A PROBABILISTIC FRACTURE MECHANICS MODEL FOR THE TUBING DEGRADATION OF THE KOEBERG STEAM GENERATORS

by

Randolph Damon

A Dissertation Submitted in Partial Fulfilment of the
Requirements for the Degree MSc (Engineering)

Department of Mechanical Engineering
University of Cape Town
Cape Town, January 2004

Synopsis

The susceptibility of Steam Generator (SG) Tubes (particularly tubes manufactured from Inconel 600) to primary water stress corrosion cracking (PWSCC) has been a major concern to the nuclear industry since 1971, when this phenomenon was first observed outside the laboratory.

Since the susceptibility of Inconel 600 to PWSCC in pure water was first established as a certainty, various electricity utilities have devoted considerable resources to determining the exact nature of this degradation phenomenon and to predicting its consequences. Whereas, the study of the nature of this degradation mechanism has led to many conflicting conclusions, the predictive methods developed have been more successful. Initially, the establishment of the Leak Before Risk of Break principle has allowed various utilities to justify SG operation with cracked tubes. Later, the development of probabilistic simulation methods, most notably by EdF and the Jožef Stefan Institute (JSI), have led to further justification of the existing maintenance regimes and also allowed the ability to do sensitivity studies with regards to various influencing parameters.

The current maintenance regime at the Koeberg Nuclear Power Station (near Cape Town, South Africa) utilises tube plugging (when cracks exceed a certain length limit) and online leak detection (based on detection of radioactive Nitrogen 16) as the main means of ensuring safe SG operation. However, the plugging limit used is based on a conservative deterministic analysis, which may be penalising in some situations. Thus, the need for risk-based SG life-time optimisation was evident.

The probabilistic fracture mechanics model developed in this study has been based on various aspects of the EdF and JSI approaches. A direct Monte Carlo Simulation (MCS) was used to determine the True Crack length distribution, the Critical Crack length distribution, and the resultant Tube Rupture probability. This particular study was based on the latest inspection data for the SG, considered most degraded at Koeberg.

The Post Inspection crack length distribution indicated that increasing the plugging limit above the current plugging limit of 13 mm has no significant effect on the resultant tube rupture probability. In addition, it will be shown that a significant decrease in tube rupture probability can only be achieved by reducing the plugging limit to 7 mm.

The Critical Crack length distribution generated by MCS clearly indicated the disadvantage of traditional deterministic methods. It will be shown that the plugging limit used at Koeberg is well within limits even for postulated accident conditions. A sensitivity analysis performed on the parameters, which define the critical crack length, revealed which parameters were most influential.

The calculated SG Tube rupture probabilities were well below the established limits and provides confidence in the maintenance and operating regime presently in place at Koeberg.

Declaration

I declare that this dissertation contains only my own original work, except where reference is made with acknowledgement to contributions from others. I also declare that this material has not been submitted for any other purpose or examination to any other department or university.

Signed this 28'th day of January 2004.

Randolph Damon

Acknowledgements

I would like to extend my thanks to the following people for the assistance they provided during the course of my thesis. Their advice was invaluable to the successful completion of this project.

- Prof. R B Tait for his supervision and guidance.
- ESKOM for sponsoring this project
- Frikkie Ellis and Haco Nicolson for initiating this project and for their guidance and support.
- David Hearne, Craig Wicker, and Anton Kotze for their guidance and support especially for their valuable insights into the metallurgical aspects of the project.
- Neil Foster for his valuable insights into probability theory
- Deon Jeannes for his support and for allowing the time needed to complete this project whenever required.

Table of Contents

Page

List of Figures

Page

List of Tables

Page

Glossary and List of Symbols

ASM	American Society for Metals
ASME	American Society of Mechanical Engineers
AVB	Anti-Vibration Bar
AVT	All-Volatile Treatment
BC	Bobbin Coil
CANDU	Canadian Deuterium-Uranium reactor (heavy water reactor)
CDF	Cumulative Distribution Function (Denoted F_X)
CEGB	Central Electricity Generating Board
CIT	Crack Initiation Time
CNS	Council for Nuclear Safety (SA licensing authority)
CPP	Condensate polishing plant
EdF	Electricité de France
EFPH	Effective full power hours
EPRI	Electric Power Research Institute (USA)
FAC	Flow assisted corrosion
FORM	First Order reliability Methods
FWLB	Feed water line break
HAZ	Heat Affected Zone
HL	Hot leg
IGA	Intergranular Attack
IGSCC	Intergranular Stress corrosion cracking
ISI	In-Service inspection
JSI	Jožef Stefan Institute (Slovenia)
LBRB	Leak before risk of break
MA	Mill Annealed
MCS	Monte Carlo Simulation
NACE	National Association of Corrosion Engineers
NDE	Non-Destructive examination
NRC	U.S. Nuclear Regulatory Commission
ODSCC	Outside diameter stress corrosion cracking
ORT	Operation at reduced temperature
PDF	Probability Density Function (Denoted f_X)
PFM	Probabilistic Fracture Mechanics
PL	Plugging Limit
POD	Probability of detection
PSI	Pre-service inspection
PSM	Probabilistic Structural Mechanics
PWR	Pressurised Water Reactor
PWSCC	Primary Water Stress corrosion cracking
RCV	Reactor coolant volume
RPC	Rotating Pancake coil
RTZ	Roll Transition Zone
RUB	Reverse U-bend specimen

SCC	Stress corrosion cracking
SG	Steam Generator
SGTR	Steam Generator tube rupture
SMiRT	Structures and Mechanics in Reactor Technology
SORM	Second Order reliability Methods
TSP	Tube support plate
TT	Thermally treated
URPC	U-Bend Rotating Pancake coil
UBHT	U-Bend Heat Treatment
VBA	Visual Basic for Applications

a	True Crack length	(mm)
a_0	Crack length at time 0	(mm)
a_C	Critical Crack half length	(mm)
a_e	Measurement error	(mm)
a_m	Measured Crack length	(mm)
C	Constant	
COV	Coefficient of Variation	
C_{TOT}	Total Carbon content	(% by weight)
C_{SOL}	Soluble Carbon content	(% by weight)
E	Activation Energy	kJ/mol
$f_X(x_1, x_2, \ldots, x_n)$	Joint probability density function for X_1, X_2, ….., X_n	
I_m	Material sensitivity index ()	
k	Flow stress factor	
$K(a)$	Stress Intensity factor as a function of a	($MPa\sqrt{m}$)
m	Parameter defining crack propagation law	
M	Number of cracked tubes	
M^*	Bulging factor in RTZ	
n_S	Inspection sample size	
N_f	Number of failure occurrences	
N	Number of simulation iterations	
P_f	Pressure propagating crack	(MPa)
P_P	Primary side pressure	(MPa)
P_S	Secondary side pressure	(MPa)
p_{SGTR}	SG Tube Rupture Probability	
p_{TR}	Tube Rupture Probability	
R_G	Universal gas constant	(1.987 cal/mol)
R	Tube radius	(mm)
t	Tube wall thickness	(mm)
t_F	Time to failure	(hours, days, etc.)
T	Temperature	(^{0}C/K)
X_i	Basic Random variables	
Z	Performance function (Resistance - Load)	

ε	Residual non detection probability	
σ	Stress	(MPa)
$\sigma_{TYPE1/2/3}$	Type 1,2,or 3 secondary U-bend stress	(MPa)
σ_f	Plastic flow stress	(MPa)
σ_θ^*	Equivalent membrane hoop stress	(MPa)
σ_Y	Yield Stress	(MPa)
σ_{UTS}	Ultimate Tensile Stress	(MPa)
$\varnothing$	Tube outside diameter	(mm)

1 Introduction

Koeberg Nuclear Power Station (~ 40 km outside of Cape Town), is a sea-cooled, twin unit (2 x 920 MW) Pressurised Water Reactor Plant, with a Framatome steam supply system. The two units have been operational since 1985. One of the major concerns of nuclear power plants of this type and age is degradation of the Steam Generator (SG) tubing, particularly primary water stress corrosion cracking.

The vertically mounted SG's (three per unit) are heat exchangers that transfer heat from a primary system (Reactor cooling system) to a secondary circuit to produce steam to drive the turbine generator. See Figure 1 for an overview of the primary system layout.
The tubing and tube sheet fulfils the following important roles:

- It provides a barrier between the radioactive primary circuit and non-radioactive SG circuit (the secondary nuclear barrier)
- Leaktightness
- Pressure boundary
- Heat transfer surface.

SG tube failures cause contamination of the secondary system and may also lead to major plant transients.

Figure 1: Primary System Layout

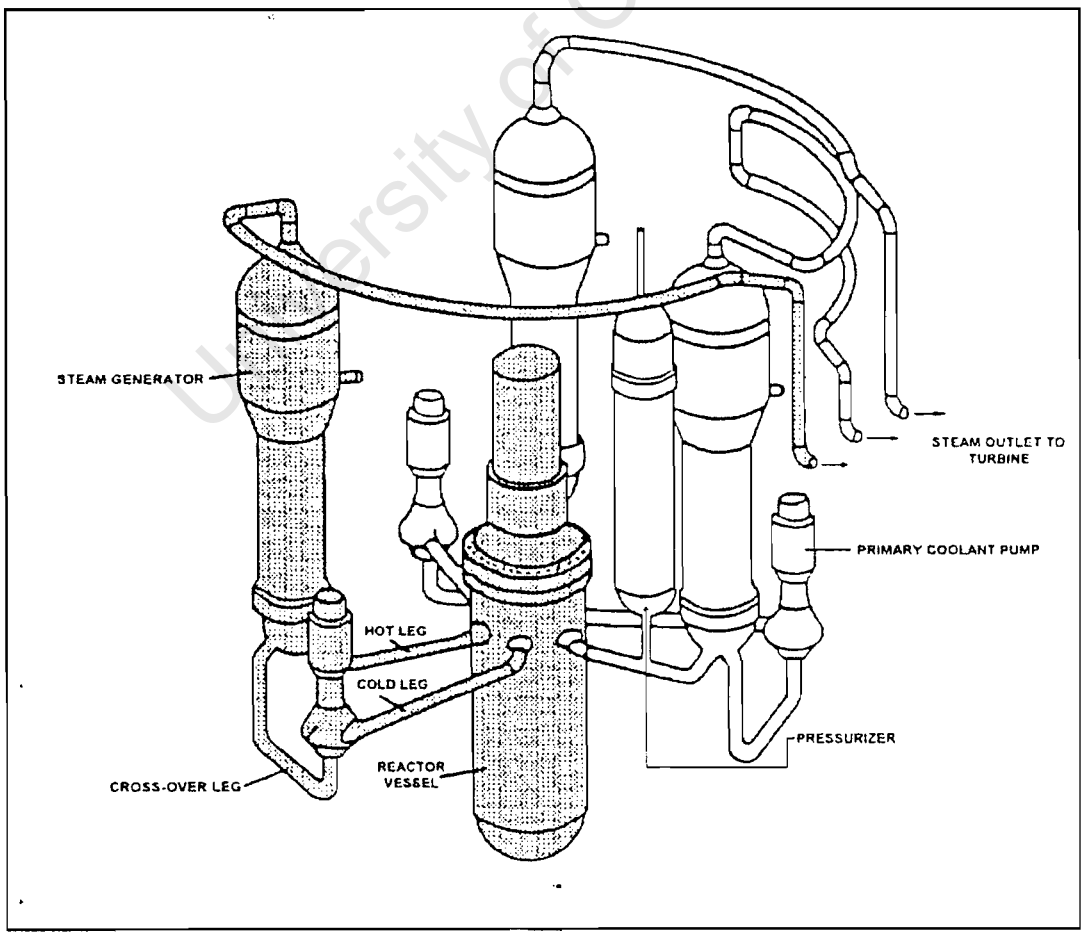

There are generally three types of steam generators in use worldwide:

- Vertical U tube
- Horizontal
- Once through

Most American, Japanese, French, and German PWR suppliers use the vertical U-tube design with inverted tubes (as does Koeberg).
Westinghouse, Combustion Engineering (CE), and Kraftwerk Union (KWU) produce variants of the inverted U-tube design, but there are important differences of detail between vendors and between the older and current designs. Babcock & Wilcox (B&W) use the once-through design. This design is a straight through tube with a vertical steam generator and vertical tubes. The Russian VVER and Canadian CANDU reactor designs use horizontal steam generators, which have the tubes mounted horizontally. No particular advantage has been seen from the horizontal versus the vertical designs.

Eskom was aware that the SG's were considered to be the "Achilles Heel" of pressurised water reactors when Koeberg was ordered in 1976. The Koeberg SG's combined with ancillary plant design (including a condensate polishing plant) and operating specifications were considered to offer adequate protection against the known tubing degradation mechanisms.
During commissioning of the Koeberg plant (Unit 1 in 1984 and Unit 2 in 1985) Electricité de France (EdF) made Eskom aware of primary side stress corrosion cracking in the tube to tube sheet expansion transition zone in reference to French steam generators.
Following EdF's advice, Eskom chose to follow a "defect specific" analysis approach to deal with the threat of stress corrosion cracking.

The defect specific analysis approach has provided Koeberg with a rigorous basis for maintaining the tubing integrity and the implementation of preventative and remedial measures. It also serves as a platform to launch the life cycle management program for the SG's.

Although this program has maintained tube integrity and availability over the past 15 years, the need still exists for an integrated plant life cycle management program, which avoids sub-optimisation.

The increasing number of preventative and remedial measures available, and the improved modelling and predictive tools (probabilistic measures) for tubing degradation, has made the development of a more comprehensive approach possible.

1.1 The Koeberg Steam Generators

The Koeberg SG design was based on the original Westinghouse recirculating pressurised water reactor (PWR) steam generators, which were manufactured under licence by Framatome. The SG tubing was manufactured using mill annealed (MA) Inconel 600. One SG on unit one was manufactured with thermally treated (TT) Inconel 600 for improved primary water stress corrosion cracking (PWSCC) resistance.

Figure 2 shows a cutaway drawing of a Koeberg SG with the essential features listed.

Figure 2: Cutaway view of a French 900MWe SG

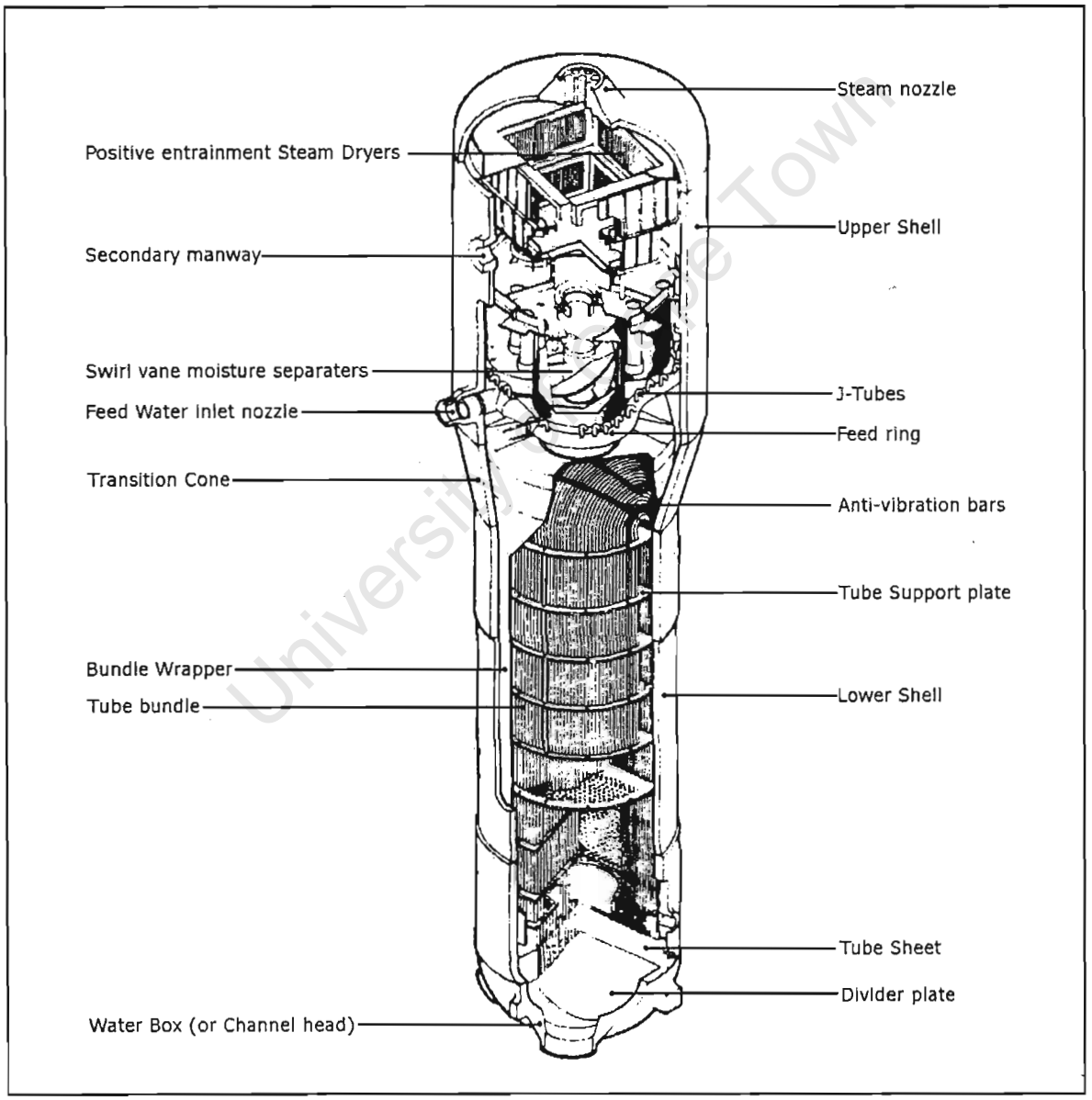

1.1.1 Design

The Koeberg SG's are Framatome type 51B, an improved version of the original type 51A SG's. Changes were made to reduce or eliminate some of the secondary side corrosion mechanisms; denting, corrosion at the tube support plates, corrosion by residual phosphates (wastage) in the sludge zone, and tube to tube sheet crevice corrosion. The following design changes were incorporated:

- Improved circulation above the tube sheet.
- Flow slot baffles were installed to reduce lane cross-flow.
- Full depth expansion – designed to prevent corrosion of the tubes within the tube sheet area by eliminating the tube to tube sheet crevice.
- Kiss roll – designed to reduce the overall residual stress in the area of diameter change, i.e., roll transition zone (RTZ). This feature is explained in more detail on pg. 8.
- Introduction of a flow redistribution baffle, with a circular orifice in the centre, 500 mm above the tube sheet, to control the upward fluid flow near the outside of the tube bundle creating a higher velocity flow along the tube sheet and minimising the number of tubes exposed to low flow velocities. This concentrates the low velocity area in the centre of the tube sheet where the blowdown extraction facilities are sited.
- Improved blowdown – additional orifices were provided on blowdown tubes in the vicinity of the lowest flow velocities.
- Quatrefoil broached support plates – corrosion was minimised at the support plates by using cruciform-broached (See Figure 13, pg. 43) support plate penetration ports instead of the round penetration ports (increased flow through the gaps).
- 13% chromium tube support plate material – to prevent oxide jacking and hence denting of the tubes at the tube support plate level. The tube support plate thickness was increased from 19mm to 30mm.
- Asymmetric distribution of J-tubes in the feedwater ring generating relatively cold feedwater for the hot leg.

The SG has a primary side and a secondary side. The primary side of the unit is in the lower half. It consists of a hemispherical cap (known as a channel head), divided into inlet and outlet halves by a partition plate. The reactor coolant flows into one half of the channel head, through Inconel U-tubes, and back to the other side of the channel head where it exits to the reactor loop. The heat from the reactor coolant is transferred through the tube walls to convert the secondary side feedwater (flowing through the tube bundle) into steam.

The U-tubes connect the two sides of the channel via a tube sheet. Together, the tube sheet and the tubes form the boundary between the primary and secondary sides. The tubes are welded to the tube sheet and full depth roller expanded to eliminate the crevice between tube and tube sheet, and hence to prevent leakage between the primary and secondary sides.

The secondary side consists of a pressure boundary shell surrounding the lower tube bundle and an upper steam drum containing the moisture separation equipment. Feedwater enters through the feedwater nozzle, and spills from inverted J-tubes on the upper side of a feedring; this prevents the ring from draining which could cause water hammer.

The feedwater then flows down an annular gap between the inside of the lower shell and the wrapper barrel, which surrounds the U-tube bundle. The wrapper barrel ensures that the feedwater enters the U-tube bundle at the level of the tube sheet. As the feedwater flows upwards through the tube bundle, the heat from the reactor coolant raises the feedwater temperature to saturation; thereafter steam is generated until, at the exit from the tube bundle, approximately 30% of the water has been converted to steam. Since the turbine cannot accept this mixture of steam and water, the entrained water must be removed. This is achieved by a set of centrifugal moisture-separators (known as primary separators), located directly above the tube bundle; steam dryers (secondary separators), at the top of the steam generator just before the nozzle, improve the steam quality to at least 99.75% (i.e. 0.25% moisture)

The entrained water that was removed by the primary and secondary separators is returned to mix with the incoming feedwater from the feedring, and hence to recirculate through the tube bundle

The main design parameters are listed in the table below:

Table 1: Main Operating Parameters

Design Parameter	Value
General	
Power per SG (MW – thermal)	928.33 MW
Number of tubes per SG	3330
Number of tube rows	46
Number of tube columns	94
Heat transfer area	4699 m^2
Primary Side Characteristics	
Inlet temperature	314 ^{0}C
Outlet temperature	277 ^{0}C
Average temperature	295.9 ^{0}C
Flow rate	4492.96 kg/sec
Pressure	155 bar
Pressure drop	2.45 bar
Secondary Side Characteristics	
Feedwater temperature	219.4 ^{0}C
Feedwater flow rate	502.78 kg/sec
Steam pressure	58.17 bar
Pressure drop	1.72 bar
Dimensions and Masses	
Overall height (approximate)	20,800 mm
Mass - Empty	298 Tonnes
Mass – 100% charge	364 Tonnes
Condenser characteristics	
Tube material	Titanium
Cooling Medium	Seawater
Full flow condensate polishing plant	Yes

The SG tubing material is a Nickel-Iron-Chromium alloy designated INCONEL* 600 (UNS NO6600). These alloys are noted for their superior corrosion and heat resistance and are used extensively in nuclear and fossil-fuel steam generators, heat treating equipment, heater element sheathing, and thermocouple tubes.
These alloys are within the broad austenitic, gamma-phase field of the ternary Ni-Fe-Cr phase diagram. Inconel alloy 600 is a solid solution alloy with good strength and toughness from cryogenic to elevated temperatures and good oxidation and corrosion resistance in many media [1]. However, it has been found that this alloy is susceptible to SCC in primary (pure) water, which is the dominant tube degradation mechanism in SG's of the Koeberg type. Inconel 690 (UNS NO6690) was then developed, with further additions of chromium (~ 30 % Cr concentration as compared with 14 to 17 %), for use in the nuclear industry and is particularly noted for its resistance to corrosion by high purity water.

Additional information regarding SG components can be viewed in appendix A. the following tables are provided.

- *Table A1:* Gives a description of the main components of the tube bundle and the various materials associated with them.
- *Table A2:* Shows data for the tubes for each SG obtained from heat certificate data. (values given are mean per SG)

* INCONEL is a trademark of the Inco family of companies.

1.1.2 Manufacture

All six SG's at Koeberg were assembled by Framatome at Saint Marcel. The heavy sheet and plate fabrication was carried out at the Creusot Loire plant. The following table gives some general information:

Table 2: General SG Manufacturing Information

General SG information	
Design	Westinghouse
Manufacturer	Framatome
Model Number	51B
Type	CP1
Number of SG's	3 per unit (3 loop/920 MW)
Date of commercial operation	Unit 1 – April 1984
	Unit 2 – May 1985
SG Tube information	
Billet manufacturer	Imphy
Tube manufacturer	Vallourec

The SG's have the following manufacturing designations:

Unit 1: SG1 96
SG2 95
SG3 77
Unit 2: SG1 98
SG2 99
SG3 100

Fabrication began with the production of the tube sheet and first shell. The lower surface of the tube sheet (which makes contact with the reactor coolant) was clad with Inconel 600. Multiple pass submerged arc welding with automatic strip feed was used. The cladding was machined and inspected using NDE (ultrasonic and liquid penetrant).

The tube sheet was then drilled (2 x 3330 holes) for penetration of the Inconel 600 U-tubes. Drilling was performed using a numerically controlled drilling machine (single and multi-spindle). The tube sheet and first shell were then joined by welding. The shells were fabricated by bending and welding of rolled steel plate. The transition cone consists of two shallow drawn sections assembled by welding. The separate shell sections were then welded together.

The Inconel 600 alloy used for the tube bundle was produced in an electric furnace and processed in a vacuum or electroslag re-melting furnace. A typical range of thermo-mechanical treatments is given below:

- Forging or hot rolling of billets.
- Hot extrusions of forged (rolled) billets
- Cold rolling.
- Intermediate annealing at 1000 – 1050 ^{0}C.
- Cold rolling or drawing.

For SG's 95, 96, 98, 99, and 100 the above treatments were followed by a final heat treatment at 950 – 980 ^{0}C, cleaning on the inside and external polishing, and finally cold bending. In addition to the above, the tubes of SG 77 were heated for 12 hours at approximately 700 ^{0}C before undergoing bending into final shape. SG 77 was acquired because, during construction, one SG was rejected by Eskom and replaced by Framatome. Thus, 5 SG's were manufactured using Mill Annealed (MA) Inconel 600 tubes while the sixth (SG 77) was fitted with Thermally Treated (TT) Inconel 600 tubing. Tubes of this type are considered to be significantly less susceptible to SCC than MA tubes [2, 3] and this has been confirmed by Koeberg experience.

The tubes were welded to the cladding on the reactor coolant side of the tube sheet in a single pass. The welds were slightly recessed in the tube sheet to prevent accidental damage. Automatic gas tungsten-arc welding (GTAW) was used, with no filler metal, producing a uniform Ni-Cr-Fe alloy weld. The welds were visually checked after each bead was laid down and underwent liquid penetrant examination at the final stage. Leak tightness was checked using a nitrogen leak test at 1.4 MPa.

The tubes were then expanded along the entire thickness of the tube sheet. Anchoring the tubes in this way is considered to have several advantages:

- Ensuring leak tightness
- Stress reduction at the tube to tube sheet weld.
- Increased mechanical strength of the assembly.
- Crevice between tube and tube sheet is virtually eliminated

A second intermediate tube expansion (kiss roll) was performed to reduce the external residual stresses in the roll transition zone (RTZ) between the expanded and non-expanded sections of the tubes in order to minimise the risk of circumferential cracking. Figure 3 illustrates the difference between normal full depth expansion and expansion with a kiss roll.

Figure 3: Tube Expansion

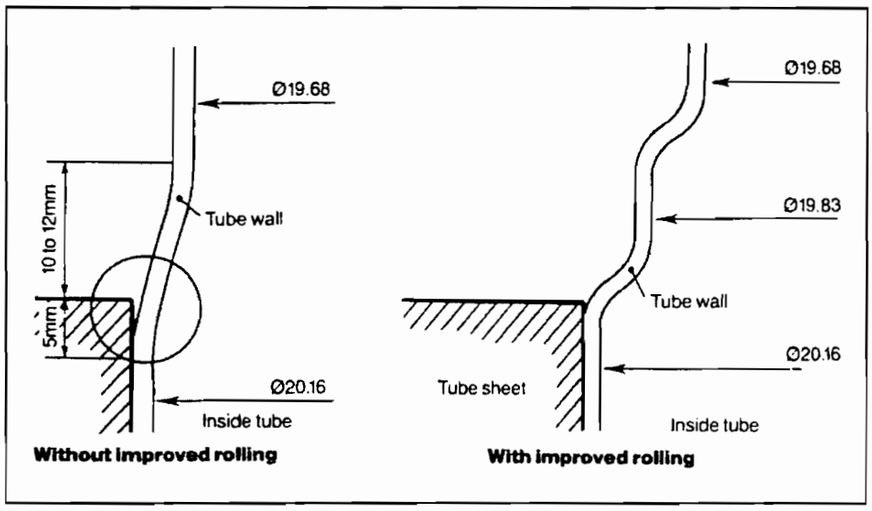

The SG's were then subjected to final qualification as follows:

- Examinations of welds for pressure rated joints. These examinations cover:
  a. Longitudinal and transverse tensile tests, bending and impact tests to determine the mechanical characteristics of the joint (parent metal, weld metal, and heat affected zone (HAZ)).
  b. Hardness profile across the joint.
  c. Chemical composition of the weld metal
- All Ferritic weld joints and zones affected by cladding operations underwent at least one stress relief treatment at a temperature between 595 and 625 ^{0}C.
- The full SG assembly was then subjected to an on-site hydrotest at 1.33 x design pressure for the primary side and at 1.5 x design pressure for the secondary side.

The SG's were then positioned over their bunkers and lowered onto the vertical supports and secured.

A number of manufacturing abnormalities was observed during manufacture and the Pre-Service Inspection (PSI). They are listed below:

- ***Tube sheet anomalies***: SG 98 had three locations with incorrect tube sheet drilling. No tubes were inserted and the tube sheet was plugged at those locations. SG 99 had one location (cold leg side) where the tube sheet had not been drilled. The corresponding hot leg side hole was thus plugged.
- ***Volume loss***: Six tubes showed small volume loss signals of over 40% wall thickness during the 100% Bobbin coil examination of the PSI. These six tubes were preventatively plugged.
- ***Dents***: More than 200 dents were detected under the upper four support plates in the peripheral zones of the SG's of Unit 1. No dents were found on Unit 2. The dent pattern was consistent with the position of the non-broached and reduced diameter holes in the upper support plates. It was concluded that the dents were caused by excessive manipulation of the tubes during installation. The size of the dents was determined by performing a supplementary signal analysis using a reference tube with simulated dents. The most severe dents were sized at 0.4 mm. The presence of deformations at the fourth support plate prevented the passage of the BC probe. Three peripheral tubes were identified as having dents and were preventatively plugged. These dents were attributed to impact or bundle twisting during final shell welding stages.
- ***Expansion Anomalies***: Some 126 tubes with tube to tube sheet expansion anomalies were detected with a multi-frequency BC eddy current probe. Two tubes had multiple anomalies. Some of the expansion anomalies were re-expanded on-site and a repeat inspection was carried out. None of the expansion anomalies were considered significant enough to warrant plugging.

In the period between the startup of units 1 and 2, EdF reported PWSCC in the roll transition zone of tubes of similar material and expansion design as the Koeberg SG's. To anticipate this threat, the PSI data, stored on magnetic media, was re-examined to characterise the data in the hot leg roll transition zone and classify the expansion anomalies in terms of possible preferential susceptibility to PWSCC. Eskom/Koeberg, with the recommendations of both EdF and Framatome, considered that any tube with defined anomaly classifications would require special surveillance. These were therefore included in the inspection scope in addition to routine sampling.

1.1.3 Design Modifications

The SG's of both Unit 1 and 2 were shotpeened in the hot leg roll transition zone during outages 102 and 201 respectively. The purpose of shotpeening is to create a compressive residual stress on the inner surface of the roll transition zone to prevent the initiation of PWSCC. It is predicted that shotpeening will have little effect on the propagation of existing defects in the roll transition zone. On this basis, unit two should have fewer instances of PWSCC since the shotpeening was carried out much earlier in its operational history than Unit 1 (9,148.8 EFPH compared to 14,323.2 EFPH). This has been verified by tube degradation statistics (see section 1.2 below).

Experience world-wide has shown that PWSCC can occur in the U-bends (rows 1 and 2) of the small radius U-bends due to residual stresses caused by tube bending during manufacture of the tube bundle. This has led to an extensive preventative plugging programme of small radius U-tubes. To prevent this, Koeberg heat treated the U-bends of rows 1 and 2, on both units during outages 105 and 205 respectively. The heat treatment employed was 2 to 6 minutes between 700 and 840^0C.

Initially the plugs used at Koeberg were manufactured from Inconel 600. However, due to French and world-wide experience of stress corrosion cracking of the plugs themselves, all Inconel 600 plugs at Koeberg have been removed and replaced with Inconel 690 plugs.

1.2 Current Status of the Koeberg steam generators

As predicted by the defect specific analysis performed during the initial operational phase, both units at Koeberg are affected by axially orientated, primary water stress corrosion cracking (PWSCC) in the roll expansion transition zone. This is the only significant form of tubing degradation to manifest itself after 13 cycles[†] (~ 18 years) of operation. Tables, A5 and A6 (Appendix A) details the extent of PWSCC and tube plugging for each SG at each outage:

It is clear that the main cause for tube plugging on Unit 1 is PWSCC indications, which accounts for 31% of the tubes plugged to date. Manufacturing defects accounts for 15.6% of tubes plugged, OD wall loss due to loose parts makes up 9%. The balance is caused by a variety less common degradation mechanisms.

Unit 2 has a much lower incidence of tube plugging and has not had any tubes plugged due to PWSCC. Again, this can be attributed to the application of shotpeening to Unit 2 before Unit 1.

The main cause of tube plugging in Unit 2 was due to manufacturing defects, which accounts for 35% of all tubes plugged to date. The rest is caused by U-bend indications (24%), loose parts damage (18%), and a variety of other less common degradation mechanisms.

Plugging, however, is not a very useful indication of the state of SG tube bundle degradation. The decision to plug is based on many parameters. Often it is more convenient and cost effective to plug a tube preventatively i.e. before the mandatory plugging criteria are met. This is sometimes done to minimise the primary to secondary leak rates during the next cycle. EdF's plugging policy has evolved as plant experience and research has progressed, and thus the decision to plug at each outage has been based on different areas of focus.

Although the plugging data cannot be used conclusively to determine the major degradation mechanisms, experience at Koeberg and internationally has indicated that PWSCC is the dominant tube degradation mechanism for Inconel 600 tubed SG's. The extent of PWSCC at Koeberg (number of cracked tubes) is considered a better indication of the state of SG tube bundle degradation and is shown graphically below.

[†] A Cycle refers to the period between successive refuelling outages for a particular unit. Koeberg uses 18 month fuel cycles and has currently undergone 11 cycles on Unit 1 and 10 cycles on Unit 2.

Figure 4: Extent of Unit 1 PWSCC*

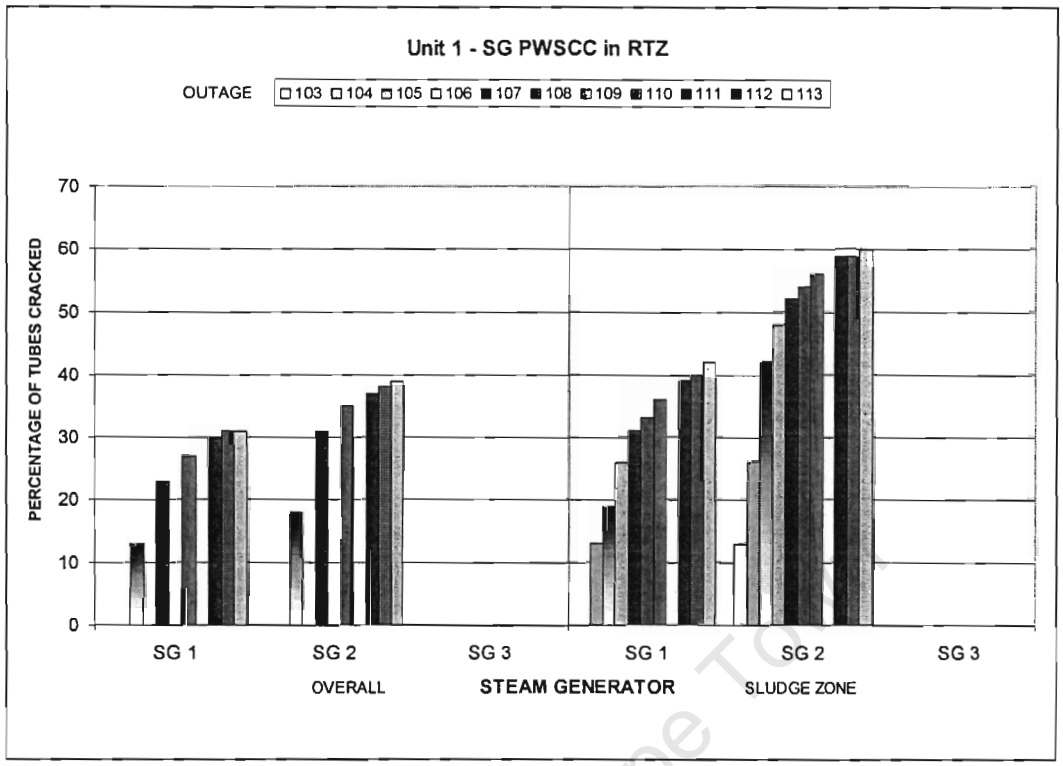

Figure 5: Extent of Unit 2 PWSCC

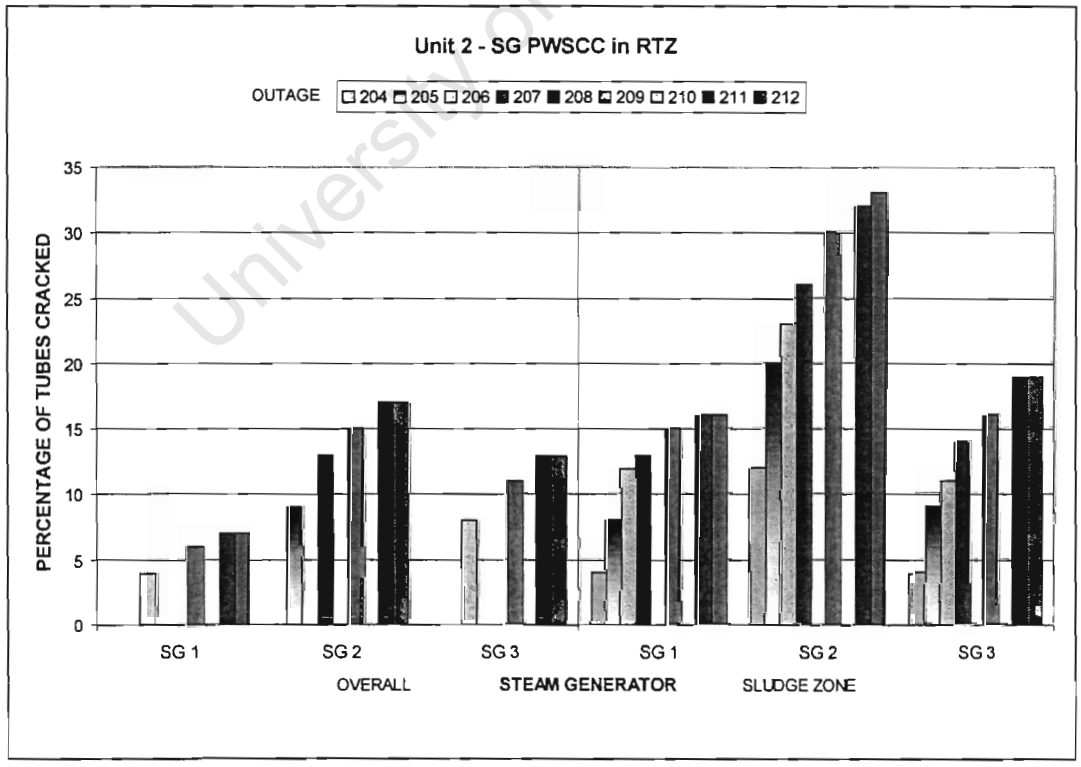

* It should be noted that the sludge zone (300 tubes) was reduced to 150 tubes from outage 110 (Unit 1) and outage 208 (Unit 2). This batch represents the reduced sludge zone (as verified by televisual inspection). Thus, to maintain consistency, the sludge zone plots do not include the results for outage 110, 208, and 210. Outage 209 was included since the entire tube bundle was inspected (i.e. the extent of cracking in the 300-tube sludge zone could be determined).

Again, the increased resistance to crack initiation by Unit 2 (by a factor of ~2) can be attributed to the application of shotpeening to Unit 2 one cycle before application to Unit 1.

The results also appear to indicate behaviour typical of the early failure region of the classic bathtub failure rate curve (this curve is fundamental to the understanding of reliability characteristics). The bathtub curve is divided into three portions. The *early failure* region is a period of high failure rate because of initial defects. It is in essence a 'shakedown' period in which weak units, with susceptible materials and improper workmanship and manufacture (e.g. improper tube expansion and loose parts) are culled out. This is evident from the decreasing failure rate observable in Figure 4 and Figure 5. The *useful-life* period follows the early failure period and is characterised by an approximately constant failure rate. Failures are at a low rate and of a random nature. Last is the period of *wear-out*. This region exhibits a sharp rise in failure rate because of ageing and wear. The SG's are designed to operate for the life of the plant and thus should not reach the wear out phase.

1.3 Fracture Mechanisms in Metals and Alloys

Intergranular fracture has been identified as the dominant fracture mechanism for SG tubing of PWR plants [4, 5, & 6]. The following section serves as an introduction to the various fracture mechanisms, particularly Intergranular fracture.

Since World War II there has been great progress in understanding the ways in which materials fracture. Such knowledge has proved essential to better formulation of fracture mechanisms. Nevertheless, it is still not possible to use this knowledge, together with other material properties, for predicting fracture behaviour in engineering terms (i.e. in a deterministic sense) with a high degree of confidence [5]. The four most common fracture mechanisms in metals and alloys are as follows:

1.3.1 Ductile Fracture

Ductile materials usually fail as a result of nucleation, growth and coalescence of microscopic voids that initiate at inclusions and second phase particles. The voids grow together to form a macroscopic flaw, which leads to fracture.

1.3.2 Cleavage

Cleavage fracture involves the rapid propagation of a crack along a particular crystallographic plane. The fracture path is transgranular in polycrystalline materials. Cleavage can be brittle, but it can be preceded by large scale plastic flow and ductile crack growth. The preferred cleavage planes are those with the lowest packing density, since fewer bonds must be broken and the spacing between planes is greater.

Cleavage is most likely when plastic flow is restricted. This occurs when insufficient slip systems for ductile behaviour are present. Face centred cubic (FCC) metals, such as nickel, are usually not susceptible to cleavage because there are ample slip systems for ductile behaviour at all temperatures.

1.3.3 Fatigue

Structures, which are subjected to cyclic loading, may fail by fatigue fracture. Fatigue cracks can be initiated in a number of ways; however , the important fact is that they are usually nucleated at a free surface from small flaws, scratches, or other stress raisers. Crack initiation and early growth occurs above a characteristic "threshold" stress intensity (ΔK_{th}) and is generally termed Stage I growth; fatigue propagation of a significant flaw (≥ 3 mm long) is termed Stage II growth; the crack grows a finite increment in each load cycle. During this stage crack growth is relatively insensitive to microstructure and flow properties. Stage II continues until the crack becomes large enough for unstable fracture, Stage III.

1.3.4 Intergranular Fracture

In most cases metals do not fail along grain boundaries. Ductile metals usually fail by coalescence of voids formed at inclusions and second phase particles, while brittle metals typically fail by transgranular cleavage. Under special circumstances, however, cracks can form and propagate along grain boundaries.
There is no single mechanism for intergranular fracture. Rather, there are a variety of situations that can lead to cracking on grain boundaries, including [4]:

- *Grain boundary cavitation and cracking at high temperatures.*
  At high temperatures, grain boundaries are weak relative to the matrix, and a significant portion of creep deformation is accommodated by grain boundary sliding. In such cases void nucleation and growth (at second phase particles) is concentrated at the crack boundaries, and cracks form as grain boundary cavities, grow and coalesce. Grain boundary cavitation is the dominant mechanism of creep crack growth in metals.

- *Precipitation of a brittle phase on the grain boundary*
  Brittle phases can be deposited on grain boundaries through improper tempering. Temper embrittlement, which occurs when an alloy steel is tempered at ~ 550 ^{0}C, involves the segregation of impurities, such as phosphorous and sulphur, to prior austenite grain boundaries. These thin layers of impurity atoms are not resolvable on the fracture surface. They can be detected in the laboratory with surface analysis techniques such as Auger electron spectroscopy.

- *Hydrogen embrittlement and liquid metal embrittlement*
  Hydrogen can severely degrade the toughness of an alloy. The precise mechanism of hydrogen embrittlement is not completely understood. It is thought that atomic hydrogen bonds with the metal atoms and reduces the cohesive strength at grain boundaries. Hydrogen can come from a number of sources, including moisture and hydrogen containing compounds.

- *Environmentally assisted cracking*
  Environmentally assisted cracking is related to hydrogen embrittlement, since hydrogen plays a role in the cracking process. High strength alloys are most susceptible to environmentally assisted cracking. The cracking is usually time-dependent and follows grain boundaries. The chemical and transport processes that lead to environmental assisted cracking are as follows:
  1. Transport of the harmful environment to the crack tip.
  2. Reactions of the environment with the crack surfaces, resulting in localised dissolution and production of hydrogen.
  3. Hydrogen absorbtion into the alloy.
  4. Diffusion of the hydrogen to an embrittlement site ahead of the crack tip.
  5. Hydrogen-metal interactions leading to embrittlement and crack propagation.

- *Intergranular corrosion*
  Intergranular corrosion involves preferential attack of the grain boundaries, as opposed to general corrosion, where the material is dissolved relatively uniformly across the surface. Intergranular attack is different from environmentally assisted cracking, since there is no embrittlement mechanism associated with the grain boundary corrosion.

In U-tube SG's, intergranular cracking of the Inconel 600 tubing has occurred at various locations e.g. within the tube sheets, just above the tube sheets, in dents at support plates, and in tight radius U-bends.
While the mechanisms causing the Inconel 600 cracks at these various locations are not well understood, their characteristics and the prevailing environment support the view that stress corrosion* is dominant [6]. Examination of pulled tubes also supports this view. Sulphur has been found on the crack faces of these pulled tube specimens, and may have been involved in crack propagation, since it has long been recognised that sulphur can induce cracking of Inconel 600.

The SG tubes are exposed to two differing environments. Pure water on the primary side and a caustic environment on the secondary side. The relative susceptibilities to SCC are affected by oxygen and caustic concentration. Inconel 600 appears to be most susceptible to SCC in weak caustic concentrations. Based on this, the hypothesis has been put forward that the phenomenon of SCC in Inconel 600 in pure water is of the same nature as that in a caustic medium [6].

Since the attack is almost always intergranular, the role of grain boundary carbides and the related chromium depleted layers in the process has been extensively studied. However, no universally accepted model is available to explain the SCC behaviour of Inconel 600, although grain boundaries carbides and the segregation of impurities (Phosphorous and Sulphur) to the grain boundaries clearly play an important role in the process.

Attempts to improve the SCC resistance of Inconel 600 have pursued modification of the grain boundary microstructure. Of the two heat-treatment processes in use, viz. a high temperature "purification" anneal and a thermal treatment, the thermally treated tubing has superior caustic SCC resistance to the mill-annealed product in all cases.
Thermal treatment in the carbide precipitation temperature range (above $\sim 597\ ^0C$) introduces a variety of grain-boundary microstructures. Grain-boundary precipitation range from fine discrete particles, to a semicontinuous layer, to large discrete particles. The maximum improvement in caustic SCC resistance is achieved with a thermal treatment of $\sim 704\ ^0C$ (for 1 to 24 hrs) and at $\sim 593\ ^0C$ (for at least 100 hrs) and $\sim 649\ ^0C$ (for 10 to 100 hrs). Thermal treatments at these temperatures and corresponding duration's have produced tubing with SCC resistance as good as, if not superior to, that of Alloy 800 [6].

* A SCC Mechanism can be defined as the combination of *mechanical*, *physical*, and *chemical* processes that accomplishes the separation of bonds at the crack tip, thereby advancing the crack.

The maximum improvement in caustic SCC resistance correlated with a grain-boundary microstructure consisting of a semicontinuous precipitate without an associated chromium-depleted layer but with phosphorous segregated to the boundaries.

Thermal treatment increases the critical stress level above which rapid crack propagation occurs, as well as decreasing the crack propagation rate. The improved SCC resistance has been attributed to a reduction in residual stress (retarding crack initiation) and grain boundary structural modification (inhibiting crack growth).
Another benefit obtained from thermal treatment is a reduction in the variability of caustic SCC resistance.
There is a large scatter in the data on the caustic SCC resistance of mill-annealed Inconel 600 presumably due to the testing of different heats of material with different thermomechanical processing histories.

Literature relevant to the intergranular corrosion of Inconel 600 in pure water and caustic environments are discussed in subsequent sections.

2 Tube Degradation Mechanisms

Pressurised water reactor SG tubes have been subject to failures/degradation's due to various mechanisms, including Primary water stress corrosion cracking (PWSCC), Stress corrosion cracking (SCC) and Intergranular attack (IA) on the secondary side, pitting, wastage, denting, fretting, vibration fatigue, and loose parts damage.
Figure 6 below illustrates these degradation mechanisms and their location within the tube bundle.

Figure 6: Tube Degradation Mechanisms and Locations

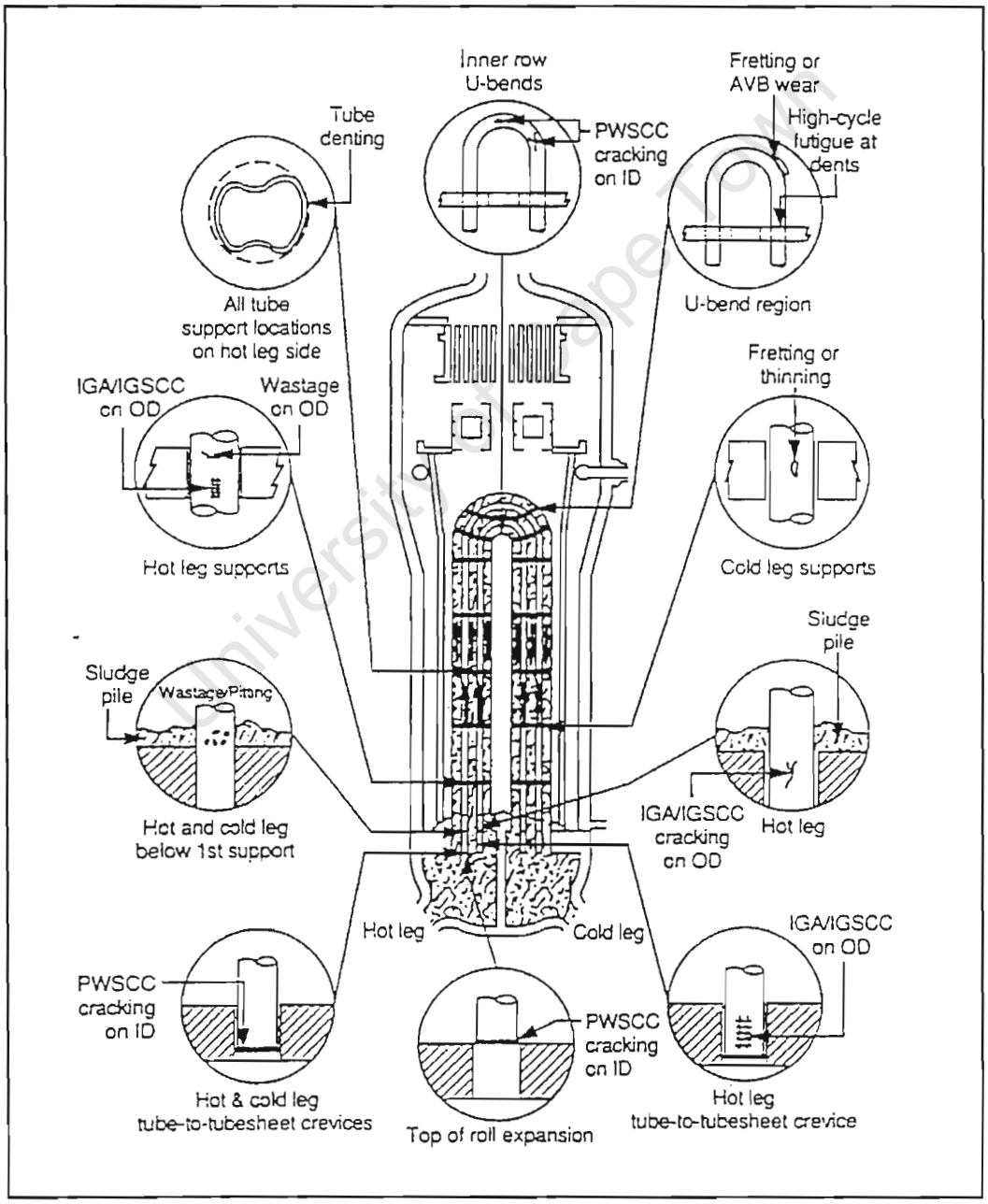

It has been observed that the dominant failure mode has changed over the years, as illustrated in Figure 7 [7] below:

Figure 7: World wide causes of tube plugging

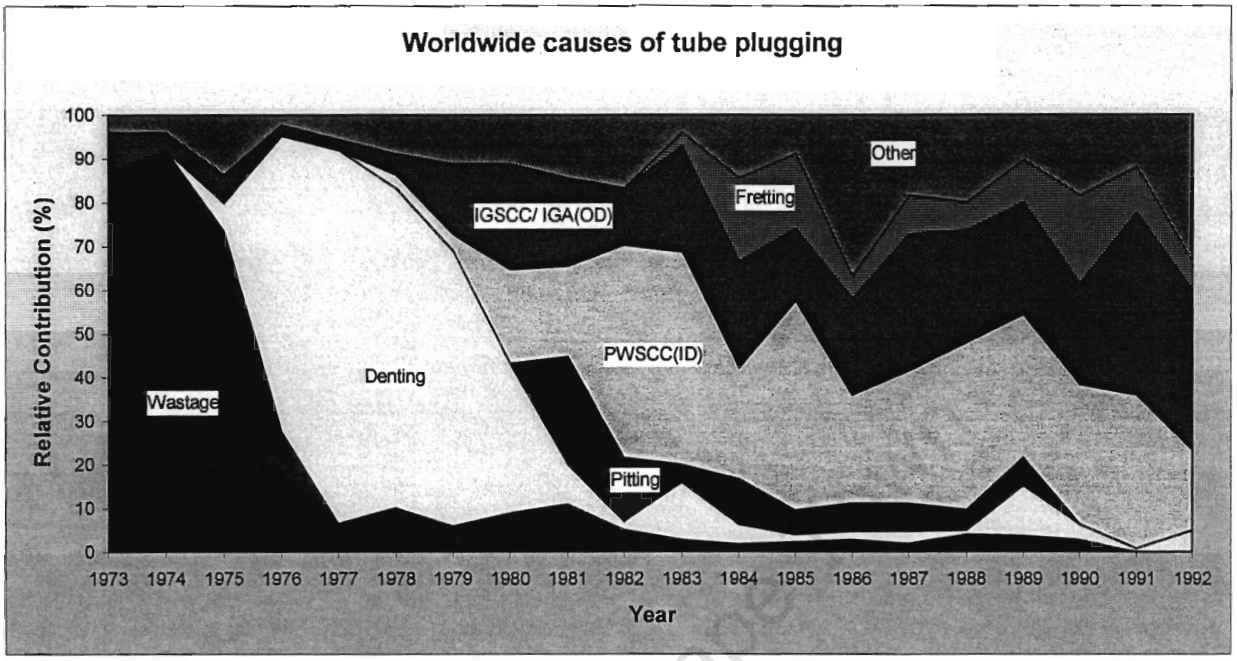

From Figure 7 it is clear that the major cause of tube failure in the early 70's was wastage. This is the corrosion on the secondary side, generally in relatively stagnant regions, which resulted in tube wall thinning. It was concluded to be acid phosphate attack resulting from the use of phosphate based secondary water chemistry. Thus, most operators changed from this to AVT (All Volatile Treatment) chemistry in the early to mid 70's. Some failures due to wastage have occurred since this time, but these have been mainly confined to those plants, which retained phosphate chemistry to a later date (e.g. Siemens/KWU). A few plants experienced wastage after the switch to AVT but this was as a result of residual phosphates, and a few where significant condenser in-leakages were believed to have introduced impurities into the SG's. Thus, the change to AVT had a significant effect on the occurrence of wastage.

The switch to AVT chemistry and its effect on wastage resulted in the emergence of denting as the predominant failure mode in the late 70's. This degradation mechanism was also largely eliminated by around 1980. For existing plants this was achieved by tightening of the secondary water chemistry controls, particularly the feedwater quality, to reduce the levels of chloride and copper ions resulting from condenser and feed-train materials.

In the longer term, i.e. for new and replacement SG's, the problem of denting has also been addressed by changes to the tube support plate material (carbon steel replaced by stainless steel) and design (drilled holes replaced by broached hole or egg crate designs). In addition, newer plants have employed high integrity condensers tubed with titanium or stainless steel to further improve feedwater quality.

During the 60's, 70's, and early 80's many tube failures occurred due to the design of the tube to tube sheet joint which left deep annular crevices around the tubes on the secondary side thereby providing stagnant regions where aggressive species could concentrate, leading to denting, wastage, and SCC.
This condition was aggravated by sludge accumulations at these regions, which could help provide the aggressive species and assist in their concentration, thus leading to further such failures and also to pitting at and just above the tube sheet. Modifications were therefore carried out to eliminate tube annular crevices. Early explosive expansion techniques largely achieved this aim, but resulted in residual stresses in the tubes, which in some cases led to SCC. Later, tube expansions were by mechanical or hydraulic means, the latter being generally preferred as it is believed to result in lower residual stress levels. Such measures significantly reduce the incidence of failures at the tube sheets and all manufacturers now employ full depth tube expansion.

Since the early 80's the proportion of tubes plugged (and sleeved) due to PWSCC on the primary side and SCC/IGA on the secondary side has increased. In 1994 PWSCC accounted for about 22% of all tubes plugged.

The Koeberg SG's have followed these worldwide trends and suffers mainly from PWSCC in the roll transition zone, U-bend cracking, and secondary side IGA/SCC

2.1 Tube Degradation Mechanisms at Koeberg

2.1.1 Primary Water Stress Corrosion Cracking (PWSCC)*

PWSCC of Inconel 600 was identified in the laboratory as early as 1959, when Coriou *et al.* [8] reported cracking of this material in high purity water at 350^0 C. In that early work, the researchers proposed "that there exists in high temperature austenitic iron – chromium nickel alloys a special kind of intergranular sensitivity not related to chromium carbide precipitation" [9]. In 1971 this laboratory cracking phenomenon in high purity water became an in-service degradation mechanism, with the first confirmed primary-side cracking of hot leg roll transition regions at the tubesheet and suspected primary cracking in U-bends at Obrigheim+. Initially this behaviour was thought to be an anomaly due to the apparent absence of water born contaminants that would promote this type of failure. Subsequent lab tests and, more importantly, SG tubing service experience confirmed the IGSCC susceptibility of Inconel 600 in primary water. An interesting historical account of known SG tube ruptures (SGTR's) is given in Appendix B.

2.1.1.1 Degradation Mechanism

In spite of the extensive research work carried out since 1960, the mechanisms causing PWSCC are still not fully understood. The main causes are thought to be anodic dissolution of material in the region of the cracks and a hydrogen induced cracking mechanism [10, 11]. Totsuka *et al.* [12] has found that the IGSCC of Inconel 600 on exposure to a slightly alkaline (pH ~ 8) aqueous solution at 350 ^{0}C is cathodically controlled and occurs only at potentials more negative than ~ -0.835 V_{SHE} (V_{SHE} indicates potentials referred to the standard hydrogen electrode scale). He also suggests that the entry of hydrogen and its accumulation at locations where a state of high complex stresses and strains exist is mainly responsible for intergranular cracking. The entry of hydrogen into the alloy was found to be affected by oxide (hydroxide) films on the surface. Recently, Thomas and Bruemmer.[13] examined the microstructure of PWSCC affected material using advanced methods of high resolution analytical transmission electron microscopy (ATEM) to gain insight into the mechanism of PWSCC. The observations suggested that an active-path dissolution or oxidation process controlled PWSCC. However, like many studies of this nature, more questions were raised than answered, and more work is still needed to fully understand the mechanisms causing PWSCC.

* The terms Primary Water Stress corrosion cracking (PWSCC) and Intergranular stress corrosion cracking (IGSCC) refer to the same degradation mechanism. The term PWSCC emphasises the fact that IGSCC is initiated on the primary side of the SG.

+ Obrigheim: Two loop German PWR (340 MWe) built by Siemens (Operational since 1969).

2.1.1.2 Main Influencing Factors

The most important factors influencing PWSCC are:
- Coolant temperature.
- Water chemistry parameters such as hydrogen content and possibly also the lithium concentration in the coolant.
- Material properties: Annealing temperature, strength, grain size etc.
- Tensile Stress, particularly internal stresses due to cold working.

2.1.1.3 Crack Initiation Times and Time to Failure

The formation of cracks as a result of these factors generally occurs after operating times of a year (8,760 hours) or more [14]. However, axial SCC was first detected at Koeberg after 20,000 operating hours on the primary side, hot leg, RTZ of a mill annealed SG [15].
Accelerated tests [16] undertaken on reverse U-bend (RUB) specimens in high purity water with hydrogen addition at 365^0C, indicated that all regular alloy 600 tubes, both mill annealed (MA) and thermally treated (TT) had cracked after 20,000 hrs. These results can be extrapolated to an equivalent time of 45 years at 320^0C.

PWSCC generally occurs in the hot leg side, RTZ (initiating from the inside diameter) of recirculating SG's. The high residual stresses in the RTZ contribute significantly to the onset of cracking and subsequent time to failure. Some sources [17] have shown that the time to failure is inversely proportional to stress raised to the fourth power i.e.

$$t_{FAILURE} \propto \frac{1}{\sigma^4}$$

In common with many stress corrosion phenomena, lifetime-to-failure of Inconel 600 in primary water can be fitted to an empirical formula of the form [18]:

$$t_{FAILURE} = C\frac{1}{\sigma^4 I_m}\exp\left(\frac{E}{RT}\right) \qquad \textbf{Equation 1}$$

where:

	$t_{FAILURE}$	Time to failure (hours)
	C	Constant
	σ	Applied Stress (MPa)
	I_m	Material sensitivity index (Table 3)
	E	Activation Energy (180 kJ/mol in this case)
	R	Universal gas constant (1.987 cal/mol)
	T	Absolute temperature (K)

The temperature and operating stress can be calculated or measured, however, the intrinsic material sensitivity to SCC as represented by I_m is more difficult to estimate. This is due, in part, to the difficulty in determining the carbide morphology of an Inconel 600 component still in service. Thus for assessment purposes, a system of material indexes (Table 3) deduced from minimum observed times-to-failure in

service or in laboratory tests has been devised [18]. The reference point for this system of material indexes for Inconel 600 is $I_m = 1$ when the temperature is 325 ^{0}C, the stress is 450 MPa, and the minimum time-to-failure observed is 10,000 h.

Table 3: Maximum Indices for Inconel 600 sensitivity to PWSCC [18]

Material	*Index (I_m)*	*Comment*
SG tubes, Mill annealed, very resistant, or thermally treated, very significantly improved.	0.2	
SG tubes, Mill annealed, not very sensitive, or thermally treated, improved.	0.5	
Pressure Vessel bottom head penetrations	0.6	
SG tubes, Mill annealed, sensitive, or thermally treated, little improved, SG partition plates, reactor support pads.	1.0	*Reference Point.* 325 ^{0}C, 450 MPa 10,000 h (min)
SG tubes, Mill annealed, very sensitive.	2.0	
Pressure Vessel upper head penetrations	2.5	

2.1.1.4 Stress Contribution

The stress state has a significant effect on crack susceptibility. Domain *et al.* [19] have observed that the absence of lateral branching in cracks suggests that a high elastic stress is necessary for crack growth. If crack growth was less dependent on stress, then branching of the cracks in directions other than normal to the principle fibre stress would have occurred. High stresses occur in the RTZ, due to the mechanical rolling process used to expand the tube into the tube sheet.
Woodward *et al.* [17] indicates that roller expansions introduces longitudinal tensile stresses towards the outside diameter and circumferential tensile stresses towards the inside diameter. The maximum stresses are greater than 150 MPa,
which is about 50% of the yield strength of Inconel 600. This condition is further aggravated by expansion anomalies introduced during mechanical rolling of the tubes into the tube sheet. These anomalies include; excessive rolling, over expanded kiss roll, and over diametering of tube sheet bore. These anomalies were detected and in some cases re-expanded during the pre service inspection (PSI) at Koeberg.

2.1.1.5 Temperature Contribution

PWSCC of mill annealed Inconel 600 tubing is also a highly temperature dependent phenomenon and can be described using an Arrhenius* relationship with an activation energy of ~ 40 kcal/mol (167.47 kJ/mol) [9, 20]. The activation energy is, however, characterised by a high degree of scatter. Economy *et al.* [21] have suggested a range of 30 to 70 kcal/mol and Scott [18] has observed a typical value of 43 kcal/mol with a scatter band of 19 to 53 kcal/mol.

EdF's work to date as cited by Nicholls [22] indicates that time to crack (t_C) is given by the following relationship:

$$t_C = \frac{k_1 E}{k_2 T} \qquad \textbf{Equation 2}$$

where
k_1 and k_2 are constants dependant on materials processing etc.
T is the temperature (K) and
E is the activation energy (kcal/mol).

Andresen [23] has shown that water chemistry strongly effects the dependence of crack growth rate on temperature, especially above 200 ^{0}C. His research has shown that in pure water (associated with ≤ 200 ppb O_2) crack tip chemistry was more benign, a peak in crack growth rate was observed at about 200 ^{0}C with a rapid drop in crack growth rate observed above 250 ^{0}C.

2.1.1.6 Crack Morphology

Two forms of PWSCC have been observed, axial cracking and circumferential cracking. Axial cracks are usually numerous around the circumference and originate where the residual stresses are the highest i.e. between the roll expansion and the kiss roll. Circumferential cracks are less common and only two tubes with indications of this type have been detected at Koeberg to date. These types of cracks have also been observed in French plants. Circumferentially cracked tubes are plugged upon detection. This is because a circumferential crack failure leaves a tube severed. The tube is thus free to whip around inside the tube bundle and may damage the surrounding tubes.

* Arrhenius' Law is a rate law, which has great generality. It states that the rate increases exponentially with temperature (or that the time for a given amount of corrosion, creep, oxidation etc. decreases exponentially with temperature).
If the rate of a process which follows this law is plotted on a ln scale against 1/T a straight line with slope –Q/R is obtained, where Q is the activation energy (kJ/mol) and R is the Universal gas constant (8.31 J/mol.K). [24]

Axial cracks are allowed to grow and are plugged when their free length (measured from the last point of contact with the tube sheet) is in the region of 13mm. These cracks generally become through wall when their length is approximately 6mm long. After 12mm the inside diameter crack length and outside diameter crack lengths are almost similar [15]

The levels of cracking are highest in the sludge zone with a progressive reduction in cracking from the centre of the tube sheet outwards to the periphery. Wicker [15] has analysed Koeberg's crack growth rates and cracking trends and found that some benefit was derived from shotpeening the hot leg RTZ's of both units. On Unit 2, where shotpeening was performed one outage earlier (Outage 201) there appears to be a considerably lesser incidence of cracking.

2.1.1.7 The Leak-Before-Risk-of-Break Principle (LBRB)

The stability of axial cracks up to a free length of 16mm under a feedwater line break condition (this is the most severe transient since maximum depressurisation, $\Delta P \approx 170$ bar, of the secondary side occurs) has been shown by Hutin and Billon [25]. The acceptable free length increases to 16.5mm in the transition zone due to the tube sheet reinforcement effect. The plugging criteria for axial cracks in the RTZ is that its free length does not exceed 13 mm. The safety margin of 3.5 mm was derived from statistical analysis [26] and is based on the following:

- 2 mm RPC length evaluation uncertainty (i.e. an error of ± 1 mm can be expected).
- 1.5 mm potential crack propagation per cycle of cracks with initial lengths greater than 10 mm.

Scott [18] has observed that in thermally treated Inconel 600 tubes, axial cracks at ~ 10 mm long arrest, for all practical purposes. Thus, provided the overall leak rate is acceptably low, there is no need to plug these tubes in contrast to their mill-annealed counterparts.

It was further shown that a significant primary to secondary leak should precede tube failure. This has become the basis for the principle of Leak Before Risk of Break (LBRB) and has allowed the operation of SG's with limited leak rates. The Koeberg safety case KSS 6.46 [22] demonstrated that as long as a 30 litres/hour per SG leak rate limit was maintained, the tube integrity under normal and accident conditions was assured for IGSCC defects.

2.1.1.8 The Influence of Metallurgical Parameters

A fairly good correlation between crack initiation time (CIT) and certain metallurgical parameters has been shown by various studies [10, 16, 19, 21, 27, 28, 29, 30, 31]. It is, however, important to emphasise that there is not a single product called "mill-annealed" Alloy 600 tubing. Each tubing manufacturer employs a different process to produce "mill-annealed" Alloy 600 tubing, and the resistance to SCC varies greatly with the process. Additionally, the resistance to SCC may vary for different Heats (batches) of tubing by the same manufacturer.

The findings for the effects of the metallurgical parameters are summarised below:

- ***Annealing*** [*] ***Temperature***: The final annealing temperature has considerable influence on CIT. A linear relationship has been observed, See Figure 8 below. It can be seen that a high annealing temperature has a beneficial influence. A high annealing temperature is required to dissolve the majority of the carbon in the alloy into solid solution. For heats given a low annealing temperature that is not sufficient to solutionize the carbon, the benefit of thermal treatment is not as great [21].

Figure 8: Influence of Final Anneal Temperature [16]

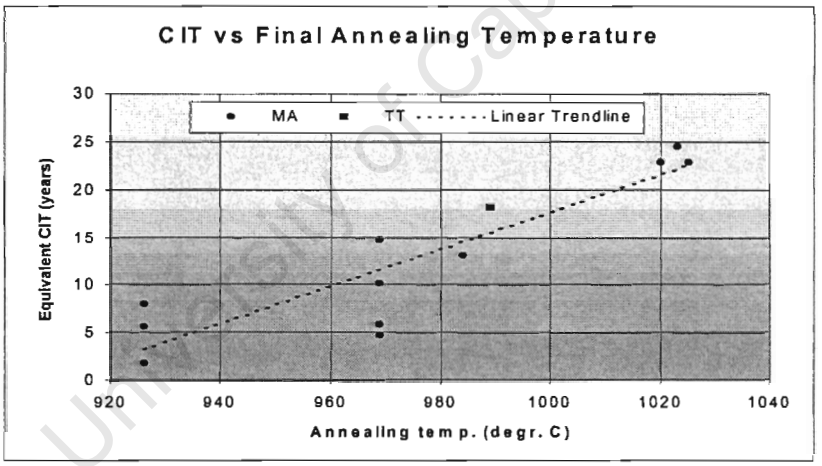

[*] When metals are forged, rolled or drawn, they work harden. After a deformation of perhaps 80% a limit is reached, beyond which the metal cracks or fractures. Further rolling or drawing is possible if the metal is annealed (heated to about 0.6 T_M)
T_M = melting temperature. During annealing, new, undeformed grains replace old deformed grains, and the working can continue for a further ~80%. [32]

- ***Carbon Content***: No correlation was found between total carbon content (C_{TOT}) and CIT. However, fairly good correlation has been obtained between carbon content and CIT if the difference between total carbon content and soluble carbon content is regarded i.e. ($C_{TOT} - C_{SOL}$). This represents the carbon content that could not have been dissolved. See Figure 9 below. EdF [26] has suggested that post manufacture heat treatment limits the risk of PWSCC especially when the level of carbon in the material is less than 0.035 %. This limit prevents excessive chromium depletion due to carbide precipitates during heat treatment. Excessive undissolved carbides can also inhibit grain growth during annealing [2].

Figure 9: Influence of Carbon Solubility [16]

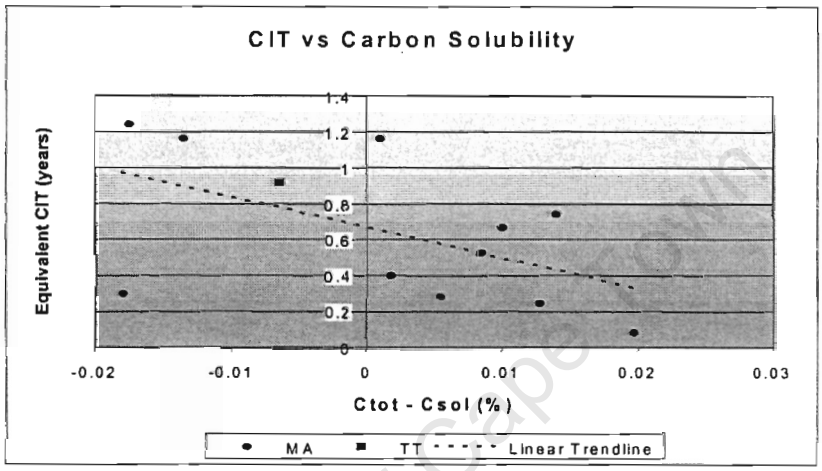

- ***Grain Boundary Carbides***: A linear relationship has been observed between the amount of grain boundary carbides and CIT (see Figure 10 below, NB. 0 = no carbides at all and 5 = grain boundaries are completely covered). Bruemmer *et al.* [27] has suggested that dislocation source activity at grain interfaces are critical in controlling IGSCC susceptibility. Effective sources such as grain boundary carbides promote crack blunting (because of their effectiveness as a dislocation source), decreasing the crack tip stress state, and thus increases resistance to cracking.

Figure 10: Influence of Grain Boundary Carbides [16]

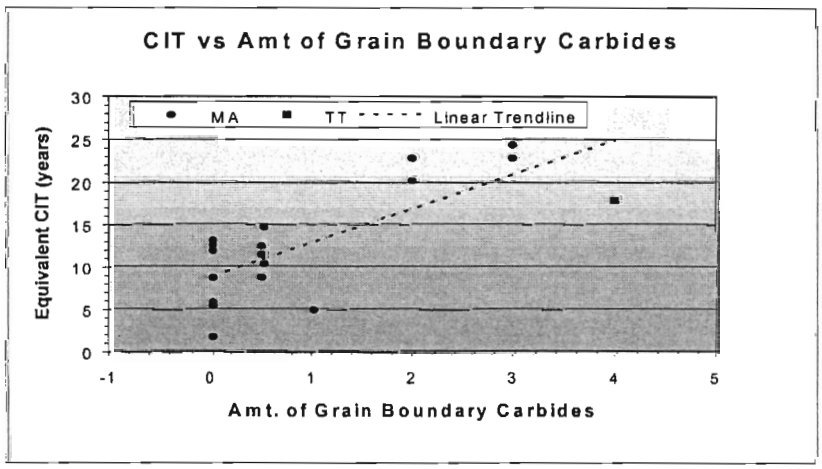

- ***Grain Size and Yield Stress***: Good correlation has been shown between these parameters and CIT, but it could not be concluded if this just reflects the influence of annealing temperature. Both parameters are strongly dependent on final annealing temperature. The laboratory results indicate that a larger grain size and lower yield strength reduce susceptibility to cracking.

A good example of the resistance due to larger grain size is Doel 1 and 2* [22]. Both units have the same design and are operated identically, but Doel 2 has had major SG tube problems whereas Doel 1 had virtually none [Doel 1 having significantly larger grain size (ASTM 9) than Doel 2 (ASTM 7)]. An inconsistency has been noted in the literature. References 27, 21, 30, 22 support the correlation between large grain size and SCC resistance, however Norring *et al.* [16] suggests the opposite. This discrepancy could be attributed to the small sample size used during these tests (10 MA and 1 TT specimen).

Tubing performance of Combustion Engineering designed SG tubing has been enhanced by employing a specification that aims at obtaining a yield strength of 310 MPa with an upper limit of 379 MPa [30]. This control prevents the use of a low temperature annealing and avoids the high yield strength and carbide free boundaries that contribute to primary side SCC susceptibility. A typical yield strength trend is shown in Figure 11 below.

Figure 11: Influence of Yield Strength [16]

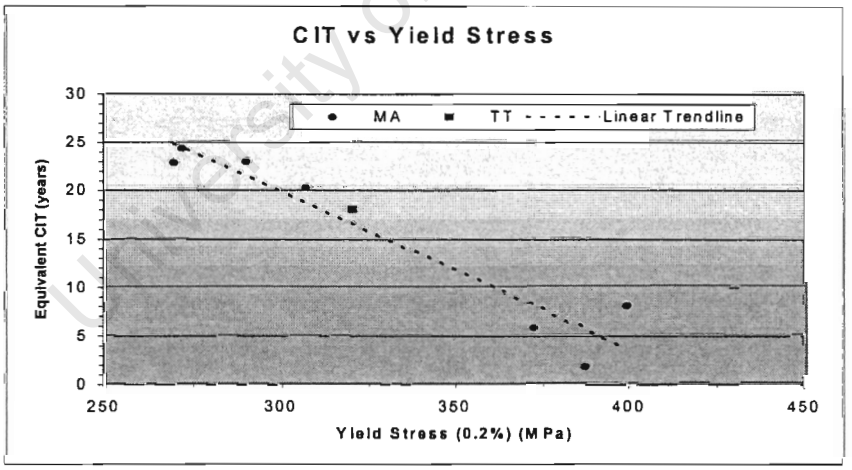

* Doel 1 and 2 are Belgium Pressurised Water Reactors (392 MWe), operational since 1975.

- ***Chromium Content***: Tsai *et al.* [28] have shown that chromium depletion due to carbide formation during heat treatment processes reduces the resistance of Inconel 600 to SCC. The chromium content should thus be sufficiently high to mitigate this effect. An EPRI study [33] has indicated that a thermal treatment (15h at 705 ^{0}C), following annealing (at 980 ^{0}C to 1010 ^{0}C), provides enough time for grain boundary chromium content to recover. The major benefit derived from a high chromium content is that the area immediately surrounding carbide particles retains enough chromium to resist sensitisation. Tsai *et al.* [28] have shown that there exists a critical chromium concentration, ranging from ~8 to 10 % (wt), above which corrosion does not take place.

- ***Nickel Content***: Sedriks *et al.* [29] have shown, using RUB specimens, that the resistance of Inconel 600 to SCC increases with increasing Nickel content. The reasons for this Nickel trend have however not been ascertained. It has been noted that increasing Nickel content is accompanied by a change in crack propagation path from transgranular to intergranular. Any model proposed for this trend should thus take this into account.

The results of these trends, obtained from literature, are summarised below:
The specifications for a "SCC resistant generation of Alloy 600 SG tubing", as recommended by Stein [31], are also included.

Table 4: SCC Resistant Metallurgical Parameters

Parameter		***Parameter value for SCC resistant tubes***	***Reference***
Metallurgical Parameters			
Anneal temperature (Final)		High (>950 ^{0}C)	16, 27, 21, 30
Carbon content	($C_{TOT} - C_{SOL}$)	Low	16, 19
	C_{TOT}	0.025 – 0.050 %	34, 31, 26
Chromium content		Above ~ 8 %	28
Nickel content		High (≥72.0 %)	29,31
Co content		0.015 % Max	31
Ti content		See Text below	
Si content		0.50 % Max	31
Mn content		1.0 % Max	31
Fe content		6.0 – 10.0 %	31
Cu content		0.50 % Max	31
Al content		See Text below	
Grain Size		*Small*	*16*
		Large	27, 21, 30
Grain boundary carbides		High	16, 19, 27, 21, 30, 2
Mechanical Properties			
Yield Stress (Room temp.)		Low (~310 to 379 MPa)	16, 30
Ultimate Tensile Strength		552 MPa Min.	31

It should be noted that these trends exhibit a high degree of scatter and are based on a small sample of laboratory specimens, however, the studies are all in agreement on the overall trends, except for the grain size discrepancy mentioned above. The scatter could be accounted for by variations in processing history. Bandy and van Rooyen [34] have suggested that the susceptibility of Inconel 600 cannot be judged on the basis of micro-structural analysis alone, since small variations in processing history also have a significant effect.

It is difficult to ascertain if resistance of a given alloy to SCC derives from resistance to initiation, propagation or both. This uncertainty is especially true for the resistance due to high Nickel content.

No data was available for the effects of aluminium and titanium content. However, the ASM handbook of Metallographic Techniques and Microstructures [35] indicates that the aluminium and titanium content and the aluminium/titanium ratio are very important for the performance of Nickel-base alloys. Increasing the aluminium/titanium ratio improves high temperature properties. Exact compositional values were not obtainable.

2.1.1.9 Inspection Method

Tubing degradation assessment is by means of eddy current non-destructive testing methods. A rotating pancake coil (RPC) is used to detect cracking in the RTZ. The inspections are either 100% (3330 tubes) or concentrated in the sludge zone (300 tubes). The sludge zone scope has been reduced to the reduced sludge zone since outage 110 and 208.

2.1.1.10 French Experience

No unplanned outages have occurred in French plants due to axial PWSCC since 1988, therefore the frequency of SGTR can be estimated to be less than *2.32E-3* (1/(36 plants x 12 years)). EdF have carried out a probabilistic study which indicates that the actual frequency of SGTR from axial PWSCC in the RTZ is less than 10^{-7} for up to four additional cycles assuming the current maintenance regime and plugging criteria are employed at each shutdown.
No unplanned outages have occurred in France since 1984 due to circumferential PWSCC in the expansion transition zone. Therefore the frequency of SGTR due to this form of degradation can be estimated as less than *1.74E-3* (1/(36 plants x 16 years)) [7].

2.1.2 U – Bend Cracking

This form of tube degradation constitutes the second most significant damage mechanism in French plants.

Cracking has been found to be intergranular and although no corrosive medium has been identified this form of cracking has been termed SCC. It is assumed that the same dependencies on metallurgical parameters as described for PWSCC are applicable.

Cracking occurs in the apex of the U-bend and the transition between the straight section and bent section. The defects on the Westinghouse tubes initiate from the inside of the bend and those on the Vallourec tubes initiate from the outside.
The tubes most susceptible to this form of degradation are the row 1 and 2 U-tubes (smallest bend radius) especially those without a pre-fabrication thermal treatment or a post fabrication stress relieving heat treatment. Koeberg applied U-bend heat treatments (UBHT) to both units during the fifth outage.

Because of the limited incidence of this type of cracking and the limited NDE data available, the crack initiation times and crack propagation rates are not well known, however some observations have been made. Cracks have been detected in Westinghouse manufactured row 1 tubes after 24,000 hrs and in row 2 tubes after 57,000 hours (no UBHT had been performed).The defects on these tubes have gone through wall inside 1 fuel cycle [22]. Vallourec tubing of the type Koeberg has, has been shown to be significantly less susceptible to this problem. Vallourec manufactured row 1 tubes have been shown to crack after 35,000 hrs without UBHT [15].

The EdF SG's with Westinghouse tubes have had all their first row (small radius) U-bends plugged preventatively because of potential leakage problems. The same practice has not been followed for the Koeberg SG's. Currently three tubes have been plugged preventatively at Koeberg due to U-bend indications (SG 99).

The causes of U-bend cracking are as follows:

- Corrosive environment / Material susceptibility
- High Stress levels due to: Primary Stresses
  Secondary Stresses
  Residual Stresses

Primary stresses are those due to the pressure gradient across the tube wall during operation (100 bar during normal operation and 170 bar during accident conditions – Feed water line break)

Le [36] has shown, analytically, that secondary stresses are significant and usually high due to severe operating conditions. The following secondary stresses have been identified:

- *Type 1*: Stresses due to temperature drop across the tube wall.
  $\sigma_{TYPE\ 1}$ = 60 MPa for a temperature drop of 30 ^{0}C.
- *Type 2*: Stresses due to axial movement of the two legs of a U-tube as a result of the temperature difference between the two legs.
  $\sigma_{TYPE\ 2}$ = 110 MPa for a U-tube having a bend radius of 6r (r = mean radius of tube cross section).
- *Type 3*: Stresses due to thermal expansion of the bend radius.
  $\sigma_{TYPE\ 3}$ = 5 MPa for Inconel 600 tubes with Stainless steel TSP's.

It has also been suggested that, due to the severe operating conditions, the overall stresses in the U-bend region of the small radius U-bends (with a bend radius of less than 6 times the tube diameter) may experience very high stress levels, because of secondary stresses, so that this may constitute the leading cause of short failure times of tubes by SCC.

Residual stresses are due to the cold bending of the U-tubes during manufacture. This is usually accompanied by significant ovality of the tube cross section. To prevent this, Koeberg heat treated the U-bends of rows 1 and 2, on both units during outages 105 and 205 respectively. The heat treatment employed was 2 to 6 minutes between 700 and 840^{0}C. It is difficult to assess the effect of UBHT due to the limited data available. Crombie [7] has thus suggested that the current scope and frequency of inspection for the row 1 and 2 U-bends be maintained until an adequate data base (Koeberg and world wide) can be built to develop further inspection policies.

Flaw detection is by means of U-bend rotating pancake coil (UBRPC). The results obtained from this method are extremely conservative in both flaw detection and sizing estimates. However, some plants have experienced leaking tubes in the U-bend region immediately after 100 % examinations of the inner two rows [7].

The frequency of SG tube rupture (SGTR) due to this form of degradation has been estimated at *3.9E-3* [7].

2.1.3 Secondary Side IGA and IGSCC

Intergranular attack and Intergranular Stress corrosion cracking (IGA/IGSCC) have been experienced within crevices between tubes and tube support plates and within crevices between tubes and tube sheets of SG's in PWR plants. This form of degradation also occurs in the region of the sludge pile (See Figure 6 above).

2.1.3.1 Crack Morphology

There are distinct differences between IGA and IGSCC. The corrosion morphology for IGSCC consists of single or multiple *major* cracks with minor to moderate amounts of branching. Experience suggests that IGSCC require stresses greater than 0.5 yield in order to propagate rapidly. At lower stress levels crack propagation rates may be very low, and the corrosion may take another intergranular form [37].
IGA may be described as general intergranular attack or volumetric intergranular attack. Its morphology is characterised by uniform attack on all grain boundaries over the surface of the tubing. In the purest case, stress does not contribute substantially to the morphology of IGA, which distinguishes this phenomenon from IGSCC. However, there is a close relationship between IGA and IGSCC, since major cracks (IGSCC) often initiates at regions weakened by IGA.

The general nature of this form of degradation is thus extensively intergranular with breakdown on planes perpendicular to the principal stress plane (for IGSCC). Outside diameter IGSCC is the dominant form of this degradation type [7].

2.1.3.2 The Influence of Metallurgical Parameters

Unlike PWSCC, no consistent dependence of IGSCC on microstructure has been established. It has also been shown that the metallurgical structure and the IGSCC susceptibility for mill-annealed samples varied from heat to heat with no apparent correlation [3].

2.1.3.3 Environmental Requirements

IGA of Alloy 600 MA occurs when either a strong alkaline or acidic condition exists together with free caustics and an oxidising environment [38].

It is difficult to establish the exact sources of these caustics (corrosive products) and oxidants. Some of the possibilities put forward are as follows [38]:

Caustics are thought to be generated from welding slag and fumes remaining in the secondary system during the construction phase and introduced into the SG during trial operations. The introduction of make-up water also contributes to these caustics.

Dissolved oxygen concentrations in the condensate was high during the initial stage of trial operation. It is thought that copper oxide and hematite* existed in the SG secondary side, which contributed to the *oxidants* present.

SG's with full depth crevices are especially susceptible to IGA/IGSCC [39]. The build-up of impurities in these tube sheet crevices over time can lead to a highly corrosive environment. The Koeberg SG's do not suffer from this problem since the tubes are expanded to the full depth of the tubesheet. The crevice is further reduced by the kiss roll transition (see Figure 3). The Koeberg SG's are however susceptible to IGA/IGSCC above the tubesheet (in the sludge zone) due to the accumulation of bulk water impurities, which concentrate in crevice regions and sludge. This is refered to as 'hideout' and this phenomenon occurs continuously during normal operation.

Silicon compounds have been found to occur abundantly in hideout returns and in the deposits of pulled tubes, however their effect on the behaviour of SG tube material has not been adequately studied. A recent study by Navas *et al.* [40] indicated an inhibiting effect of silicon compounds on the IGSCC of mill annealed Alloy 600. The inhibiting effect appeared to be related to the incorporation of silicon in the oxide layer.

* Hematite: A hard translucent mineral consisting mainly of ferric oxide

2.1.3.4 Temperature and Stress Contribution

The operating temperature and stress state also plays a significant role in the initiation and propagation of IGSCC. However, in comparison with the chemical driving forces, the stress appears to be a contributing factor rather than a dominant factor [41].

The stress intensity factor (K) at the crack tip and the environmental conditions are considered key parameters in IGA/IGSCC propagation behaviour. Kawamura and Hirano [42] have studied the effects of K at the crack tips on the IGA/IGSCC propagation behaviour of SG tubes. Their findings may be summarised as follows:

- K at the crack tips increased with increasing crack length. For a long crack, K decreased with an increasing number of cracks. However, for a short crack, K decreased only slightly with an increasing number of cracks.
- Double cantilever beam (DCB) test results showed IGA/IGSCC cracks did not propagate rapidly with K ranging from 0 $MPa\sqrt{m}$ to 60 $MPa\sqrt{m}$, which was considered typical of the IGA/SCC crack tips of typical SG tubes under PWR operating conditions. Also, the crack velocity decreased with decreasing temperature.
- In general the relationship between crack velocity and stress intensity could be divided into three regions (i.e. regions of stress dependent crack growth [Region 1], stress independent crack growth [Region 2], and rapid increase crack velocity with increasing stress [Region 3]). In region one the crack velocities were assumed to be controlled by the kinetics of a chemical reaction between the metal and the environment that filled the crack. In region two it was believed that the crack velocity was limited by the transport of hydroxyl ions to the crack tip. The resultant curves are typical for SCC [5]. See Figure 12 below:

Figure 12: Effect of K on Crack Velocity [42]

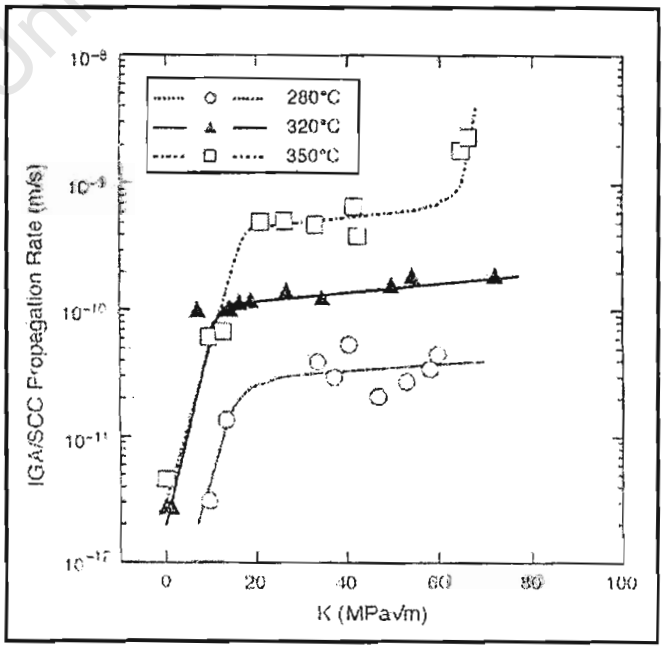

2.1.3.5 Preventative Measures

Various preventative measures are in use world wide. The main purpose being to improve the secondary side water chemistry to reduce impurities and to establish a reducing environment. These measures include the following:

- Na/Cl molar ratio control using ammonium chloride (NH_4Cl).
- Corrosion potential reduction by high hydrazine (H_2NNH_2) operation.
- Lab tests have demonstrated that boric acid (H_3BO_3) injection can inhibit the initiation and growth of IGA/IGSCC in MA Alloy 600 in caustic environments [39]. The mechanism by which this inhibition occurs has, however, not been determined. The use of boric acid in the SG secondary side has been qualified.
- Feedwater de-aeration to minimise oxidant levels.
- Full condensate polishing plant.
- The use of high integrity condensers with titanium tubing, thus limiting the risk of condenser in-leakage.
- The heat treatment of areas with high manufacturing residual stresses such as the small radius U-bends.
- Tube sheet crevice flushing (TSCF) operations help reduce IGA/IGSCC in deep sheet crevices [39]. This has been shown in laboratory tests and from operating experience. TSCF operations cause boiling to occur within the tube sheet crevice thus forcing concentrated (or dilute) liquids out. These operation are repeated several times depending on the available outage time.
- Titanium dioxide (TiO_2) has been identified as the cracking inhibitor that is most effective in caustic environments. It results in the formation of a protective nickel titanate ($NiTiO_2$) film on the tubing surface. This inhibitor has been applied at Kori-1 with positive results [41].
- Thermal treatment of the tube bundle during manufacture (typically 700 ^{0}C for 16 hrs) has significantly decreased the IGSCC susceptibility in caustic solutions [2, 3]. Koeberg's SG 77 was thermally treated at 700 ^{0}C for 12 hrs.
- SG's with Inconel 690 TT and Incoloy 800 (Siemens/KWU plants) tubing have shown significant resistance to IGA/IGSCC compared to Inconel 600 [38]. Their application, however, would imply expensive replacement of SG tubing or the entire SG.

2.1.3.6 Crack Initiation Time

The apparent incubation times, before IGA/IGSCC is observed non-destructively, are in excess of ~ 40,000 h, even in the worst case, but from that point the problem develops more rapidly than primary side cracking [18]. It is thought that these long incubation periods are linked to the fouling of crevices and development of the local environment conducive to IGA/IGSCC.

2.1.3.7 French Experience

No unplanned outage has occurred in France due to this degradation mechanism and therefore a conservative estimate of the frequency of SGTR is considered to be less than *2.0E-3* [7]. The frequency of SGTR for this degradation mechanism for Koeberg is considered to be even lower than this due to improved local thermo-hydraulic conditions of the model 51B, tubesheet lancing, strict control of secondary side chemistry and condenser leak tightness.

2.2 Other Tube Degradation Mechanisms

The following degradation mechanisms have not yet been detected on Koeberg SG's. They have, however been detected on many types of SG's throughout the world. These degradation mechanisms are of interest since it is thought that some of them may eventually manifest themselves as the Koeberg SG's age.

2.2.1 Vibration and Mechanical Problems

Mechanical problems due to flow induced vibrations were first identified in 1973, but have only become significant during the last decade.

This degradation mechanism has manifested itself as fretting/erosion. Fretting is a corrosion mechanism which generally occurs at the tube/tube-support structure intersections as a result of tube vibration. It is essentially a wear process, which could be better described as erosion, continually creating new surfaces which become available for electrochemical corrosion processes, thereby tending to accelerate degradation. Fretting has been noted to some degree in all major PWR steam generator designs, e.g. at the anti-vibration bars (AVB's) in the U-bend regions of Westinghouse and Combustion Engineering units, and at the support plates in Babcock and Wilcox once-through SG's [7]. The Koeberg type SG's are mainly susceptible to AVB wear and damage due to loose parts.

2.2.1.1 AVB wear

Fretting has been observed at the large radius U-bends/AVB interface of PWR SG's (See fig. 2 for the location of the AVB's). AVB wear could potentially affect up to 500 tubes, however few are in fact affected. Wear is created by the impact/fretting between the large radius U-bends and the AVB's.

AVB wear has been observed after 6 cycles of operation in 900 MW units of the Koeberg type. The average wear rate was observed to be 2% / year, with a maximum observed wear rate of 17% / year. The critical dimensions for the worn area are 74% of the wall thickness for accident conditions and 85% of the wall thickness for normal conditions [15].

The problem has been reduced by design and operating modifications. Some plants have replaced their AVB's with those of improved design (shape and clearances) and/or materials. Chromium plated Inconel 600 was used in the early mid 80's (the Koeberg AVB's are of this type) but stainless steel was used in later designs. However, these modern designs/materials have not mitigated this degradation mechanism.

This problem seems to be developing only very gradually. In addition, it has been shown that such wear cannot lead to real tube rupture given the small size of the defect. EdF has thus determined that no additional action appears to be necessary [26].

2.2.1.2 Loose Parts Damage

The presence of loose parts in the secondary side can cause severe damage due to flow induced fretting between the object and the tube. Loose parts originate as detached structural pieces or objects left behind during manufacture or maintenance. Thus, loose parts damage is most common shortly after commissioning of a new plant.

Most commonly, loose parts result in localised wear on peripheral tubes. It has been found that loose parts, which do penetrate to the centre of the tube bundle, have a low wear potential due to their small dimensions and limited flow excitation [15]. Because loose parts settle on top of the tube sheet, tubes are usually affected on the outside diameter of the RTZ.

Loose parts damage is not generally manufacturer/design specific, but is more often a consequence of human error; thus it cannot easily be "designed-out" and reduction in such incidents may be best achieved by attention to procedures, quality assurance, and cleanliness during maintenance.

A total of 12 tubes (9 in SG96 and 3 in SG99) have been plugged at Koeberg due to loose parts damage. The latest incident resulted in two plugged tubes during outage 107. However, the incidence of loose parts damage is expected to decrease significantly as the SG's age and cleanliness is maintained during outages.

This type of damage is random in nature and the effects, in terms of plugged tubes, is low in comparison with those for other types of degradation [7].

2.2.1.3 High Cycle Fatigue

The incorrect positioning of the AVB's and embedding of a tube at the upper tube support plate can significantly increase the risk of rupture of the tube at the level of this plate due to vibration fatigue over a large number of cycles. The presence of "aggravating factors" (denting etc.) affecting the integrity of the tube at the level of the upper tube support plate or bend, can also increase the risk of tube rupture.

The latest data indicates that two SG tube ruptures have occurred due to this reason, North Anna (USA) in 1987 and at Mihama (Japan) in 1991 [26].

2.2.2 Pitting

This degradation mechanism is characterised by small diameter tube-wall penetrations. Pitting is usually observed in regions where flow is restricted (thus, regions where aggressive chemicals can concentrate) such as the sludge pile region.

Pitting has been attributed to the ingress of condensate demineraliser fines and cooling water inleakage. Chloride ions, sulphate acids, copper, and oxygen have been identified as possible promoters of this degradation mechanism [7].
The result of these concentrated corrodents is local acidic conditions adjacent to tubes which can lead to the formation of local corrosion cells and pitting.

Examination of a typical SG pits [43] has revealed a laminar appearance, which is caused by the presence of metallic copper layers. In addition, the corrosion deposit was enriched in chromium and depleted in nickel and iron compared to the base metal.

The following thus causes pitting:
- Presence of chlorides
- Low pH
- Presence of oxidants such as cupric chloride ($CuCl_2$) or oxygen.

Pitting has not been observed in Koeberg's SG's.

2.2.3 Wastage/Tube Thinning

Initially phosphate was used to control the coolant pH of PWR SG's. However, it was soon observed that these phosphates caused secondary side corrosion damage in the form of wastage/tube thinning.

The mechanism of wastage/tube thinning or "phosphate thinning" is still not completely understood. Garnsey [44] proposed the following viable mechanism although it is only a qualitative approach. He bases his model on the sodium phosphate phase diagram, which indicates that, above 546 K (273 ^{0}C), solutions with an Na/PO_4 ratio of between about 2.8 and 2, when sufficiently concentrated, will precipitate an immiscible liquid phase. This phosphate-rich liquid phase, which is a molten sodium hydroxyphosphate, is extremely corrosive to both ferritic steels and high nickel alloys.

As a result of this degradation mechanism, most of those SG's that were initially operated with phosphate were converted to all-volatile treatment (AVT), utilising hydrazine or morpholine. Since Koeberg also employs AVT, phosphate thinning is not expected to affect the SG's.

2.2.4 Denting

The conversion from phosphate to AVT water treatment (including new units started with AVT) resulted in a decrease in tube wastage and pitting but introduced a new damage process, termed "denting", which is considered to be much more serious [45].

Denting is a circumferential inward movement, or dent, of SG tubing at support plates and at tube-sheet locations having open crevices. Distortion of the tubes is caused by the volume expansion of oxides that form when accelerated corrosion of carbon steel occurs in the drilled holes of support plates. The oxide volume expansion also distorts the support plates, which can have serious side effects, such as deformation and sometimes cracking of inner-radius tubing of U-bends.

Mild steel can be oxidised to magnetite (Fe_3O_4) in aqueous conditions at 570 to 670 K (297 to 397 ^{0}C) and the oxide growth is non-protective in the presence of ferrous, nickel (e.g. in the vicinity of Fe-Ni-Cr alloys), and chloride ions. The nickel is believed to act as an efficient cathode in an electrochemical metallic oxidation reaction under cathodic control.

Sample intersections of tubes and support plates removed from dented SG's have shown local chloride concentrations of over 4000 ppm in the dented region [37]. The high local chloride concentration is caused by local thermal-hydraulic conditions within the crevice between the tube and the tube support plate. The chloride source is generally condenser leakage, especially at plants cooled by seawater. This is not a problem at Koeberg since the titanium-tubed condenser effectively prevents condenser in-leakage.

The denting by itself has not threatened tube integrity, however, the increase in tensile stress in the tube wall can lead to PWSCC or IGSCC local to the dents. Cracking has been observed on both the inside and outside surfaces of the tubes in the region of the dents.

Three tubes were plugged at Koeberg due to manufacturing dents, which caused probe blockage, in Unit 1 during the pre-service inspection (two tubes in SG 96 and one tube in SG 95). Since then denting has not been observed at Koeberg. This may be attributed to the following:

- High AVT chemistry regime
- High pH (9.6)
- Titanium-tubed condenser (Minimise chloride in-leakage)
- The use of broached quatrefoil (improves fluid flow) martensitic stainless steel tube support plates, see Figure 13.

Figure 13: Broached Quatrefoil TSP

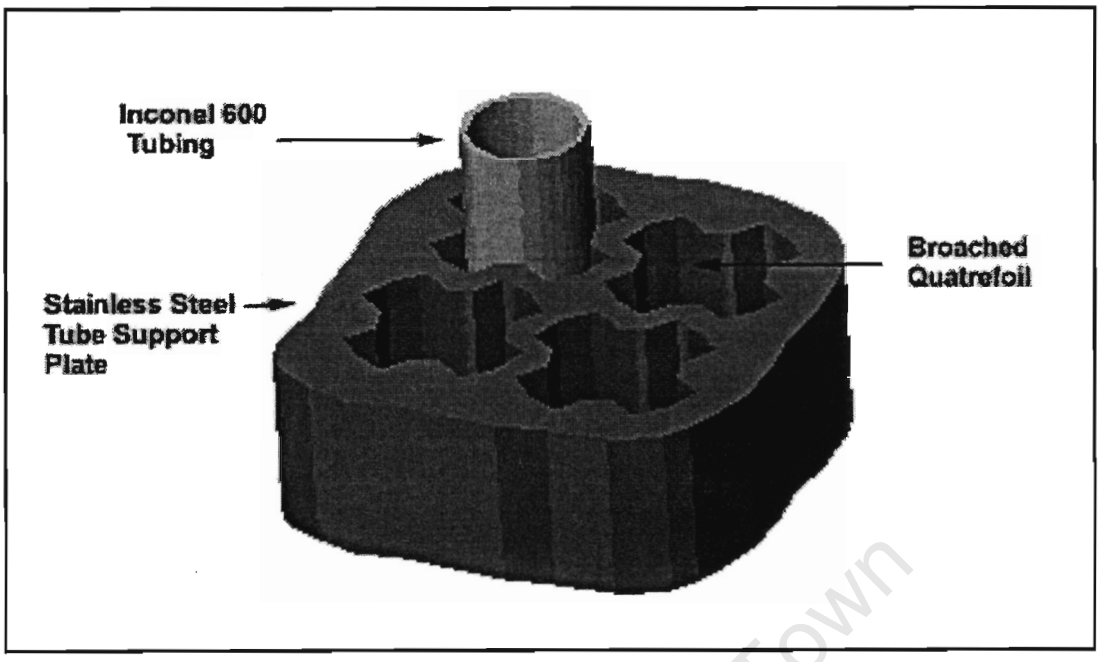

2.3 Environmental effects

The factors, which affect corrosion damage, are as follows:

- Hydraulic design
- Thermal design
- The presence of concentrators such as crevices or sludge
- The presence of impurities

In an operating unit, thermal and hydraulic designs and the presence of concentrating regions are not easily alterable. Thus, efforts to reduce the impact of the generic degradation mechanisms have concentrated on the primary and secondary side chemistries, since the presence of impurities and sludge concentrators are more easily controlled.

2.3.1 Primary Coolant Chemistry

The primary coolant chemistry is responsible for the following:

- To control the reactivity throughout the fuel cycle
- To control the level of radioactivity within the circuit.
- To minimise corrosion and the associated problems of corrosion products.

These requirements are achieved by the addition of the following chemicals:

Hydrogen
Radiation adversely affects the primary chemistry since water molecules dissociate under these conditions into hydrogen and oxygen. This leads to the corrosion of metal surfaces in the primary system. Corrosion in the primary circuit can be minimised by reducing the level of dissolved oxygen, maintaining an alkaline pH, and by removing impurities from the coolant. The dissociation of water is controlled by dosing the reactor coolant with 25-50 cc/kg of hydrogen in accordance with EPRI guidelines as indicated by Davies [46].

Boric Acid
Boric acid (H_3BO_3) is added for reactivity control. The concentration of boric acid is varied to control long term reactivity changes, such as fuel depletion and fission product build-up. The quantity of boric acid maintained in the reactor coolant is usually plant specific. In general it ranges from ca 2000 ppm boron or less at the start of a fuel cycle to ca 0 ppm boron at the end [1]. Boric acid can affect the pH, which can affect the corrosion rates in certain circumstances.

Lithium Hydroxide

Lithium hydroxide (LiOH) is used to control the coolant pH and acts as a crud* inhibitor. The pH is currently maintained at 7.25 at 295 ^{0}C in accordance with EdF practice as indicated by Davies [46]. Research [47] has indicated that PWSCC is dependent on LiOH and Boron concentrations in the primary circuit. A decrease in boron concentration (at constant LiOH concentration) results in an increase in PWSCC susceptibility. However, application of LiOH/B chemistry control is difficult due to the variability of plant to plant conditions. Currently, a limit of 2.2 ppm LiOH has been set by the fuel manufacturer used by Koeberg. This may change in the future due to recommendations by the fuel manufacturer to maintain pH above 6.9 with maximum LiOH concentrations of 3.5 ppm for limited periods of time [46]. However, the high lithium values, required for pH values between 6.9 and 7.4 at 300 ^{0}C, during the initial part of the fuel cycle, have the potential of accelerating the corrosion of Zircaloy fuel cladding and of increasing the susceptibility of mill-annealed Alloy 600 tubing to PWSCC [1].

In addition to the chemical additions, the following operational interventions are in place to limit radioactivity and to mitigate PWSCC:

RCV Cleanup

The primary side operates with continuous RCV (Chemical and Volume control system) cleanup at 15 tonnes/hr, with a maximum of 30 tonnes/hr. This is done to limit radioactivity in the primary circuit. It also reduces the quantity of aggressive contaminants, such as chloride ions, reaching the SG's [46].

ORT

Koeberg adopted operation at reduced temperature (ORT) in July 1994 (Unit 1) and December 1994 (Unit 2). Reducing the primary coolant temperature can mitigate PWSCC problems. Thus, ORT resulted in a 10 ^{0}C reduction in average reactor coolant outlet temperature without a significant decrease in unit output. The effect on PWSCC susceptibility has, however not been quantified.

Additional Primary system specifications (values given are for normal power operation) are given below in Table 5.

Table 5: PWR Primary System Specifications [1]

Parameter	*Normal Value[1]*	*Normal Value [Koeberg]*
O_2, ppb	< 5	< 5
H_2, ml/kg H_20 (at STP)	25 - 50	25 - 35
Cl, ppb	< 50	< 50
F, ppb	< 50	< 50
SO_4, ppb	< 50	< 50
Suspended solids, ppb	< 350	< 50
SiO_2, ppb	< 100	< 200

ppb = parts per billion

* Crud: Generic term for the corrosion products in the primary system that circulate with the flow and settle on other components in the primary side, such as the core. These are primarily Fe, Co, Mn, Ni, and Cu-based compounds produced by corrosion of the steel surfaces.

2.3.2 Secondary Side Chemistry

On the secondary side of the PWR, the objective is to ensure that corrosion rates are as low as possible, particularly of non-stainless materials in the feed train, as well as to minimise sludge transfer to heat transfer surfaces.

Koeberg has a carbon steel secondary circuit which suffers from flow assisted corrosion (FAC). This is an electro-chemical process, which is accelerated by fluid flow (the fluid dissolves the magnetite metal oxide layer faster than it is formed). This results in the presence of corrosive substances (the principle source) and the accumulation of sludge deposits in regions of low flow velocity. The following parameters influence FAC; Material composition, Component configuration, Fluid velocity, Turbulence, Steam quality, Oxygen, Temperature, and pH.

The following measures are in place to minimise FAC:

Ammonia Regime / Ethanolamine (ETA) Regime

The secondary side chemistry at Koeberg is characterised by a high AVT and high pH regime. The advantage of AVT is that it can protect both the feedwater and steam systems. The chemicals added (Hydrazine, Ammonia, and ETA) are volatile, which means that they are carried out of the SG in the steam flow rather than concentrating in the liquid phase and being removed by the SG blowdown system. As the chemicals are carried through the steam system, they are able to protect the whole of the secondary circuit including the turbines.

From the outset, AVT of the secondary circuit using ammonia was selected by EdF due to world-wide experience of phosphate tube wastage (the phosphate treatments were non volatile and gave rise to chemical reactions resulting in precipitation [26]). A feedwater pH of 9.5 was maintained until January 1989. After this date the pH was raised to 9.7 still using ammonia. Hydrazine (N_2H_4) is added to the condensate (70 – 100 ppb) to scavenge for oxygen and maintain a reducing environment. Hydrazine also breaks down to ammonia, thus assisting with pH control.

In 2000, Koeberg changed from ammonia treatment to Ethanolamine (ETA) treatment. This is to produce a more uniformly basic environment throughout the secondary system. ETA has a higher steam/water partition coefficient and as such, remains in the water phase to a greater extent than morpholine (alternative amine used on all EdF stations) and ammonia which are highly volatile. It is considered that implementation of ETA would reduce corrosion products to almost negligible levels and result in a significant reduction in the risk of tube rupture due to secondary side induced degradation. Additionally, significant cost savings could be achievable since the frequency of sludge lancing could be reduced. Since the implementation of ETA the amount of sludge deposited in the SGs has been steadily reducing to approximately half that of ammonium hydroxide. However since it is not possible to run on ETA conditioning with the ATE (Condensate polishing plant) plant in service, Koeberg must change back to ammonium hydroxide conditioning whenever there is a condenser tube leak. The changing of conditioning chemicals has an adverse effect, and results in more sludge being deposited in the SGs.

Condenser

The Koeberg condensers are cooled by seawater. These condensers are titanium-tubed to minimise inleakage and provide defence against faulted water chemistry conditions.

Condensate Polishing Plant (CPP)

Although the titanium-tubed condenser minimises the risk of inleakage, the water, on its journey through the rest of the cycle, can pick up metallic ions such as iron and copper from pipelines. Thus to maintain continual flow of high quality water a condensate polishing system is used. Condensate polishing is accomplished by passing the condensate through large demineralizing vessels that contain both cation and anion resins. The resins remove dissolved solids and act as filters for impurities and suspended solids.

Each unit has a full flow (3780 m^3/hr) deep bed CPP. These plants are comprised of five cations followed, through a common header, by five mixed beds.

Initially full flow condensate polishing resulted in high sodium concentrations, detected in the SG blowdown, during startup operations. This was a result of sodium slippage from the CPP. As an interim measure, partial flow condensate polishing was adopted to mitigate this problem. Subsequently, the regeneration of the mixed bed resins was optimised to a level where SG blowdown sodium can be maintained below 1.5 μg/kg even with full flow polishing. The Na cation conductivity* is regularly maintained at less than 0.12 μS/cm. Normal operation is considered to be within 6 μg/kg and 0.8 μS/cm [46].

Blowdown

This is another measure to control feedwater purity. Blowdown lines periodically remove a portion of the water, which is then cooled and treated for reuse. A common treatment uses cartridge filters to remove suspended solids, notably iron and copper oxides, through the use of filters and demineralizers. In PWR SG's the general practice is to use throwaway filter cartridges followed by demineriliziers.

Koeberg operates with relatively high continuous blowdown (~ 30 tonnes/hr) at the expense of power output to minimise sludge build up and impurities.

This loss in power output is proportional to the blowdown flow and is in the region of 7 MWe, at a blowdown flow of 50 tonnes/h. At Koeberg's 1999 cost of production of approximately R60/MW hour, this equates to about R3 700 000 per year. This loss has to be compared to the replacement costs of steam generators (which are currently about R500 million per unit) that would eventually be a consequence of poor steam generator chemistry.

It therefore follows that a balance between thermal losses and water chemistry conditions is necessary and the operators and chemists need to be aware of and work closely towards this.

* Conductivity is proportional to the ionic concentration of the solution i.e. the number of cations and anions present. Therefore, water purity is indicated by the ability/inability of a solution to conduct current. The unit μS/cm (micro Siemens/cm) is equivalent to μmho/cm where mho is the unit of conductance i.e 1/Resistance.

Wet and Dry Conservation

During plant shutdowns, special care is taken to minimise secondary side corrosion. General corrosion is caused if water and oxygen are present simultaneously in the system. Thus, two strategies have been adopted for lay-up of the secondary system, namely wet and dry conservation.

Wet conservation is the preferred option, however, it cannot be used for refuelling outages. If the outage is of short duration (less than 10 days, mid-cycle shutdown) then wet conservation is used. The SG is enclosed in a Nitrogen blanket to prevent oxygen ingress and normal feedwater is circulated. If the duration is greater than 10 days, and the SG can remain closed, then wet conservation can still be used, but the feedwater is dosed with hydrazine and ammonia. In addition, nitrogen is bubbled through the SG to maintain oxygen levels below 100 ppb.

Dry conservation is adopted for refuelling outages. The rate of general corrosion of non-alloyed steel in atmosphere is proportional to the relative humidity*. A low relative humidity is thus required to minimise general corrosion. The corrosion rate is negligible below 60 % and is nearly zero below 35 % [46]. At Koeberg, the SG's are drained as early as possible after they reach a temperature of 120 ^{0}C so that the residual heat can dry the SG. A compressed air system is connected to maintain a continuous air flow for the duration of the dry conservation. This ideal procedure is, however, not always practical since SG's are on the Outage critical path and maintenance and inspection operations interrupt the dry conservation.

Sludge Lancing

Sludge lancing of the top of the tubesheet is carried out whilst the SG's are still wet for each refuelling outage. However, there has been no significant reduction in sludge accumulation during the operational history of the SG's at Koeberg [46].

* Relative Humidity: The ratio of the Amount of moisture the air holds to the Maximum Amount of moisture the air can hold at the same temperature.

Additional secondary side system specifications (values correspond to normal power operation) are given below in Table 6.

Table 6: PWR Secondary Side Chemistry General Specifications [1]

Parameter	*Feedwater*		*Blowdown Water*	
	[1]	*KBG[c]*	*[1]*	*KBG[c]*
Components (ppb)[a]				
Hydrazine (N_2H_4)	< 100	70-100		
O_2	< 5	< 1		
Na			ca 2	< 2
Cl			ca 2	< 5
Fe (Total)	< 5	< 5		
Cu (Total)	< 1			
SO_4			ca 3	< 5
Cation Conductivity at 25 ^0C ($\mu S/cm$)				
Corrected[b]	≤ 0.2	< 0.1		< 0.15

[a] ppb = parts per billion

[b] Corrected for the presence of organics such as acetates and formates

[c] KBG (Koeberg) values listed are Target values

The following figure summarises the primary and secondary chemistry regimes in place at Koeberg.

Figure 14: Summary of the Koeberg Water Chemistry

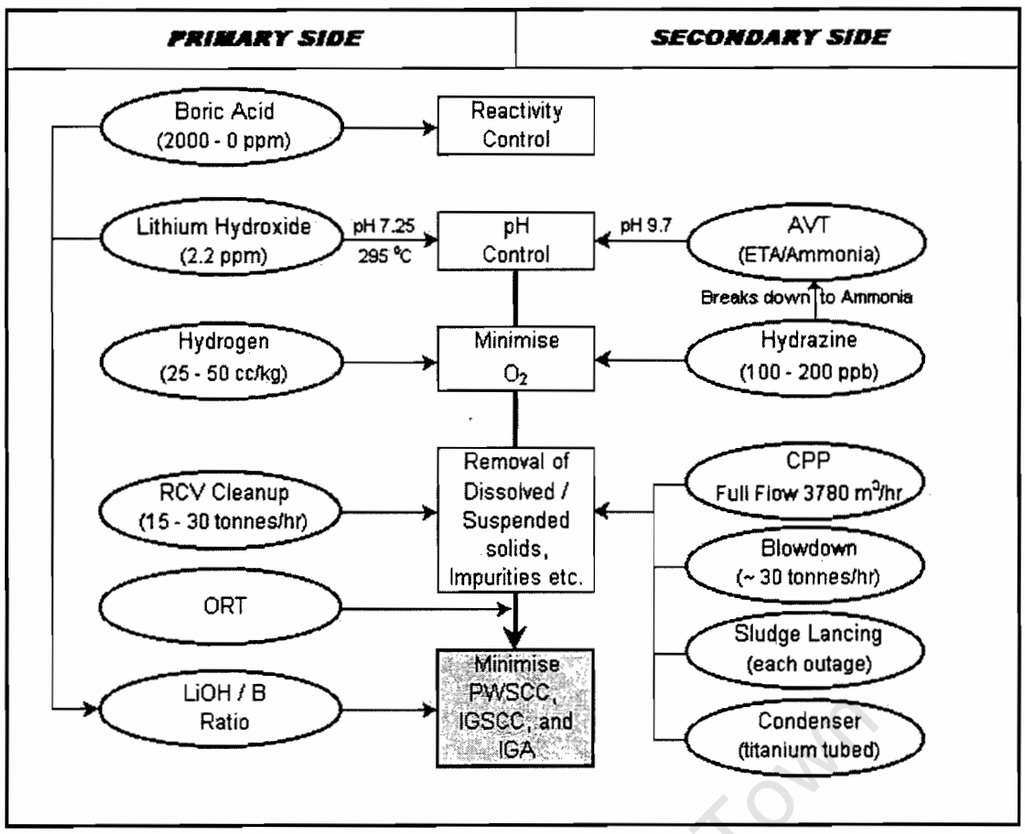

3 Tube Inspection Programme

The SG maintenance strategy has the following objectives:

- *SAFETY:* The prevention of an SGTR
- *AVAILABILITY:* The prevention of an unplanned outage due to large primary to secondary leaks exceeding operational technical specifications.

The overall in-service inspection (ISI) requirements for Koeberg are based on Section XI* of the ASME Boiler and Pressure vessel code (1980 edition). However, during preparation of the Koeberg In-service Inspection Programme (1981), it was realised that strict adherence to the ASME code requirements would not provide the best strategy to ensure safety and availability at Koeberg [22]. The code specified single frequency eddy current examination, limited plugging criteria and inspection sample selection criteria which were both difficult to use and did not take into account specific defect characteristics. As a result, in joint agreement with the CNS (SA licensing authority), Koeberg based the ISI requirements on the NRC Regulatory Guide 1.83 (1975). It was the joint position of the CNS and Eskom that defect specific acceptance criteria, inspection scope selection criteria, and corrective action criteria would be justified on a case-by-case basis.

The defect specific analysis approach consists of identifying and analysing the degradation mechanisms which could affect the SG tubing, and using this analysis to determine measures which have to be taken in order to keep the risk of tube failure at an acceptably low level. This approach requires continuous monitoring during operation and an extensive outage inspection programme during refuelling outages. The EdF specific analysis [26] is considered to be appropriate because of the similarity in construction and operating regimes of the SG's in France and at Koeberg. The specific non-destructive examination programme, leak monitoring regime, and corrective action criteria was established in Koeberg Safety Case 6.48 [48]. However, the analysis will remain under active review based on Koeberg, French, and world-wide experience.

3.1 Continuous Monitoring

The leak before risk of break principle (LBRB) has been accepted, in several countries, for certain types of defects affecting the safe and economic operation of PWR's, notably PWSCC of SG tubing. For a proven LBRB defect, initiation would be followed by a period of stable crack growth before complete tube rupture and the defect would manifest itself as a small but detectable leak. EdF consider that monitoring primary to secondary leaks during operation provides a good indication of tube degradation and is the best means of SGTR prevention [26]. Evolution of leak rates during a cycle may provide insight into the levels of inspection required at the next outage.

* ASME Boiler and Pressure Vessel Code. Section XI: Rules for Inservice Inspection of Nuclear Power Plant Components.

A Koeberg specific LBRB safety case [22] was established for PWSCC. This safety case was based on extensive theoretical and experimental work done in France. These tests have shown that the critical crack size corresponds to leak rates of over 100 litres/hour [25], however, to ensure that adequate safety margins are maintained a limit of 30 litres/hour/SG was set. The case thus justifies a plugging criteria based on crack length with observance of limiting primary to secondary leak rates. Even for defects where the LBRB concept has not been rigorously proven, EdF consider that rupture is, in most cases, preceded by a limited but rapidly growing primary to secondary leak which, if acted upon promptly, will allow plant shutdown prior to tube rupture [26].

The principle source of primary to secondary leaks at Koeberg is PWSCC in the RTZ. During normal operation, these leaks are typified by a gradual increase in leak rate (below 5 l/hr/SG) corresponding to defect growth. Plugging of tubes during outages is intended to limit the stabilised leak rate to 5 l/hr/SG (i.e. after the peak due to startup).

The leak rates vary not only according to defect growth but also according to the stages of the operational cycle. Start-ups are accompanied by initially high leak rates, followed by a slow decrease in leak rate before stabilisation after 20 to 30 days of operation. Certain transients can induce significant variations in leak rates, up to 20 l/hr/SG. Below a threshold of 150 ppm, the decreasing concentration of boron during the cycle leads to an increase in leak rate. This occurs at the end of a cycle and stabilises during stretch-out.

At Koeberg, the evaluation of changes in the primary to secondary tube leak rate is based on continuous monitoring of N_{16} (Nitrogen 16) and chemistry grab samples.

EdF consider this to be the best means of prevention of SGTR [26]

3.2 Outage Inspection

The inspection techniques generally used on SG tubing are internal eddy current inspection, visual inspection of the peripheral and sludge zone regions at the tubesheet level and leak testing using helium or water.

The outage inspection programme is implemented at a general level and at a defect specific level. The objective of the general inspection is to detect the appearance of possible tube degradation (in tubes considered sound). This is achieved by a sampled whole length tube inspection with the Bobbin Coil probe. At Koeberg a sampled 1 in 8 Bobbin Coil inspection was performed on all SG's during the first refuelling outage. Table 7 below summarises EdF's general inspection programme, based on the plant condition.

Table 7: Summary of EdF General SG Inspection Programme [49]

Condition of Plant (Proportion of tubes affected by defects)	*Eddy Current Inspection Programme*	*Leak Tests*	
		If Leak detected during operation	*If Leak not detected during operation*
< 5 %	On one SG each Year: 1 tube in 8	Hydraulic Test	
5 % to 10 %	On two SG's each Year: 1 tube in 8	Hydraulic Test plus Helium Test if small leak	
> 10 %	On two SG's each Year: 1 tube in 4	Hydraulic Test plus Helium Test	Helium Test

The defect specific programme follows the general programme if tube degradation is detected. The objectives of this programme are to monitor defect development and determine the extent and nature of the affected zone. The first refuelling outage at Koeberg was followed by an indexed sample on one SG at each subsequent refuelling outage. Tubes that have an increased risk of damage augment this sample. EdF has developed special inspection programmes for each of the following degradation mechanisms [26]:

- Expansion zone PWSCC
- U-bend PWSCC
- Tube support plate (TSP) PWSCC
- Expansion zone secondary side corrosion
- TSP secondary side corrosion
- AVB wear
- High cycle fatigue
- Secondary side wear – Loose parts
- Corrosion near flow distribution baffle
- Plug degradation.

Visual inspection of the peripheral tubes of each SG at each refuelling outage before and after sludge lancing was also specified.

To augment the defect specific analysis, full RPC inspections were performed during the fourth and fifth (ISI 105, 205, 106, and 206) refuelling outage on both units and the sixth (ISI 107) refuelling outage on Unit 1 on selected SG's to determine the full extent of the SCC problem.

Specific Eddy current techniques have been developed by EdF to detect and analyse the various degradation mechanisms.

3.2.1 Eddy Current Techniques

Eddy Current inspection is based on the principles of electromagnetic induction and is used to identify or differentiate among a wide variety of physical, structural, and metallurgical conditions in electrically conductive ferromagnetic and non-ferromagnetic metals and metal parts.

This method consists in studying the variations in impedance in two coils of an inspection probe placed near to a non-ferromagnetic conducting part (the SG tube). When a defect is encountered, the electrical balance of the device becomes modified. A defect signal is recognisable from its amplitude, its phase, and its form. The signal can be analysed in the form of a Lissajous curve on a cathode ray screen. Certain combinations of signals at different frequencies can reveal the characteristics of particular defects.

One of the rapidly increasing applications for this method is the inspection of thin-wall (0.9 to 1.5 mm) Inconel 600 SG tubing and heat exchanger tubing [50]. SG tubing has been extensively tested using these multifrequency techniques since 1977. The focus of SG tube inspection by eddy current has shifted from concentrating solely on the detection of and characterisation of tube wall denting and wastage to more complex tube wall degradation mechanisms. These complex degradation mechanisms include intergranular attack (IGA), stress-corrosion cracking (SCC), mechanical wear, and pitting. In response to the complexity of these newer problems, eddy current instrumentation has also evolved from a single-frequency to a multiple-frequency configuration. The analog instrumentation has been replaced by digital multiple-frequency instrumentation, offering more consistent data acquisition. The wider dynamic range offered by the digital instrumentation allows analysis of eddy current data obtained from traditionally difficult areas, such as dented tube support/tube sheet interfaces and roll transition/roll expansion areas within the tubesheet.

The following Eddy current probes are in use at Koeberg during refuelling outages:

3.2.1.1 Bobbin Coil (BC)

This is the basic method for monitoring of 900 MW and 1300 MW SG tubes. The BC is used to inspect the full length of the tubes because of its general detection capability and the speed of inspection. The following types of defects can be detected:

- Material loss due to wear (Loose parts or AVB wear)
- SCC in U-bends, TSP zone, and free span.
- SCC in expansion or expansion transition zones. (This has been replaced by the RPC)
- Expansion anomalies
- Dents and impacts, especially at the TSP zones
- Measure the height of the sludge above the tubesheet
- Measure the proximity of tubes to one another.

3.2.1.2 Rotating pancake coil (RPC) (STL)*

The RPC is used to detect and characterise tube end cracking. This is a pinpoint probe comprising 2 parallel coils on ferrite cores set at 45^0 to the tube generating line. The coil follows a helical movement allowing for inspection of part of the tube length. The characteristics of several cracks of a single tube can be detected. The detectable characteristics include; location in relation to the tubesheet, crack length, crack depth, and crack orientation (axial or circumferential). EdF have developed auto analysing software (ESTELLE), allowing for good levels of reliability of measurements and allows for faster analysis [26].

The uncertainty associated with this detection method is 2 mm or ± 1 mm† [46].

3.2.1.3 U – Bend Rotating pancake coil (URPC) (STS)

The U – Bend Rotating pancake coil (URPC) is used to inspect the small radius U – bends. The tube is inspected from the bend to 10mm below the upper TSP on the other side. The URPC consists of a head and coil assembly, a series of beads that comprise a flexible neck and a rigid probe body with a drive motor and an optical position encoder. The probe is based on an American design and the detection capability is claimed to be better than the Bobbin Coil probe [51, 26].

In addition to the necessity for inspecting with inside coils (BC, RPC, and URPC), all test probe positioning for tube selection and probe insertion/withdrawal functions must be performed remotely due to the radiation levels in the vicinity of the tube access areas.

3.2.2 Helium/Hydro Tests

Helium and Hydro leak testing are performed to check for leaking tubes, which may contribute to the overall SG leak rate. These tests are not mandatory, but are used to maintain the SG leak rates within the allowable specified leak rate limits.

Hydrotests are performed by pressurising the secondary side of the SG with a volume of water (as high as 45 bar) and checking for leaks from the tube ends (in the channel head). A fluorescent substance can be added to secondary side water to increase the sensitivity of this method of detection. The hydrotest is used to measure large leaks and it is generally accepted that this method will reveal a tube with a leak, during operation, of more than 20 l/hr [26]. For smaller leaks or when the overall leakage may be the result a large number of leaking tubes, this method is not always sufficient.

* The acronyms STL and STS are used by EdF

† Nureg/CR6365 recommends ± 1.5 mm or 3 mm RPC length uncertainty.

The Helium test is used to detect and measure, for each tube, the leakage rate of a mixture of 5% (sometimes 10%) helium and air, held at a pressure of 5 bar in the SG secondary side. An air current is sent from the cold channel (primary side) and a mass spectrometer is used to measure the concentration at the other end of the tube. For through wall cracks due to PWSCC at the tube ends, information obtained from the RPC is increasingly being taken into account to select important leaks.

3.2.3 Visual Inspection

Visual examination of the tube bundle periphery is performed on all SG's at each refuelling outage to check for loose parts and post plugging tube damage. Additionally, visual examination of the sludge zone is carried out on a less frequent basis.

A detailed listing of the inspections performed at each refuelling outage is given in Appendix A, Table A3 and A4.

3.3 Destructive tests

3.3.1 Examination of Pulled Tubes

Examination of pulled tubes have been practised widely for several years, more than 350 tubes had been examined in this way by 1997 [26].

The tubes are examined in the EdF Hot Cell Laboratory (SCMI) at Chinon. Examination generally involves carrying out one or several of the options below, as required:

- Leak test at 100 bar and 172 bar.
- Burst test.
- Radiological inspection of degraded areas
- Visual inspection of both the inside and outside diameter walls before and after opening and flattening of the tube.
- Dye-penetrant inspection of the tube material.
- Chemical analysis
- Noting of mechanical and geometric characteristics of the tube.

The process of pulling a tube and its subsequent expert examination constitutes a costly method of monitoring that must remain exceptional. Thus, no decision to pull must be taken without firmly founded justifications. It is not expected that Koeberg will have any tubes pulled, but will rely on experience gained from French analysis of pulled tubes.

4 Preventative Measures

4.1 At Koeberg

Numerous methods have been implemented internationally in an effort to minimise and even prevent tube degradation due to SCC. The following have been implemented at Koeberg.

4.1.1 Shot Peening RTZ

Shot peening to produce residual surface compressive stresses is a well-known approach for providing resistance to SCC [37]. This method has been investigated for use inside tubes in the RTZ [52, 53] and its benefits have been established. A general trend towards stabilisation of the number of indications has been observed [54]. It is suspected that peening will serve to prevent initiation of new cracks, but will not prevent growth of existing cracks through the wall thickness.

In this procedure, shot (metallic beads) is blown up the tube so that it impinges on a conical deflector located in the area to be peened. It is important that the compressive stresses developed on the tube inside diameter must be balanced by tensile stresses in the remaining wall thickness. Excessive peening could result in increased susceptibility to secondary side IGSCC.

The Koeberg SG's were shot peened in the RTZ on the hot leg during outages 102 and 201. Unit 2 has a much lower incidence of tube cracking. This can be attributed to the application of shot peening to unit 2 before Unit 1, and is a clear indication of the effectiveness of this method.

Only the hot leg side of the SG tubes were shot peened because the higher temperature (~ 314 ^{0}C) makes this side more susceptible to PWSCC. The cold leg temperature is approximately 279 ^{0}C. At this temperature and from predictions based on activation energy, initiation time, and temperature calculations, it is anticipated that cracking may occur on the cold leg side from approximately 60,000 hrs. For this reason it may become advisable to shot peen the cold leg side of the Koeberg SG's in the near future [15].

4.1.2 U-Bend Heat Treatment

World-wide experience has shown that PWSCC can occur in the U-bend regions of small radius (rows 1 and 2) Inconel 600 SG tubes [53, 51]. Cracking occurs primarily at the apex and near the tangents of the U-bends. This is due to the residual stresses caused by tube bending during manufacture of the tube bundle. To prevent the risk of rapid degradation of these regions, operators adopted an extensive plugging programme of small radius U-bends.

To mitigate this problem and prevent loss of heat transfer surface area, Koeberg heat-treated the U-bends of rows 1 and 2 on both Units during outages 105 and 205. The U-bend heat-treatment (UBHT) employed was 2 to 6 minutes between 700 and 840 ^{0}C [46].

The effectiveness and relative speed of in-situ UBHT has been demonstrated in laboratories and operating units [53, 51]. Vaccaro *et al.* [53] claims that UBHT in combination with shot peening of the roll transition zone (RTZ) will extend SG tube life beyond the design life. The effectiveness of induction heating methods for the stress relief of the RTZ has also been noted [52, 17]. The results show that the optimal temperature for stress relief heat treatment of this region is in the range of 700 to 750 ^{0}C.

A novel means of delivering in-situ heat treatment of welded or expanded tube ends has been proposed by Tait [55] and is currently under development at UCT. This method utilises a high intensity light bulb (1.0 to 1.5 kW) as the heat source. Light bulb heat treatment can attain 600 ^{0}C in 10 min. However, the effectiveness of this method in different situations, and its effect on the residual stresses in the surrounding tubes, still needs to be quantified.

4.1.3 Operation at Reduced Temperature (ORT)

During the commissioning of the Koeberg plant (1984-1985) EdF made Eskom aware of PWSCC in the tube-to-tube sheet expansion transition zone, in reference to French SG's. This type of tube degradation was first detected in the Koeberg SG's during the second outage in the central hot leg zones (two tubes in Unit 1 and six tubes in Unit 2, located in the sludge zone). Initial studies indicated that if this degradation type were allowed to propagate without intervention, the SG's would not last for their full, 40 year, design life.

One way to reduce tube degradations due to SCC is to operate the units with a reduced primary coolant temperature. The dependence of SCC on temperature has been well established [37, 20, 9, 21, 18]. This reduction in temperature results in both an increase in crack initiation time and a decrease in the crack growth rate. Several other plants, such as Ringhals 3 (Sweden) have implemented reduced primary coolant temperature with positive results [15].

Koeberg thus adopted operation at reduced temperature (ORT) in July 1994 (Unit 1) and in December 1994 (Unit 2). ORT is an operating regime whereby the temperature of the reactor coolant is reduced while the nominal power output is maintained by redefining the operating windows and changing set points.

The disadvantages associated with ORT is as follows:
- A reduction in electrical power output
- ORT is limited by the turbine operating characteristics (moisture carry over limits) and can lead to erosion-corrosion problems in the associated pipework.

The implementation of ORT at Koeberg resulted in a drop in average reactor coolant outlet temperature by ~ 10 ^{0} C. This resulted in an initial reduction in power of 0.9% for Unit 1 and 2.8% for Unit 2. The reduction in primary temperature on Unit 2 resulted in an increase of the moisture content of the steam to the turbine. A modification was performed on the steam drying equipment (upper internals) during the seventh outage to return the steam moisture content to specification (0.25%). A further modification to the Unit 2 governor system has allowed this unit to operate at 99.9% nominal power.

A study done by FRAMATOME (Doc. No. EE/G–DC–1612) suggested that the benefits of ORT for Koeberg (Unit 1 only) to be the following:

- SCC growth rates reduced by ~ 20%
- PWSCC at the top of the tube sheet would be avoided on SG 77 until 1,000,000 EFPH.
- Small radius U-bend cracking on SG 77 would be postponed until 50,000 EFPH
- U-bend cracking postponed from 32,000 to 38,000 EFPH for SG 96 and SG 95.

4.1.4 Secondary Side Water Chemistry Control

The control of the secondary-side water chemistry is achieved by the following measures:

- High AVT
- Titanium tubed Condenser
- Condensate Polishing plant (Full flow)
- Continuous Blowdown
- Sludge Lancing (at each refuelling outage)

These measures and their effect on SCC prevention have been discussed in section 2.3.2.

4.2 Additional Preventative Measures

Additional preventative measures, not implemented at Koeberg, are discussed below.

4.2.1 Nickel Plating

The nickel plating repairing technique was deemed sufficiently attractive by FRAMATOME and BELGATOM to launch important development programs on it.
Nickel is applied to the inside surface of the SG tube by electrochemical means. This nickel deposit fulfils three functions:

- *Bridges the through wall cracks* and stops primary water leakage into the secondary system,
- *Prevents the penetration of primary water in the crack tip region* and thus arrests PWSCC propagation,
- *Prevents contact between the primary water and the tube wall* and avoids initiation of new cracks.

An important part of the development work was to select an adequate plating procedure and to develop tooling for use inside the small diameter tubes. This was achieved successfully and the entire process requires a single tool (except for the initial brushing of the surface) inserted in the tube [56]. All the parameters of the process are continuously checked and monitored on charts during the operation.

This method has the following advantages:

- It is harmless to the tube because the residual stresses generated in the tube or the plating are very low and no subsequent heat treatment is required.
- It can be applied anywhere in the straight part of the tube and the RTZ.
- The tube retains its functional characteristics after plating with no significant decrease in heat transfer.
- No significant geometrical restriction occurs for inspection equipment or for any other maintenance equipment.
- The process is considered reversible. If necessary, the nickel deposit can be stripped chemically without damage to the tube.
- Nearly all the tubes of the SG can be reached by the plating device.

The one major drawback of nickel plating is that it does not impart structural strength to the tubes. Additionally, secondary side corrosion can damage the tubes to such an extent that tube rupture can become a possibility. The use of nickel plating is not recommended as a remedial measure, but rather as a preventative measure for tubes that have not yet cracked and as such, its effectiveness depends on how early it is implemented.

Another disadvantage of this method is that it invalidates the use of the eddy current rotating pancake coil (RPC), since the nickel layer constitutes a barrier to the small magnetic field created. Consequently, a new ultrasonic inspection technique has been developed [56]. This system uses a rotating mirror concept that focuses the ultrasonic beam in the tube wall to ensure the detection of either axial or circumferential PWSCC defects. The probe uses a high-resolution transducer with a focal spot of 0.5 mm. The qualification tests show that there is nearly no influence of the nickel layer on the ultrasonic signals and that the detectability for small width PWSCC is higher with the ultrasonic than with the eddy current technique.

Another issue which required extensive research was the validity of the leak before risk of break (LBRB) criteria for a nickel plated tube. Under the unlikely assumption that a crack would grow undetected under the plating, it had to be shown that the nickel ligament would rupture (allowing detection of a leak) before the crack length reached the critical length. Initial results have indicated that the nickel film does indeed rupture [56].

All the laboratory tests, as well as the operational experience on nickel plating at DOEL 2 and 3 (Belgium) since 1988, have demonstrated the adequacy of nickel plating as a repair method for tubes affected by PWSCC in the transition zone. The optimised procedure developed during these trials has allowed FRAMATOME to offer this repairing technique at an industrial scale. This method was however, developed too late for implementation at Koeberg since cracking had already occurred in the RTZ of several tubes by 1989 and the preventative intent would have been lost.

4.2.2 Chemical Cleaning

Chemical cleaning is used to remove the hard sludge, which accumulates on top of the tubesheet in the region of low flow velocity. Hard sludge is very difficult to remove by sludge lancing and this facilitates the concentration of aggressive chemical species in tube-tubesheet crevices. These chemical species cannot always be removed by boiling during an outage [15].

Chemical cleaning is the only method capable of cleaning these areas as well as the whole tube bundle. Its action can be of two types:

- *Preventative*, with a shorter treatment time but carried out periodically, in order to avoid the formation of hard sludge.
- *Corrective*, with a longer treatment time necessary for the removal of hard deposits present on the tubesheet, and the oxides filling the tube-tube support plate crevices.

The process was developed and patented by the Groupement des Laboratoires of EdF. Framatome has acquired the world-wide license. The EdF chemical cleaning process is applied in two phases and three stages:

Phase 1: Dissolution and disintegration of sludge using a chemical solution.

The solution is comprised of the following:

Gluconic acid	7.5% (approx.)
Citric acid	4% (approx.)
Multiserv corrosion inhibitor "P6"	0.8% (initially)
Ammonia to obtain a pH of	3.3
Process temperature	85 ^{0} C

- Stage 1: The solution dissolves the magnetite.
- Stage 2: An oxidant (air bubbling) is added and the pH is adjusted to 9.5 (by adding ammonia) to ensure dissolution of copper.

Phase 2: Finishing phase

- Stage 3: Remove residual Sulphur

  The inhibitor P6 contains sulphur. Although laboratory tests have not been able to show any harmful effect of these compounds, a complementary finishing phase is put into effect in order to remove this residual sulpur.

  The composition of the solution used is as follows:

Citric acid	0.4%

  pH adjusted to 3.3 by addition of monoethanolamine
  Inhibitor without sulphur
  Alcanization of this solution ensures surface passivation.

The sequencing (and possible use of several new solutions) and the duration of the treatment are chosen and adjusted in relation to the quantity of sludge to be dissolved and of its physical and chemical characteristics. The low aggressivity of the process permits long treatment times (up to 172 hours), sometimes necessary for virtually complete removal of hard or very thick sludge.

Operations carried out at Nogent 1 (1989) and Saint-Alban 2 (1990) by Framatome, Multiserv and Electricité de France [57] have demonstrated how chemical cleaning can be applied on an industrial scale and in a controlled manner. The process has been improved for further applications in more severe situations (i.e. SG quite heavily fouled up, with no prior cleaning). Even if this treatment does not stop the corrosion, it can cause it to slow down, delaying the time for SG replacement.

Chemical cleaning is currently under consideration for use on Koeberg's SG's. It is hoped that this process will reduce the possibility of IGA or IGSCC on the secondary side.

4.2.3 Primary Side Zinc Addition

Research has indicated that the addition of Zinc to the primary water of PWR SG's delays the initiation of PWSCC of Inconel 600 (Mill-annealed). However, the inhibitory effect of zinc addition and its mechanism has not been clarified. Research is still ongoing and as yet this preventative measure has not been implemented internationally.

Kawamura *et al* [58] have recently attempted to clarify the inhibitory effects of zinc on PWSCC susceptibility of Inconel 600 (Mill-annealed) in the as-received condition and after extended exposure to primary water at 360 ^{0} C, creating an oxide prefilm. It is well known that the stability of the oxide film formed on the material plays an important role in the initiation and growth of SCC. Therefore, it is very important to clarify the variation of the oxide film characteristics accompanying a modification of water chemistry.

The study found that a double layered oxide film was formed on Inconel 600 MA. The outer layer was composed of $NiFe_2O_4$, and the inner layer was composed of $NiCr_2O_4$. With the addition of zinc at approximately 10 ppb in PWR primary water, zinc was incorporated into the inner spinal structure, the outer inverse spinal oxide was diminished or thinned so that the oxide thickness was reduced.

It was concluded that zinc addition (> 10 ppb) into the simulated primary coolant suppressed the hydrogen reduction reaction on the surface of Inconel 600 MA and enhanced the formation of a stable oxide film composed of a zinc-chromium phase. It was suggested that these oxide film characteristics are the contributing factors to PWSCC resistance in Inconel 600 MA.

Some PWR utilities are planning to modify the primary water chemistry by zinc addition with the objective of reducing radiation field build up, SCC, and maintenance costs. Currently, Koeberg does not intend to implement primary side zinc addition [15].

4.2.4 Increased Boron concentration in secondary water

An increase in the boron concentration in the secondary side water has been shown to decrease the incidence of IGA. However, no estimate can be made of its effectiveness [37].

On-line addition of boric acid has been employed at several plants, however, this intervention is not being considered for Koeberg.

5 Remedial Measures

In operating nuclear power plants, failure of a SG tube may be regarded, not simply as an SGTR, but as a state of unacceptable risk. This limit is reached when crack lengths are in excess of the acceptable limits discussed previously. When this occurs, a tube may be removed from service by plugging, or repaired by sleeving or laser surface remelting.

5.1 Tube plugging

A tube that poses a safety risk may be removed from service by means of plugging. The plugs used (Inconel 600 or Inconel 690) are of various types:

- Welded to the tube
- Mechanical, expanded in the tube, without welding
- Removable: expanded in the tube, but to a lesser degree than mechanical plugs, allowing easy removal of the plug. See Figure 15 below

Figure 15: Removable Plug in the "inserted" position (Framatome)

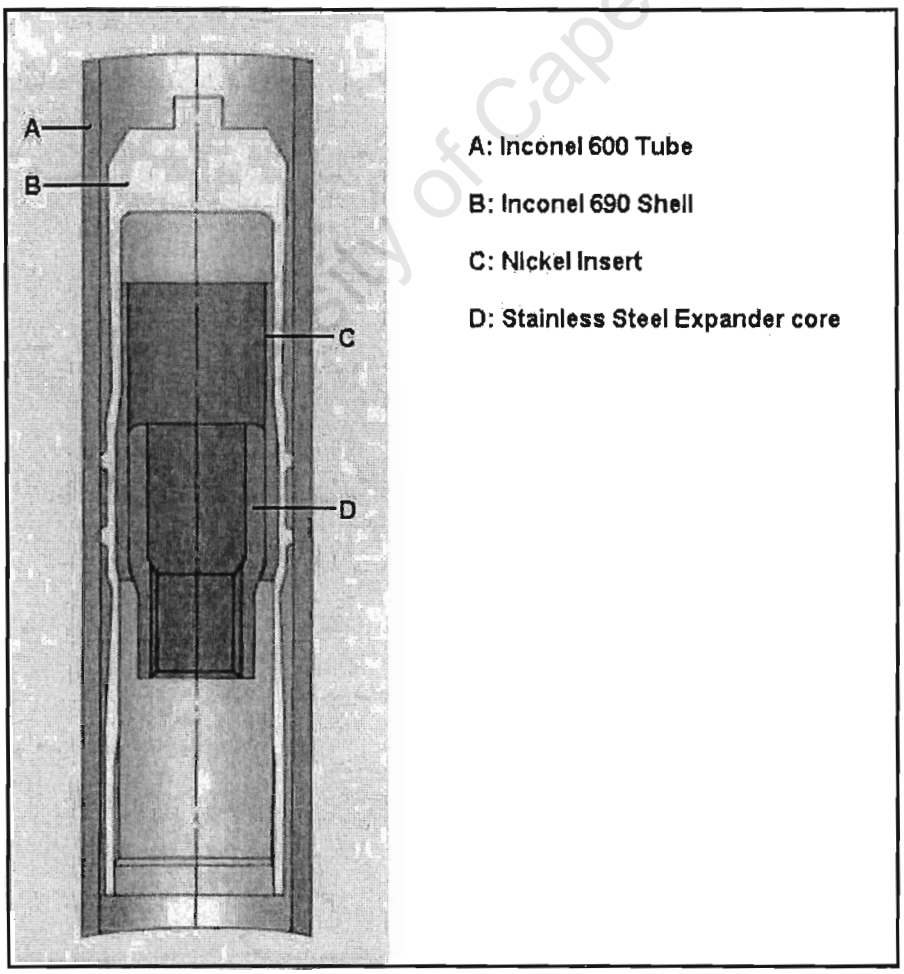

It should be noted that the technology has developed whereby even permanent plugs can be removed without extensive damage to the tube.

The plugs are inserted in both the hot and cold legs. They are seated flush with the lower end of the tube to minimise the effect of flow eddies. Initially, explosive plugs were used. In this process, the plug could be positioned in the tube to be plugged, and then explosion-welded in place instantaneously by a small amount of explosive contained in the hollow blind nipple. Problems have been experienced, however, with misfired plugs, and the eventual leaking of cold-worked plugs.

Further techniques were thus developed and currently a mechanical device is used. Plugging is achieved in two stages as follows:

- Positioning of a cylindrical plug in the mouth of the tube to be plugged,
- Drawing on a contained threaded member which expands the plug into the tube.

Removable plugs were developed to enable eventual removal, thus permitting the tube to be returned to service. The use of removable plugs means that when the plugging limit is reached, plugs can be removed and a proportion of the previously plugged tubes can be sleeved or repaired using some alternative corrective action. This increases the life of the SG with the possibility of the development of better repair procedures in the interim.

Framatome developed a removable plug with a shell made of heat-treated Inconel 690, an insert of nickel 201, and an expander core of cold drawn 316L austenitic stainless steel. Installation and removal are each performed in a single operation using the same tool.

The plugging criteria, as established by the Koeberg defect specific analysis [48] is summarised in Table 8 on the next page.

Table 8: Plugging Criteria

Category	*Plugging Criteria*
PWSCC within tubesheet	Circumferential Crack within 80 mm of the top of the tubesheet.
PWSCC in the RTZ*	➢ Axial Crack, FL ≥ 13 mm, Lower end within tubesheet or within 3 mm of the last point of contact of the tube with the tubesheet. ➢ Axial Crack, FL ≥ 10 mm, Lower end 3 mm or more above the last point of contact of the tube with the tubesheet. ➢ Axial Cracks, ≥12 cracks per tube. ➢ Circumferential Crack indication. ➢ Indication characteristic of a deformation due to oxide jacking above the tubesheet. ➢ Axial Cracks, FL ≤ 13 mm if plant availability is at risk due to large primary to secondary leak rates.
SCC in small radius U-bends	Indication characteristic of a defect within the U-bend region. (defect sizing and propagation data not available).
Wear by Loose parts on Secondary side	➢ Wall loss indication of 40 % or more of tube wall thickness. ➢ If there is contact or potential contact with a loose part that cannot be removed, even in the absence of measurable wear.
Wear due to contact with AVB's	Wall loss indication of 40 % or more of tube wall thickness.
Secondary side corrosion at the top of the tubesheet (hot leg)	➢ A 500 mV indication as characterised by the BC. ➢ An OD wall indication of amplitude > 200 mV as characterised by the RPC. ➢ An indication of external corrosion detected with the BC with an amplitude > 200 mV, together with an indication of an axial crack in the RTZ (measured with RPC) with a FL ≥ 10 mm when these two defects cannot be separated by more than 8 mm in height.
Other Modes of tube degradation	Based on specific Engineering evaluation performed to determine corrective action.

FL = Free Length (measured from last point of contact with the tubesheet)
RTZ = Roll Transition Zone

* Two axial cracks which are separated by a ligament less than 7 mm axially and 35 ^{0} circumferentially will be considered as a single crack for the application of plugging criteria.

Plugged tubes still require routine surveillance since plug cracking has been known to occur. After the rupture of an Inconel 600 mechanical plug in the USA, all of the plugs of that type, installed in the hot legs of 900 MWe SG's, were equipped with blanks (plug in plug, PIP) to limit the risk of plug rupture [26]. The nature of plug cracking in mechanical and welded plugs is as follows:

- *Mechanical Plug Cracking*:
  This damage mechanism is essentially PWSCC of the mechanical plug resulting in both axial and circumferential cracks of the plug shell, on both sides of the expanded zone. Axial cracks may lead to a pressurisation effect. Circumferential cracks may lead to the risk of plug expulsion into the tube due to the pressure differential and subsequent U-bend wall damage.

  The initiation time is estimated by EdF to be at least one cycle, therefore inspection of plugs should be carried out at every outage. The risk of this form of degradation at Koeberg has been reduced due to the use of Inconel 690 TT mechanical plugs. Additionally, the number of plugged tubes is extremely low at Koeberg (45 in total), therefore the risk of cracking is considered to be low [7].

- *Welded Plug Cracking*:
  As above, this degradation mechanism is PWSCC in the weld zone resulting in axial cracks, which may, in turn, lead to the pressurisation effect. The only case of this type of degradation detected in France had an initiation time of 11 cycles with a conical hollow welded plug design [7].

  Prior to operation, Koeberg had 13 tubes plugged preventatively with Inconel 600 welded plugs. During the seventh outage on Unit 1, a sample of these solid plugs was examined by dye-penetrant testing. No cracks were found. This established confidence that none of the welds contained any surface breaking cracks [59].

The pressurisation effect mentioned above, has also been called the 'diode effect' and the 'boiler effect' due to the circumstances which lead to the eventual tube failure.

- *Diode effect*: Refers to the crack allowing water to leak through in one direction but then restricts flow out in the reverse direction. The parameters governing this phenomenon are still not fully understood.
- *Boiler effect*: Refers to the increase in pressure of the trapped water (i.e. near constant volume) when it is heated, on start-up, from cold shutdown for example.

The actual damage to the plugged tube is caused by the cycling of water flow through defects in the plugs themselves. Water fills the tube during cold shutdown and expands the tube when heated on start-up. This plastically deforms the tube but without sufficient pressure to cause tube rupture. The plastic deformation increases the internal volume of the tube so that, during the next cold shutdown, more water can enter the tube through the cracked plug. The cycle is repeated until a sufficient volume of water is within the tube to cause tube rupture on expansion during start-up. It is estimated that tube rupture will take at least 1 to 3 cycles [7]

The extent of tube plugging is limited by operating requirements. Plugging results in a loss of heat exchanger surface area and a subsequent drop in pressure and thermal efficiency. The tube plugging limit at Koeberg is 5 % of the tube bundle (i.e. 167 tubes, 5 % of 3330). This ensures that the thermal efficiency of a SG is maintained within acceptable limits. The plugging limit of 5 % is conservative since the SG's are operated at reduced temperature (ORT) which also lowers thermal efficiency. The tube-plugging limit is between 5 to 10 % without ORT. The worst SG (in terms of number of tubes plugged) is SG 96 with 15 plugged tubes after 10 cycles (i.e. 0.45 % of the tube bundle).

Currently 45 tubes are plugged in all six SG's. Thirteen of the plugs were installed during manufacture or after the pre-service inspection, with the balance (32 tubes) being installed subsequently because of various degradation mechanisms.

5.2 Sleeving

Sleeving is the main alternative to tube plugging. Sleeving a tube involves the insertion of a tubular insert (mostly Inconel 690) into the damaged area and attaching the sleeve to sound material on either side of this area. The ends of the sleeves are expanded hydraulically or explosively and are in most cases sealed by rolling, welding or brazing. Sleeves are placed mainly in the region of the RTZ and at the levels of the TSP's where PWSCC and denting may occur.

Various methods have been developed, differing mainly with respect to the method of attachment, of the sleeve ends to the inner tube surface. These methods are as follows:

- Mechanical Sleeving
- TIG welded Sleeving (Framatome)
- Brazed Sleeves
- Kinetic (Explosive) Sleeves
- GTAW Sleeves
- Laser Welded Sleeves
- Elbowed* Sleeves.

EdF have experimented with the first two methods listed [26]. The mechanical sleeve fitting technique has been improved and is qualified; however, the TIG welded sleeving method is still under review. Laser welding (replacing TIG welding) is presently being adopted throughout the world. It gives excellent control of welding parameters and good reproducibility in implementation. In 1993, the laser welding process developed by Framatome was qualified [26].

* In order to allow for repair of tubes at the periphery of the bundle, this method consists in introducing an elbowed sleeve, which is straightened when it is introduced.

The major types of defects that can be repaired are:
- Internal and external corrosion
- Denting
- External tube wall wear.

This remedial method offers the following advantages:

- Reduced plugging rate with a consequent increase in service life of the SG's.
- The method is suitable for repairing most types of tube defects.
- The applicability of the LBRB principle (or in-service inspectability) is still considered valid by EdF [26].
- The consequences of a sleeve rupture are less than those of a tube rupture (anti-dislocation device) [26].
- The risk of sleeve corrosion is extremely low due to the use of 'mature' technologies, such as the use of Inconel 690 and stress-relief thermal treatment of welded ends.

The following disadvantages have been noted:

- The accessibility of the tube becomes limited i.e. it is not possible to install sleeves at successively higher TSP levels. This implies that tube life is limited to the time taken for corrosion damage, at the TSP level, to make the tube unserviceable.
- Slight pressure losses and heat transfer capacity losses occur as a result of sleeving. Studies have shown that 100 sleeved tubes are equivalent to 2 plugged tubes, although in practice, it has been found that 10 sleeved tubes are equivalent to 1 plugged tube [15].

Special precautions must be taken when sleeves are installed to prevent water from being trapped in the gap between the sleeve and the tube. Trapped water may result in a pressurisation effect, which occurs on start up, and can lead to tube deformation or tube rupture. In addition, the accumulation of contaminants in the gap must be avoided to prevent IGA and IGSCC.

Several thousands of sleeved tubes are in service throughout the world. These sleeves have been inserted using a variety of assembly techniques. Sleeving has been in limited use in France.

Sleeving is viewed by Koeberg as the most suitable remedial method for PWSCC tube damage in the RTZ [15]. No tubes have been sleeved at Koeberg to date due to the cost of installation (French crew required). However, it is envisaged that the use of removable plugs will allow a program of sleeving to be implemented once the plugging limit has been reached.

5.3 Laser Surface Melting / Laser Remelting

Both tube plugging and sleeving result in loss of heat transfer capacity and subsequent operational penalties. In addition, these remedial measures are limited by accessibility problems. These problems can be overcome by tube surface modification using a laser beam, which can easily reach failed parts of a tube through a beam transmission system, such as an optical fibre, to repair them. This technique has been under development by Westinghouse since 1988 and was first tested at Duquesne Light Co's, Beaver Valley – 1 in April 1993. This repair technique is the first in-situ SG repair technique that does not employ other materials such as weld overlay.

The laser surface melting (LSM) technique is essentially a preventative measure. A laser is used to melt the surface layer of the SG tubing. This effectively prevents SCC by introducing a thin barrier layer between the corrosive medium and the susceptible microstructure. Tests have shown that cracks arrest in the zone which has been laser melted.

Lim *et al.* [60] investigated the effects of sensitization* treatment on microstructural evolutions in laser surface melted Inconel 600 samples using equipment such as scanning electron microscopy (SEM) and transmission electron microscopy/energy-dispersive X-ray (TEM/EDX). A comparison was made between sensitized samples of solution annealed Inconel 600 (SA + sensitization) and those subjected to LSM (LSM + sensitization). It was found that carbon solubility was enhanced in the LSM + sensitization specimens thus minimising the carbon available at grain boundaries for chromium depletion. The minimum chromium concentration in the SA + sensitization sample was measured to be 7 wt % whereas a minimum of 12 wt % was measured in the LSM sample

The laser remelting technique is an in-situ repair/remedial measure. This is a remote technique, which uses pinpoint lasers to apply heat directly to cracks, melting and resolidifying the metal. Cracks are repaired from inside the tube and this technique can achieve up to 80 % through wall penetration. It is anticipated that 100 % through wall penetration will be achieved in the near future.

* Sensitization: In austenitic stainless steels, the precipitation of chromium carbides, usually at grain boundaries, on exposure to temperatures of about 550 to 850 ^{0} C (in this case 600 ^{0} C for 24 h – one of the most susceptible heat treatment conditions to IGA/IGSCC in this alloy), leaving the grain boundaries depleted of chromium and therefore susceptible to preferential attack by a corroding (oxidizing) medium [37].

6 Predictive Methods

Various methods have been developed to predict SG service life and to verify the safe operation of existing units with susceptible SG's. These methods are mainly of the deterministic type e.g. Arrhenius plots, finite element analysis, and the leak before risk of break principle (LBRB). Recent developments in probabilistic methods (particularly simulation based probabilistic fracture mechanics methods) have not only allowed for improved predictive capabilities but also allowed optimisation of plugging limits and inspections scopes. In the last few years, the need for rationally based tube-plugging criteria and aids for planning and decision making on remedial measures, including SG replacement, has become increasingly apparent. This need has made the probabilistic approach increasingly attractive.

The initial focus, after the first in-service cracks were confirmed in 1971, was to demonstrate the safety of the existing SG fleet. Failing which would have been disastrous to the industry (the EdF fleet alone has 170 SG's in operation equipped with tube bundles made of Inconel 600 or 690). EdF made the LBRB concept a key element of its safety policy and the resulting surveillance philosophy [61]. A vast study program was therefore developed in the 1980's, covering both break criteria and behaviour under leak conditions. These studies, which focussed on the main degradation phenomena (cracks in the RTZ), were based on theoretical models supported by numerous tests on models. Further analysis and tests on pulled tubes have been used to validate the assumptions of these theoretical studies. Since the late 1980's the focus has shifted to developing optimal plugging criteria and inspection scopes based on probabilistic methods.

It is perhaps important, at this point, to note the difference between deterministic and probabilistic methods. Deterministic Engineering seeks to answer a question with a single number, assumed to occur with certainty, while probabilistic methods provide a range of likely answers, plus a statement on the probability of a given result.

6.1 Deterministic Methods

The two important deterministic studies of relevance to Koeberg is that by Stein *et al.* [9, 20, 31, 62], and EdF/Framatome [25, 61]. These two studies establish the sensitivity of Inconel 600 SCC to temperature and the Leak-before-break principle respectively.

6.1.1 Arrhenius Plot

It is well established that failure (SCC initiation) of Inconel 600 tubing is a thermally activated process and follows an Arrhenius relationship (see section 2.1.1 above for introductory remarks concerning this relationship). The Arrhenius plot can be used to predict the minimum service life of Inconel 600 tubing in primary water.

A typical Arrhenius plot (also referred to as the Minimum Survival Curve) is shown below.

Figure 16: Minimum Survival Curve from Stein *et al.* [9]

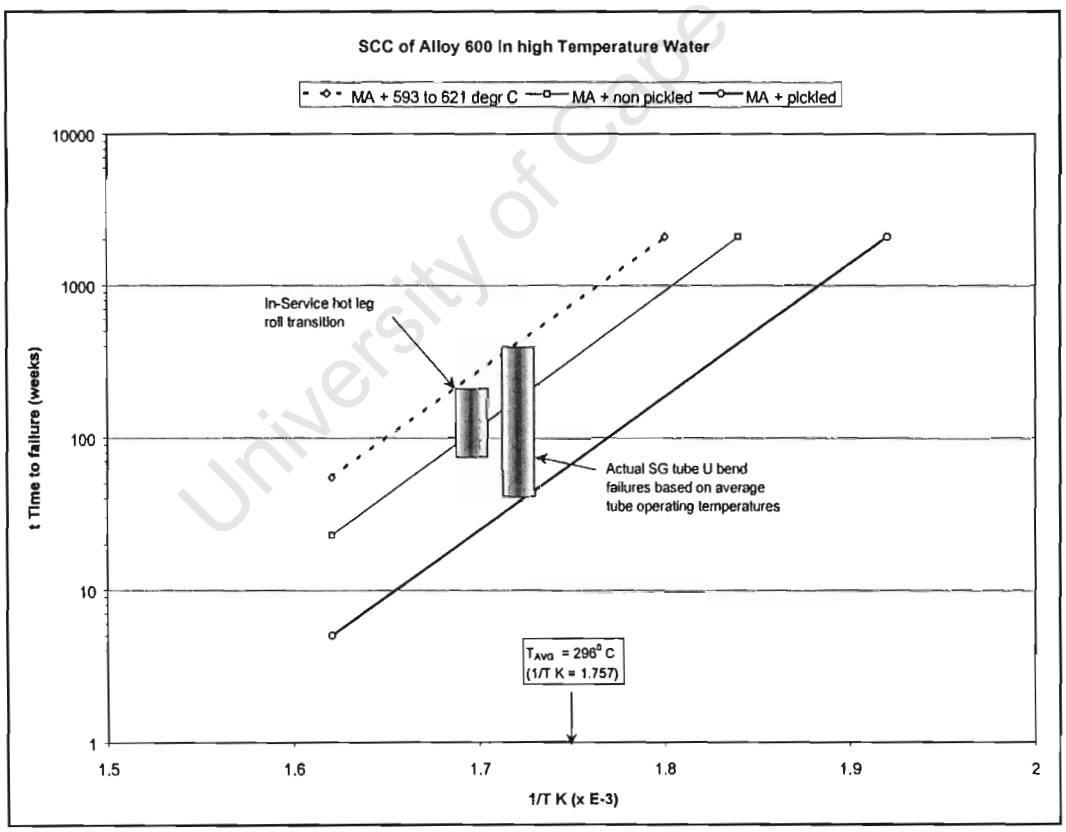

The slope of the lines is an indication of the Activation* energy (~ 40 kcal/mol-K). The activation energies observed from these results are close to the activation energy for bulk diffusion of Carbon in Nickel based alloys. The activation energy is a constant for SCC of Inconel 600 in primary water and therefore parallel lines may be drawn through the most conservative data for other material conditions plotted.

* The process of Activation is the changing of a passive surface of a metal to chemically active state.

The following conclusions may be drawn from these studies:

- The plot indicates that Inconel 600 SCC is strongly temperature dependent (Justification for Operation at reduced temperature, ORT)
- The plot indicates that heat treatments at 593 to 621 ^{0} C or 705 ^{0} C improve the SCC performance over that of the Mill-annealed conditions by at least a factor of 2.5.
- The Mill-annealed conditions are extremely important in defining the carbide precipitation characteristics and resultant SCC performance in primary water.
- By judicious choice of material processing a material can be produced that can survive the 40 year design life. (see Table 4: SCC Resistant Metallurgical Parameters required)

6.1.2 Flaw Analysis and the Leak-Before-Break Principle

Since 1981, EdF and Framatome have done considerable work to define failure criteria, critical crack lengths and ultimately establish the validity of the Leak-Before-Break principle. This was an important process to justify continued operation with susceptible SG's.

6.1.2.1 SG Tube Rupture Failure Criteria

More than 1000 burst tests on Inconel 600 tubing were performed in various test configurations. The tests have shown that the instability limit pressure can be accurately estimated using Plastic Instability Criteria (i.e. applied stress, amplified by bulging, is compared to a flow stress limit). The results have also shown that tube rupture occurs after extensive strain, as a consequence of the high ductility and toughness of the tubes.

It was also experimentally confirmed that the instability limit pressure of a tube with a crack located in the roll transition zone at the top of the tubesheet is higher than that of a tube with the same type of defect located in a straight section remote from discontinuities. The gain in critical pressure is due to two combined effects: local mechanical strengthening due to seating in the tube sheet, which limits tube bulging, and an increase in the flow stress due to strain hardening of the material in the roll transition zone during the rolling operation.

6.1.2.2 Critical Crack Sizes

Hutin and Billon [25] used failure criteria similar to the CEGB R6 approach and a finite element model to determine the critical crack sizes for the worst case transient. The most severe transient was determined to be a feedwater line break accident since this results in rapid depressurisation of the secondary side. The results obtained are as follows:

Table 9: Critical Crack Sizes

	Axial Cracks	Circumferential Cracks
Free Span	2a = 16 mm	$2\alpha = 180^0$
Roll Transition Zone	2a = 16.5 mm	$2\alpha = 180^0$

It should be noted that these are lower bounds of a_{CRIT} due to conservatism's, especially of material properties. Koeberg has established a plugging limit of 13 mm for axial cracks and immediate plugging if any circumferential crack indications are detected.

These results, in conjunction with a leak rate model, have led to the conclusion that tube rupture due to SCC should be preceded by significant primary to secondary leakage. This would allow the reactor to be shut down before failure (tube rupture) occurs.

6.2 Probabilistic Methods

The deterministic approach to structural mechanics typically employs conservative estimates of the influencing parameters and the use of a "safety factor" to account for uncertainties inherent in these parameters. This is how probabilistic considerations are admitted "via the back door" [63].

To illustrate this point consider Figure 1 below. This figure shows the probability density functions of the Failure Parameter (or Load Parameter)* (L) and the Resistance Parameter (R), including their interference (overlap). Typical examples of load and resistance parameters are listed in the figure. It should be noted that the area of overlap is not equal to the failure probability. However, the area is qualitatively proportional to the failure probability as long as the mean value of load is less than the mean value of resistance.

The conservatism associated with the deterministic approach is also clearly shown. Load Parameter calculations are typically based on conservative assumptions and result in load values well above the mean (indicated by S_L). Safety factors are usually applied to the resistance parameter to account for uncertainties and may result in resistance values well below the mean (indicated by S_R). The typical deterministic analysis thus ensures that the Load Parameter (S_L) is less than the Resistance Parameter (S_R), given these conservative considerations.

Figure 17: Load Parameter-Resistance Curves

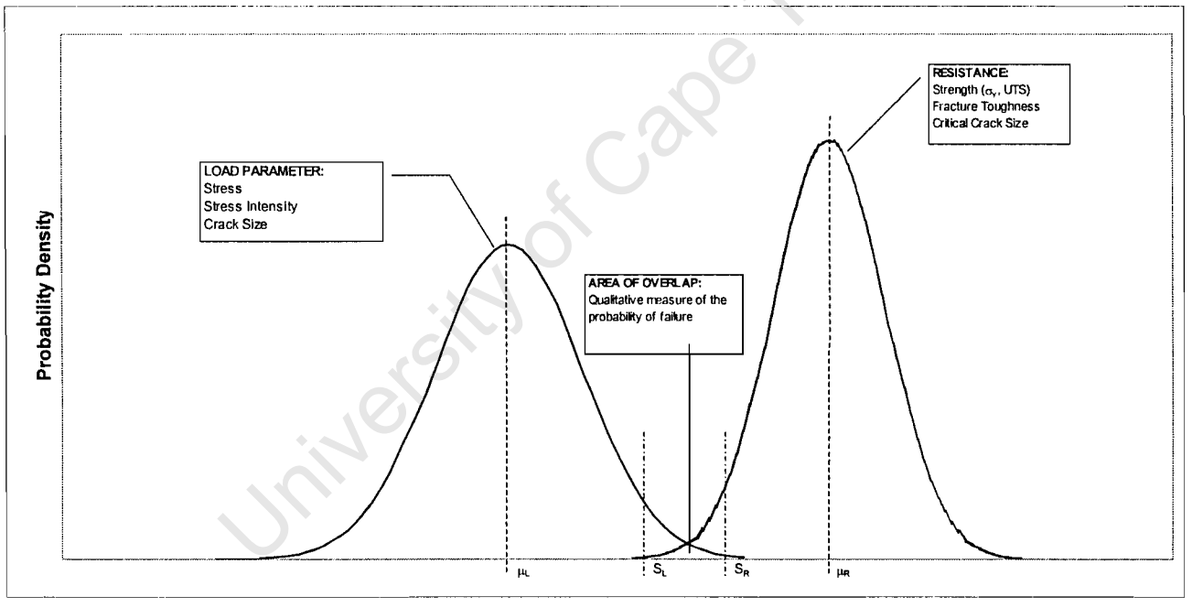

* For convenience, in the subsequent discussion the Failure Parameter, which typically includes crack size, effective applied stress, stress intensity factor, etc, will be referred to as the "Load Parameter". The use of this term is thus not restricted to applied force only, but to any of the above variables.

A better way to deal with uncertainty is by means of probabilistic structural mechanics methods. This is particularly pertinent in the case of fatigue and fracture mechanics analysis since the parameters involved exhibit relatively large degrees of random scatter.

The following section serves as an introduction to the field of probabilistic structural mechanics, which is the basis for the development of a probabilistic fracture mechanics model for the tubing degradation of the Koeberg SG's.

6.2.1 Probabilistic Structural Mechanics

Probabilistic Structural Mechanics (PSM) is an evolving and expanding field within structural mechanics. This subject has been comprehensively reviewed by Sundararajan [64]. The past four decades have seen significant advances in this field and still considerable research and development activities are in progress. The recent advances in computing power, in particularly, has led to an increasing interest in simulation based reliability methods and the subsequent ability to analyse more complex situations.

The basic concept of the classical theory of structural reliability and risk based design starts with the definition of the *performance function*. The first step towards evaluating the reliability of a structure is to decide on the relevant load and resistance parameters called the basic variables X_i, and the functional relationship among them. Mathematically this relationship can be described as:

$$Z = \text{Resistance} - \text{Load Parameter} = g(X_1, X_2, \ldots, X_n) \qquad \textbf{Equation 3}$$

The failure surface can then be defined as $Z = 0$. This is the boundary between the safe and unsafe regions in the design parameter space. The limit state function (performance function) plays an important role in the development of structural reliability analysis methods. These methods were developed corresponding to limit state functions of different types and complexity.

The probability of failure is thus given by:

$$p_{TR} = p\left[g(X_1, X_2, \ldots, X_n) < 0\right] \qquad \textbf{Equation 4}$$

A mathematical expression for the failure probability is:

$$p_{TR} = \int \dots \int f_X(x_1, x_2, \dots, x_n)\, dx_1 dx_2 \dots dx_n \qquad \textbf{Equation 5}$$

in which $f_X(x_1, x_2, \dots, x_n)$ is the joint probability density function for $X_1, X_2, \dots, X_n$ and the integration is performed over the region in which $g(X_1, X_2, \dots, X_n) < 0$. If the random variables are statistically independent*, then the joint density function may be replaced by the product of the individual density functions in the integral.

The computation of p_{TR} by the above equation is called the *full distributional approach* and can be considered to be the fundamental equation of structural reliability analysis. In general, the joint probability density function of random variables is practically impossible to obtain. Even if this function were available, the evaluation of the multiple integral would be extremely complicated.

Various methods have been developed to solve equation 5. Stress-Strength Interference methods are useful for simple applications only, where the defining probability density functions are relatively simple. First and Second Order reliability Methods (FORM and SORM) use analytical approximations of the integral that are simpler to compute and allow more complex applications to be analysed. Simulation based reliability methods have gained popularity due to the complex applications that can be analysed and the relative power of modern computers. Monte Carlo Simulations (key tool for simulation based reliability methods) are versatile and can solve virtually any probabilistic structural mechanics problem that has an underlying deterministic solution.

The Monte Carlo Simulation technique was developed during the Manhattan Project of World War II (in the development of the atomic bomb) for simulating complex physical processes, and in particular, for modelling neutron transport in atomic bomb design. Its name comes from its resemblance to gambling. This analogy to games of chance is a good one, but the "game" is a physical system and the outcome of the game is not a pot of money or a stack of chips (unless simulated) but rather a solution to some problem.

* Two events A and B are statistically independent if the outcome of one in no way affects the outcome of the other. Therefore, two random variables, X and Y, are statistically independent if information on one variables probability of taking on some value in no way affects the probability of the other random variable taking on some value. One of the most significant consequences of this statement of independence is that the joint probability of occurrence of two (or more) random variables can be written as the product of the individual marginal probabilities [65].

Direct Monte Carlo simulation techniques (classic use of simulation-based methods) can be used to estimate the probability of failure defined in equations 3, 4, and 5 above. Each random variable in a relationship is represented by a distribution function. A random number generator picks a number from the distribution with the probability of being picked proportional to the probability density function (pdf). After selecting weighted random numbers for all the stochastic variables, the relationship is calculated by feeding them into the performance function. Failure occurs when $g(X_1, X_2, \ldots, X_n) < 0$, therefore an estimate of the failure probability can be found by

$$\bar{p}_{TR} = \frac{N_f}{N} \qquad \textbf{Equation 6}$$

where N_f is the number of simulation cycles in which $g(X_1, X_2, \ldots, X_n) < 0$ and N is the total number of simulations. As N approaches infinity, p_{TR} approaches the true probability of failure.

The accuracy of equation 6 can be evaluated in terms of its variance. For a small failure probability and / or a small number of simulations, the variance of p_{TR} can be quite large. It may thus require a large number of simulations to achieve a specified accuracy. The variance of the estimated failure probability can be computed by assuming each simulation cycle to constitute a Bernoulli trial* [65]. Therefore, the number of failures in N trials can be considered to follow a binomial distribution. The variance of the estimated failure probability can then be computed as follows:

$$Var\left(\bar{p}_{TR}\right) \cong \frac{\left(1-\bar{p}_{TR}\right)\bar{p}_{TR}}{N} \qquad \textbf{Equation 7}$$

The recommended measure [64] of statistical accuracy for the failure probability is its coefficient of variation:

$$COV\left(\bar{p}_{TR}\right) \cong \frac{\sqrt{\frac{\left(1-\bar{p}_{TR}\right)\bar{p}_{TR}}{N}}}{\bar{p}_{TR}} \qquad \textbf{Equation 8}$$

* A Bernoulli trial satisfies the following assumptions [65]:

1. There are only two possible outcomes for each trial
2. The probability of success is the same for each trial
3. There are *N* trials where *N* is a constant.
4. The *N* trials are independent.

It is evident from equations 7 and 8 that as N approaches infinity, $Var\left(\bar{p}_{TR}\right)$ and $COV\left(\bar{p}_{TR}\right)$ approach zero. A small coefficient of variation thus indicates better accuracy.

The amount of computational time needed for the Direct Monte Carlo method is relatively large, however the computational effort per simulation is relatively small. Variance reduction techniques have been developed to increase the efficiency and accuracy of simulation based methods for a relatively small number of simulations, in addition to expediting convergence. However, the level of computational difficulty for each simulation cycle increases.

The Direct or Classical Monte Carlo method will be used in this study.

Specific engineering applications of PSM are to Finite element analysis, Fracture mechanics and Fatigue analysis. Some surveys have reported that ~ 80 % [64] of all failures are due to fracture and fatigue. Since the random scatter in fracture and fatigue properties of structural materials are usually wider than that in other material properties, probabilistic methods are especially apt for fracture and fatigue analysis. The figure below is a graphic representation of these various branches of probabilistic structural mechanics.

Figure 18: Probabilistic Structural Mechanics

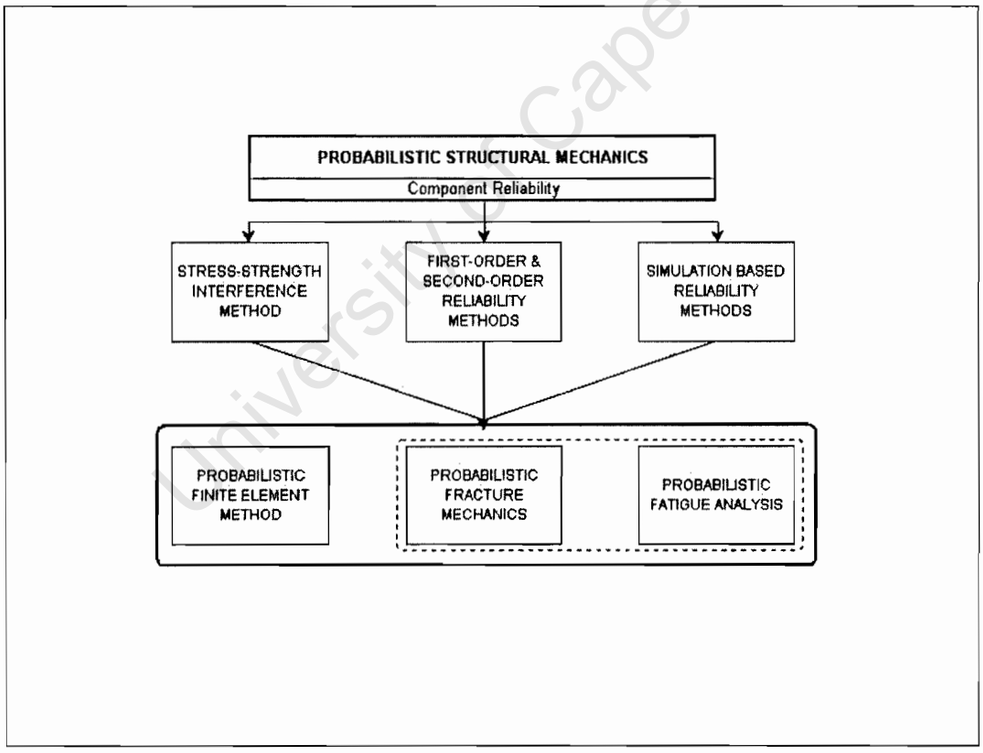

7 Probabilistic Fracture Mechanics (PFM) Model

The need for high levels of SG reliability has led to an increasing use of sophisticated in-service inspection techniques as a means of detecting and monitoring defects, and to the plugging of many tubes. This is both expensive* and may lead to early retirement of SG's due to loss of heat transfer area as a result of extensive plugging. Plugged tubes may be placed back in service by sleeving, however this is also an expensive and time consuming process. The purpose of this study is to develop a probabilistic fracture mechanics model to optimise the maintenance strategy (in terms of plugging limit and inspection scope) for the Koeberg SG's.

Steam Generator tube rupture (SGTR) accidents are considered in the design of the plant and it's probability of occurrence must be less than 10^{-2} per reactor year (third-category event, between 10^{-2} to 10^{-4}) [66]. This will be used as a target range, for the probability of a SGTR, within which to optimise the SG maintenance strategy.

7.1 Background

Initially the worlds most widely used tube plugging criteria was based on an acceptable level of tube wall degradation, allowing for a 40 to 50% tube wall thickness reduction [67]. It soon became evident that the dominant form of tube degradation was PWSCC in highly stressed areas, which was difficult to detect with the eddy current techniques employed at that time. In such cases the plugging criteria based on allowable tube wall thickness was regarded as overly conservative.

For this reason, EdF and the "Jozef Stefan" Institute, set out, independently, to develop an alternate plugging criteria that would allow safe operation with axially stress-corrosion cracked SG tubes. Both approaches rely on the ductile fracture behaviour of Inconel 600, which has been verified in independent experimental programs [61].

The PFM models developed for this purpose by EdF [26, 61, 66, 68, 69, 70] and the "Jožef Stefan" Institute [67, 71, 72, 73, 74, 75] have been the basis for the development of a similar model, specific to the Koeberg SG's.

These two models have differences with regards to certain sub modules; however, the overall approach is the same. In both cases three distinct phases can be identified:

- Estimation of Initial Crack Size Distribution
- Initiation and Growth of Defects
- Failure Analysis Module

* The time required for a full scope (i.e. all tubes) Eddy Current inspection of all three SG's at Koeberg is typically 6.5 days. This has an impact on the cost (in terms of normal costs and radiation dose to personnel) and duration of outages.

7.1.1 The EdF Approach

In 1988 EdF began work on a probabilistic maintenance study, which led to the development of the COMPROMIS* code [26, 61, 66, 68, 69, 70]. The first version of this code (available in 1992) could deal with longitudinal stress corrosion cracking in the RTZ. The initial model was based on the 1990 inspection data for Bugey 5.

The code is based on a probabilistic fracture mechanics computation, which calculates the probability of occurrence of a SGTR. The probability of occurrence can be summarised by the equation: $\mathrm{Prob}\left[a(t) > a_C\right]$ where $a(t)$ denotes the size of an existing crack at time t and a_c the critical crack size which would lead to fast fracture under the analysed loading conditions. The probabilistic approach allows for the factors which contribute to the uncertainties on sizes $a(t)$ and a_c to be taken into consideration.

The code is made up of the following three stages:

Estimation of Initial Crack Size Distribution
The ability of the in-service inspections to detect and measure defects is taken into account in the form of probabilistic detection distributions and measuring errors that depend on the size of the defect. The manipulation of these factors to produce a true reflection of the defect size distribution after inspection is based on a method developed by Barnier *et al.* [68]. This method is based on Bayes' theorem, which can account for the reliability of the inspections in detecting and sizing in order to reconstruct the exact distribution of true crack sizes.

Initiation and Growth of Defects
The purpose of the second module is to simulate, over time, the evolution of the initial defect size distribution i.e. $a(t)$. The crack propagation model was derived from a model developed for stainless steels and adapted to Inconel 600 on the basis of laboratory tests and operating experience [66]. The code covers the case of axial SCC in the roll-transition zone.

Failure Analysis Module
The last stage calculates, for each time step, the probability of a tube rupture based on a comparison of $a(t)$ and a_c and information about leaks detected in service. The analysis was performed for the most severe transient (feedwater line break) resulting in the maximum ΔP across the tube walls i.e. a ΔP of 17.2 MPa [69].

* **CO**de de **M**ecanique **P**robabiliste de la **R**upture pour **O**ptimiser la **M**aintenance et les **I**nspections en **S**ervice (Probabilistic Fracture Mechanics code of SGTR to optimise SG maintenance and in-service inspections)

The code was used primarily for the following:

- To test and compare various maintenance scenarios with a view to cost/safety optimisation (parameters considered: type of inspection, frequency, sampling strategy, plugging criteria)
- To investigate the sensitivity of the results to various sources of uncertainty, making it possible to identify the most influential weaknesses and guide research into areas, which would be most beneficial to pursue.
- To predict the operational life of a SG by simulating the number of tubes plugged versus time.

Initial results (based on the SG most affected in the French fleet with a 1/8 inspection sample) indicate that it would be necessary to wait four operating cycles without inspection for the risk to reach the limits imposed by the design rules, i.e. 10^{-2} to 10^{-4} [66]. It was also shown that a 100 % inspection has a significant influence and can substantially reduce the risk of failure especially for highly damaged tube bundles. Sensitivity studies also showed that the probabilities of failure based on worst-case (deterministic) values are greater by an order of four decades to the probabilistic approach.

These results were used to confirm the validity of the EdF SG maintenance policy. If subjected to the initial design plugging criteria, the concerned SG's would have been retired prematurely.

The lack of new literature since 1993, with regards to the COMPROMIS code, seems to indicate that further development of the code stopped after these initial results were obtained.

7.1.2 The Jožef Stefan Institute (JSI) Approach

The Reactor Engineering Division of the Jožef Stefan Institute (JSI) have developed and refined a probabilistic fracture mechanics model for the SG tubing degradation of the Slovenian Krško Nuclear Power Plant (Westinghouse D-4 SG) since 1990 [67, 71, 72, 73, 74, 75]. This model was based on the "Belgium approach" as described by Frederick *et al*. [76].

Whereas the EdF approach concentrated on supporting a particular maintenance strategy, the JSI approach proposed similar probabilistic fracture mechanics techniques to estimate the reliability of degraded SG tubing treated by a set of possible maintenance strategies. The strategies covered were based on crack length and plugging limit.

The model proposed initially by Mavko and Cizelj [67] has been further refined and expanded since 1992. These refinements include the following:

- Comparison of the failure probabilities calculated by FORM and SORM to those obtained by various Monte Carlo simulation methods [71]. This was used to validate the Monte Carlo simulation method. It was found that applying both FORM and SORM bounded the Monte Carlo solution in the range of practical interest i.e $(8\ mm < PL < 14\ mm)$.
- Implementation of the method developed by Barnier *et al*. [68] to account for the effects of inspection error on the initial crack size distribution. This is the same method used in the EdF approach.
- The development and verification of a Linear Elastic Fracture Mechanics based model describing the propagation of axial stress corrosion cracks in Inconel 600 SG tubes [73].

The JSI approach may also be broken down into three distinct phases similar to the EdF approach:

Estimation of Initial Crack Size Distribution

The initial model could account for cracks exceeding the plugging limit, which may have been missed during the inspection process. This simple model was based on the sizing error and detection probability. Based in this model, the crack length after the in-service inspection was defined by the random variable a_0:

$$a_0 = \begin{cases} a_m + a_e, & a_m + a_e < PL \\ a_m + a_e, & a_m + a_e \geq PL \text{ and } \zeta \leq P_d(a_m) \\ 0 \text{ Otherwise} \end{cases} \quad \textbf{Equation 9}$$

with

$$P_d(a_m) = 1 - e^{-0.45 a_m} \quad \textbf{Equation 10}$$

where a_m and a_e are random variables representing measured crack length and measurement error, respectively. $P_d(a_m)$ and ζ are the detection reliability function and a uniformly distributed random variable, respectively [72]. The coefficient, - 0.45, used in the detection reliability function $P_d(a_m)$ was based on a study of typical inspection performance data.

As indicated earlier, this simple model has been replaced by the more rigorous method developed by Barnier *et al.*

Initiation and Growth of Defects

The JSI model, in its current form, utilises a Linear Elastic Fracture Mechanics based model to describe the propagation of axially orientated stress corrosion cracks [73]. This propagation law was developed for axial cracks (assumed to be through wall) in the tube expansion transition zones. The residual stress field was considered as the major contributing factor driving short cracks while operational stresses dominate the growth of longer cracks. An estimate of the residual hoop stress was obtained using a non-linear finite element simulation of the tube to tube-sheet rolling process.

Failure Analysis Module

Similar to the last stage of the EdF approach, the probability of a tube rupture is based on a comparison of $a(t)$ and a_c. However, the JSI approach does not take credit for the leak detection capability and is thus conservative. In both approaches, the failure function is based on a ductile fracture mechanics model, which was verified experimentally in independent studies. The failure function is the basis for the calculation of a_c. The analysis was performed for the most unfavourable hypothetical accident conditions viz. a feedwater line break (maximum depressurisation of the secondary side) with a ΔP of 20 MPa.

The following conclusions have been drawn from the most recent JSI studies [72, 74] for the Krško Nuclear Power Plant:

- The plugging limit range of 8 to 14 mm was found to be optimal in terms of the number of plugged tubes versus SGTR probability. It was found that the SGTR probability could be changed by a factor of 2 in this range. Lower SG failure probabilities can thus be achieved at the expense of reduced SG performance.
- A hypothetical feedwater line break would cause a single SG tube rupture in approximately 0.1% of all cases and a multiple SG tube rupture in less than one in a million cases (given a PL < 12 mm). Specifying no plugging limit (i.e. $PL \rightarrow \infty$) results in virtually certain multiple SG tube rupture.
- The probability of tube rupture was found to be rather sensitive to human errors. A probability of human error in the order of about 1% increased the probability of a multiple tube rupture event by about 4 orders of magnitude. These results also indicated a need for further investigations in the field of human reliability during inspection and plugging procedures.
- Sampling size also had a significant effect. Thus, routine 100% inspections of tube bundles were recommended.
- A comparison was also made of maintenance strategies based on allowable crack depth and allowable defect length. The crack length strategy was shown to be superior in terms of SGTR probability.

The probabilistic fracture mechanics model developed in this study for the Koeberg SG's is based on both approaches discussed above. In most cases, the EdF approach is followed, as the data available is more relevant to the Koeberg SG's. The reasons for adopting various sub modules are discussed in subsequent chapters.

7.2 Deterministic Basis

The failure probability as defined in equation 5 has the following form for this particular case:

$$p_f = \int_0^\infty f(a) \int_0^a f_c(2a_c)\, d(2a_c)\, da \qquad \textbf{Equation 11}$$

where,

$f(a)$ = Probability Density Function of Observed crack lengths.
$f_c(a_c)$ = Probability Density Function of Critical crack lengths.

Both functions are joint probability density functions of different parameters. The observed crack length distribution is based on inspection data and information regarding the measurement error and detection probability (this will be discussed later).

The critical crack length calculation is based on a correlation between burst pressure and plastic flow stress $(\sigma_f)^*$. Flesch and Cochet [61] have noted a "perfect" correlation between test results and a model of this form+. This formulation was also supported and developed by Kastner *et al.* [77].

For tubes without defects, the tube rupture criteria (for the free span or non-specific zone) can be expressed by the following relationship:

$$\sigma_\theta = \sigma_f \qquad \textbf{Equation 12}$$

where σ_θ is the membrane hoop stress due to the pressure differential across the tube walls and $\sigma_f = k(\sigma_Y + \sigma_{UTS})$ where σ_Y = yield stress and σ_{UTS} = ultimate tensile stress. A conventional and conservative value of σ_f is obtained for $k = 0.5$.

* Flow stress is used to account for strain hardening.

+ This formulation for the instability criterion of a straight pipe having a longitudinal through wall crack was first established by Hahn et al. [78]

For tubes with single or multiple axial defects in the RTZ, the tube rupture criteria can be expressed by a modified version of equation 12:

$$M^{*}\sigma_{\theta}^{*} = \sigma_{f} \qquad \textbf{Equation 13}$$

where σ_{θ}^{*} is the equivalent membrane hoop stress (taking into account the pressure loading on the tube walls and crack lips) and M^{*} is the bulging factor (also referred to as the stress magnification factor) specific to the RTZ. The bulging factor accounts for crack bulging due to the internal pressure in the tube.

It was experimentally confirmed [61] that the instability limit pressure of a tube with a crack located in the RTZ is higher than that of a tube with the same type of defect located in a straight section remote from discontinuities. The gain in critical pressure is due to two combined effects: local mechanical strengthening due to seating in the tube sheet, which limits bulging, and an increase in the flow stress due to strain hardening of the material in the RTZ during the tube expansion process. It was also demonstrated that the rupture criterion (equation 13) remains applicable where there are several major cracks distributed over the entire tube circumference.

The performance function as defined in equation 3 for the specific case of SG tube integrity may now be stated as follows:

$$Z = \sigma_{f} - M^{*}\sigma_{\theta}^{*} = g\left(\phi, t, \delta, k, \sigma_{Y} + \sigma_{UTS}, P_{f}\right) \qquad \textbf{Equation 14}$$

where,

M^{*} = Bulging Factor for a specific cracked tube in the RTZ : $M^{*} = f\left(a_{i}, a_{e}, \delta, \phi, t\right)$

σ_{θ}^{*} = Equivalent Membrane Hoop Stress : $\sigma_{\theta}^{*} = f\left(P_{P}, P_{S}, P_{f}, \phi, t\right)$

σ_{f} = Flow Stress $\sigma_{f} = f\left(\sigma_{Y} + \sigma_{UTS}, k\right)$

a_{i} = Crack Length (Inner Surface)

a_{e} = Crack Length (External Surface)

P_{P} = Primary Side Pressure

P_{S} = Secondary Side Pressure

P_{f} = Pressure propagating the crack

ϕ = Tube outer diameter

t = Tube wall thickness

δ = Tube crevice depth

See Figure 19 below:

Figure 19: RTZ - Parameter Definitions

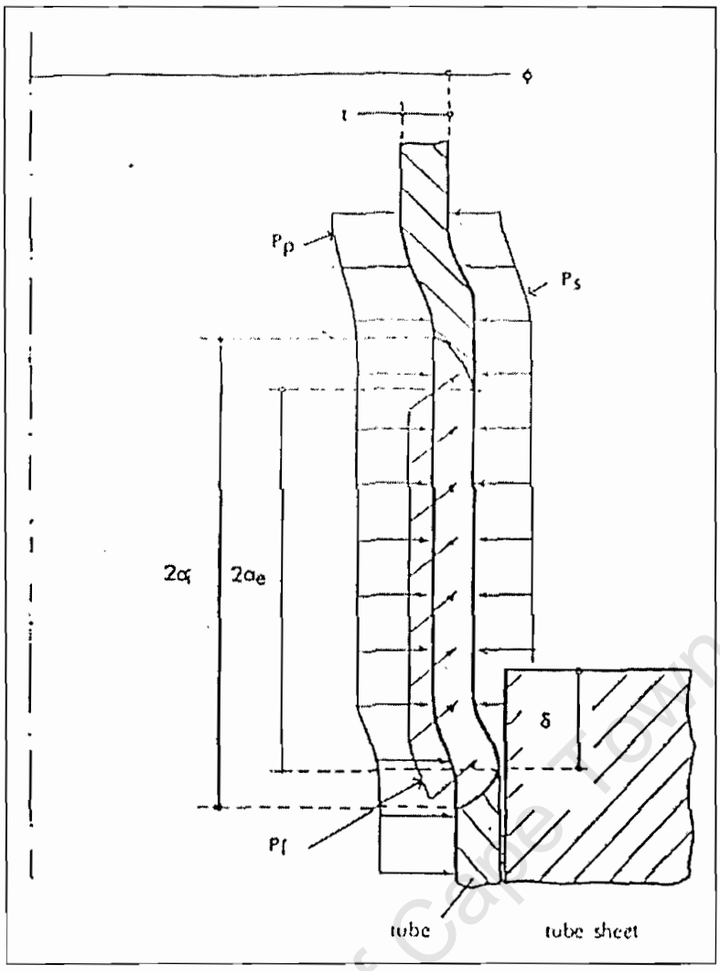

The bulging factor in the RTZ may be described as follows:

$$M^* = \mu M$$

where M is the bulging factor in the non-specific zone of an SG tube and

$$\mu = f\left(\frac{a}{\sqrt{Rt}}\right) \leq 1$$

The exact relationship between M^* and $\frac{a}{\sqrt{Rt}}$ has been determined experimentally. EdF and Framatome performed more than 1000 burst tests on Inconel 600 and Inconel 690 tubing with various types of damage located in straight sections remote from discontinuities and supports (non-specific sections), in the RTZ at the top of the tube sheet, in the vicinity of the tube support plates, and in the U-bends [61].

The empirical results for single or multiple cracks in the RTZ is as follows:

$$M^* = 0.0872 + 0.7265\, e^{\left(-1.3374 \frac{a}{\sqrt{Rt}}\right)} + 0.9858\left(\frac{a}{\sqrt{Rt}}\right) \qquad \textbf{Equation 15}$$

Inverting the bulging factor correlation for a_c (critical crack length) when $M^*\sigma_\theta^* = \sigma_f$:

$$a_c = \left(-0.128 + 1.020M^* - 6.976\, e^{-3.146M^*}\right)\sqrt{Rt} \qquad \textbf{Equation 16}$$

where,

$$M^* = \frac{\sigma_f}{\sigma_\theta^*} = \frac{k\left(\sigma_Y + \sigma_{UTS}\right)}{P_f\left(\frac{R}{t} - 0.5\right)} \qquad \textbf{Equation 17}$$

Results are plotted for $\frac{1}{M^*}$ and $\frac{1}{M}$ (this is equivalent to $\frac{\sigma_\theta^*}{\sigma_f}$ which is equivalent to the burst pressure) versus $\frac{a}{\sqrt{Rt}}$ in Figure 20below:

Figure 20: SG Tube burst criteria for Non-specific zones and RTZ [61]

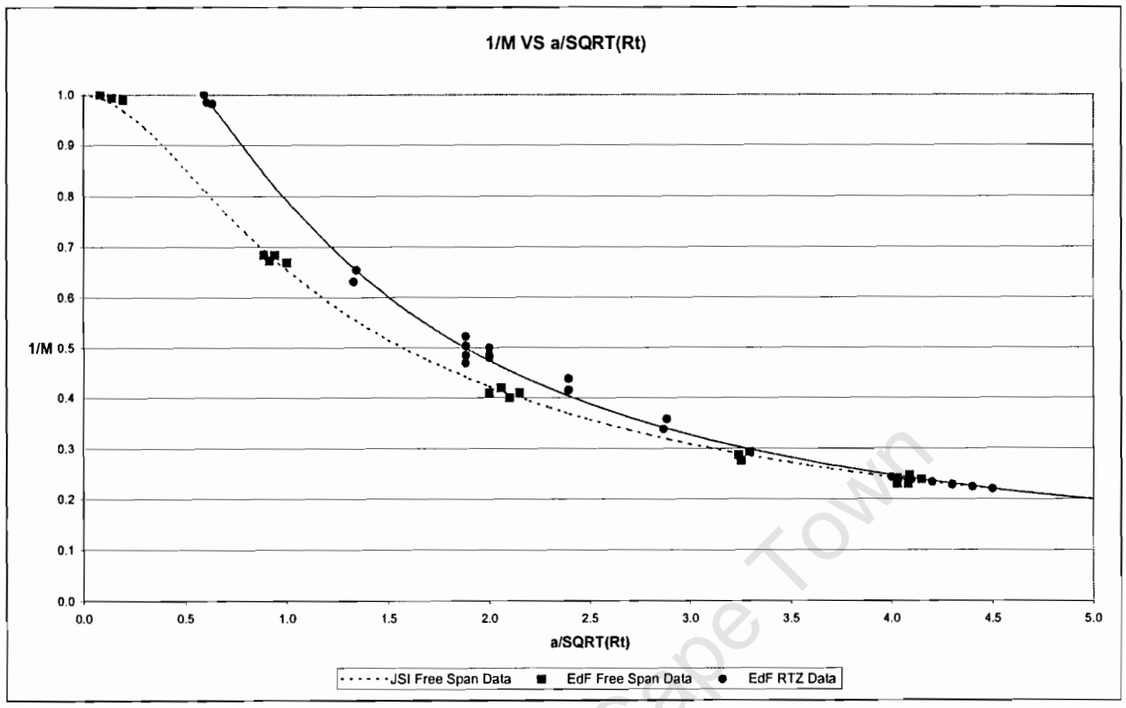

It is evident that higher burst pressures were recorded for tests performed in the RTZ given a particular crack length. The correlation between the EdF free span data and the JSI free span data is remarkably good. This is of particular interest since Hernalsteen [79] observed "large discrepancies" when he compared the published data, for burst tests in the free span, of several European laboratories.

The JSI approach was based on the free span data presented above. The additional circumferential rigidity in the RTZ was taken into account in the form of a *Tube Sheet Reinforcing Factor*, defined as a correction to the flow stress factor k. It's use was however restricted to cracks tangent to the tubesheet, which may not be true for numerous cracks propagating from the tube sheet.

It should be noted that these results are based on machined cracks (laser cut or by electric discharge machining). In both types of crack fabrication crack width was typically 0.2 mm which may be very different from the tight corrosion cracks being simulated [79]. EdF have, however, performed tests on available pulled tubes and the above curves were found to be bounding in these cases. Equations 16 and 17 can thus be used with relative confidence.

7.3 Model Outline

The probabilistic fracture mechanics (PFM) model proposed in this study is based on the EdF and JSI approaches discussed earlier. The EdF approach is of greater relevance to the Koeberg SG's due to design and operational similarities. The JSI approach was used as an additional insight into the development of PFM models of this type.

The proposed PFM model consists of three distinct sub modules similar to those developed by EdF and the JSI. These sub modules are:

- Estimation of Initial Crack Size Distribution
- Initiation and Growth of Defects
- Failure Analysis Module

The development of these sub modules is discussed in detail in subsequent sections.

The data used for the model is based on the Koeberg SG most affected by axial PWSCC in the RTZ. The inspections results used is based on Outage 113 which took place in January 2003. Important information with regards to the SG chosen for this study is listed in the table below.

Table 10: SG 95 Inspection Summary

Parameter	Value
SG ID	SG 95 (SG 2 on Unit 1)
Outage	113
Number of Tubes	3330
Inspection Scope	100 %
Number of tubes with cracks	1307
Total Number of cracks	3304
Maximum cracks per tube	13

A schematic of the proposed model is shown below:

Figure 21: PFM Model Schematic

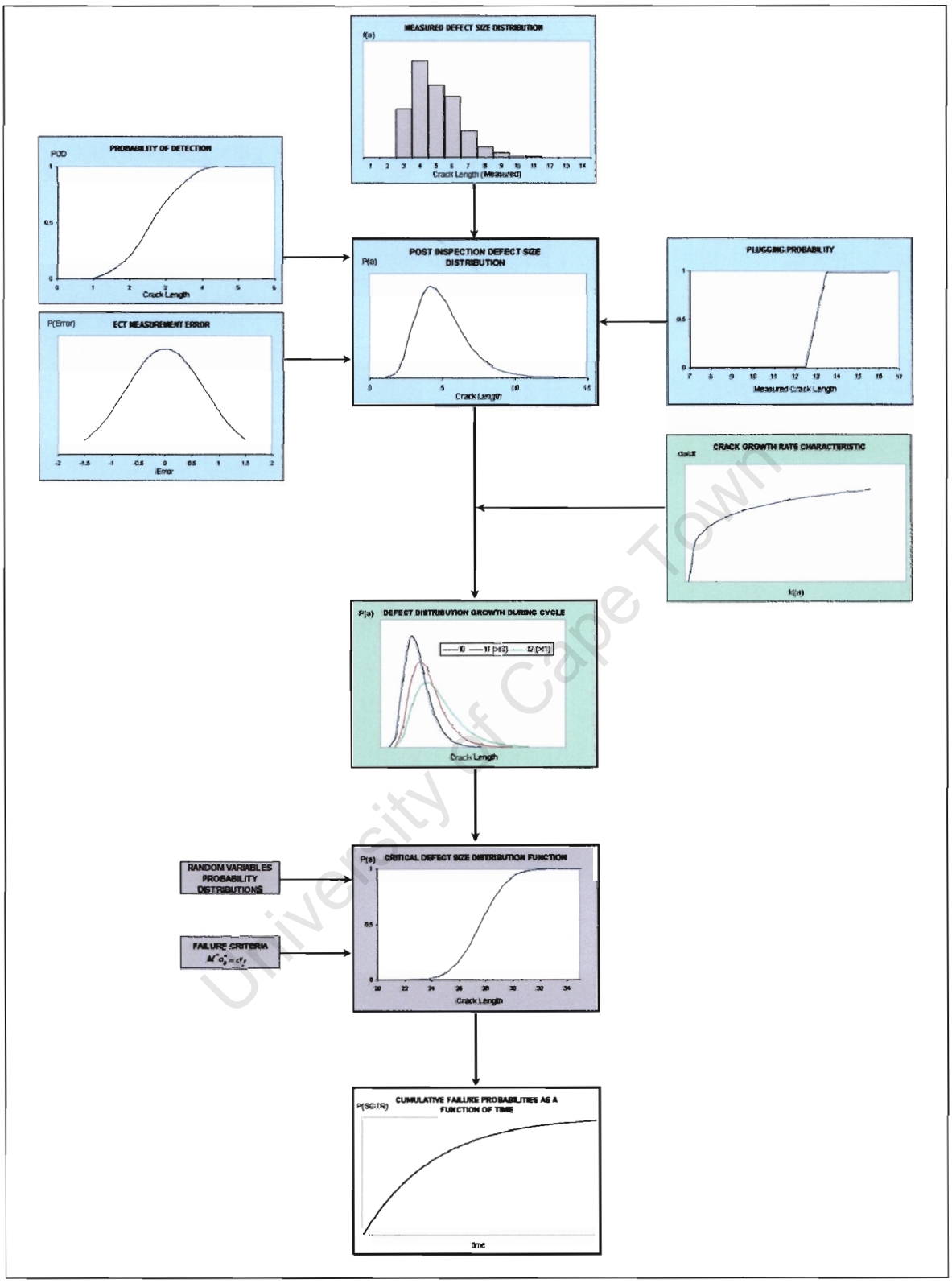

The model was developed as a Microsoft Excel spreadsheet with certain algorithms written in Visual Basic for Applications (VBA).

7.3.1 Random Number Generation

Random number generators are at the heart of all Monte Carlo simulations. These uniformly distributed random numbers are used to generate random variates from non-uniform distributions. These non-uniform distributions are typically based on the parameters, which describe the deterministic relationship being studied.

In most cases, we want the generated pseudo-random* numbers to simulate a uniform distribution (equal probability) over the unit interval (0,1), that is, the distribution with the probability density function,

$$p(x) = \begin{cases} 1, & if\ 0 < x < 1 \\ 0, & otherwise \end{cases} \qquad \textbf{Equation 18}$$

All of the references studied [63, 80, 81, 82, 83, 64] recommend the Linear Congruential Generator as a source of random numbers. The form of the generator is as follows:

$$x_i = (a\, x_{i-1} + c) \bmod m \quad \text{with } 0 \le x_i < m \qquad \textbf{Equation 19}$$

where x_i is the new random number being generated, x_{i-1} is the previous number, a is called the *multiplier*, c is called the *increment*, and m is called the *modulus* of the generator. In the above relationship, x_i is the remainder when $(a\, x_{i-1} + c)$ is divided by m. This relationship is based on a branch of mathematics called Modular Arithmetic. Interested readers may find a brief introduction to this subject by Gentle [80].

Since such a sequence repeats itself after at most m steps, the period must be required to exceed the number of random numbers involved in the experiment under consideration. It is thus important to set m to as large a number as possible to prevent cycling of random numbers.

The above relationship cannot be implemented in the VBA code since the data types available do not support such large numbers. However, the VBA code does have a built in random number generator (the RND function) which has been used for the purposes of this study. The RND function is based on the Linear Congruential method of the same form as equation 19. This function utilises an internal unsigned long data type that is not supported by the VBA language.

* Computerised processes call for perfectly deterministic generation of numbers and the product, not being truly random but cyclical in nature is referred to accordingly as pseudo-random or quasi-random.

The parameters used are as follows:

x_i = New random number

x_{i-1} = Previous random number (an initial value of 327680 is used)

a = 1140671485

c = 12820163

m = 2^{24}

These parameters are considered adequate based on the criteria set forth in reference [80]. The VBA RND function will thus be used in all the algorithms required for this study.

The sequence of uniform random numbers between 0 and 1 will be denoted as $U(0,1)$.

7.3.2 Random Variate* Generation

The generation of random variates from non-uniform distributions is usually done by applying a transformation to the generated uniform random numbers. Each realisation of a non-uniform random variate can be obtained from a single uniform or from a sequence of uniforms. Some methods that require a sequence of uniforms require that the sequence be independent.

The generation of random variates requires that:

- The relevant Cumulative Distribution Function (CDF) is invertable (or in the case of normal and log-normal variates, numerical approximations exist for the inverse of the CDF)
- A uniform random number generator is available.

Thus, if we generate a uniform $U(0,1)$ random number and substitute this into the inverse of the CDF of interest (with the relevant parameters), we obtain a realisation of a variate for this particular CDF.

For example, consider the generation of an exponential variate with parameter λ. The CDF is expressed as:

$$F_X(x) = 1 - e^{-\lambda x}$$

If we substitute u_i (a uniform $U(0,1)$ random number) for $F_X(x)$ and invert the CDF to solve for x_i, we obtain:

$$x_i = -\frac{1}{\lambda}\ln(1-u_i)$$

Here, x_i is an exponential variate with parameter λ.

It should be noted that not all distributions have closed form solutions for the CDF or its inverse (e.g. Normal, Log-normal, and Gamma distributions). In these cases, numerical approximations (in the form of algorithms or subroutines) are available. The algorithms used for generating random variates from the distributions used in this study are listed in appendix C.

The method described in the example above is referred to as the *Inverse Transform method*, which is applicable to cases where the CDF has a closed form solution. Where no closed form solutions for the CDF exists, the *Composition* and *Acceptance-Rejection* methods are used [83].

* Some authors distinguish "random numbers" from "random variates", where the term "random number" applies to pseudo-random numbers that arise from a uniform distribution over the unit interval (0,1), and the term "random variates" applies to pseudo-random numbers that arise from some other distribution. Uniform random numbers are also referred to as "uniforms" in some texts. This usage will be adopted here.

The following schematic illustrates the methods available for the generation of random non-uniform variates from uniform random numbers.

Figure 22: Generation of Non-Uniform Random Variates

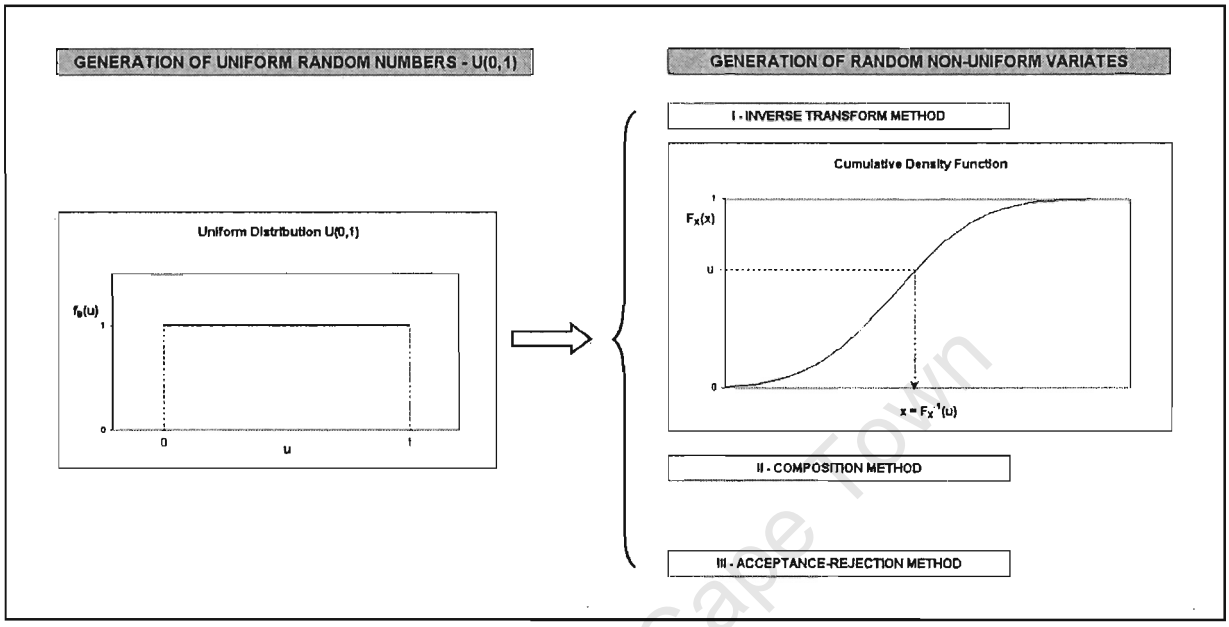

This schematic represents the essence of a Monte Carlo Simulation (MCS). The MCS process may thus be summarised as follows:

- Generate a uniformly distributed random number $U(0,1)$
- Generate random variates from the random variables describing the deterministic relationship being studied.
- Apply the deterministic relationship for each realisation of the parameters random variates.

The generic MCS VBA source code and spreadsheet it interfaces with is given in appendix D1.

7.3.3 Estimation of True Crack Length Distribution

The input to this sub module is the measured crack length frequency plot as shown below:

Figure 23: Measured Crack Length Frequency Plot (SG 95, Outage 113)

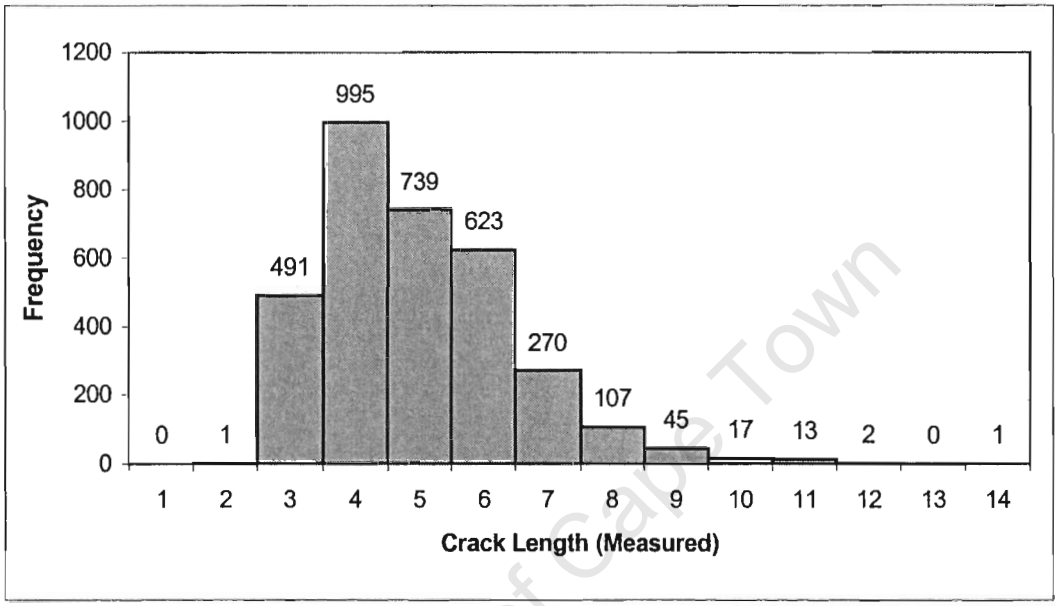

This frequency plot represents the distribution of measured crack lengths in the RTZ (the quoted length includes the portion in the tube sheet). We thus have a total of 3304 cracks in 1307 tubes. The highest number of cracks recorded in a single tube was 13.

The inspection data collected during an outage forms the bases for deciding which tubes should be plugged to ensure safe operation. However, due to crack sizing error and imperfect detectability, some of the cracks left in operation may actually exceed the plugging limit.

The objective of this sub module is to reconstruct the above distribution to be representative of the true defect size distribution, post inspection. The sources of error considered in this study are the measurement error, probability of detection (POD), and human error.

The method described here may be considered a hybrid method based on aspects of the JSI and EdF approaches. It is similar to the JSI approach (in terms of dealing with measurement error) but utilises methods developed by EdF to account for plugging probability. The method has two phases:

- Estimation of true defect size distribution by MCS analysis.
- Estimation of post inspection defect size distribution

7.3.3.1 True Defect Size Distribution

The true defect size distribution may be defined as follows:

$$a = a_m + a_e \qquad \text{Equation 20}$$

where a is the true defect length, a_m is the random variable representing measured defect length, and a_e is the random variable representing sizing error.

The sizing error is in the order of ±1.5 mm [46] and was modelled (as suggested by Cizelj *et al.* [74] as a normal distribution with a mean of 0.0 mm and a standard deviation of 0.75 mm. Thus, only random errors, independent of the crack length are considered.

The effect of sizing error was taken into account by performing a direct Monte Carlo simulation (MCS) on a_m and a_e. The simulation simply samples a value from the measured crack size distribution and adds a value sampled from the sizing error distribution. The resultant distribution is considered to be the true defect size distribution. A listing of the VBA code and the spreadsheet is given in appendix D2.

The random variables used in the MCS and the resultant distribution parameters are listed in the table below:

Table 11: Random Variables for MCS of True Defect Size Distribution

Variable	Distribution*			Unit	Truncation	Comment / Reference
	Type	Parameters				
a_m	Log-normal	$\alpha = 1.559$	$\beta = 0.291$	mm	None	Measured (Outage 113)
a_e	Normal	$\mu = 0.00$	$\sigma = 0.75$	mm	±1.5	[74]
$a_m + a_e$	Log-normal	$\alpha = 1.545$	$\beta = 0.337$	mm	-	Generated by Monte Carlo Simulation.

* For definitions of these distribution parameters see appendix C.

7.3.3.2 Post Inspection Defect Size Distribution

Given the initial distribution of true defect sizes just estimated, the plugging probability is needed to calculate the "post inspection" distribution. This allows us to account for the effect of maintenance actions taken i.e. the plugging of tubes exceeding the plugging limit. The probability that a tube is plugged is a function of the probabilities that the tube is inspected, that the defect is detected, that its measured size exceeds the plugging limit, and that there is no failure of plugging (essentially human error).

This may be stated as follows [68]:

$$P[\text{Plugging}/a] = P[\text{inspecting}/a] \times P[\text{detection}/a] \times P[a_m > PL/a] \times P[\text{Plugged}] \qquad \textbf{Equation 21}$$

where a is the true defect length, a_m is the measured defect length and PL is the plugging limit. The individual probabilities are defined as follows:

- $P[\text{inspecting}/a] = \frac{1}{n_S}$ where n_S is the sample scope e.g. a random sample of 1 in 8 tubes is typical. Since a 100 % inspection was performed on the SG under consideration, this probability takes on a value of one.
- $P[a_m > PL/a]$ may be considered to be 1 when $a \geq PL$ and 0 when $a < PL$. This simplification is possible since the sizing error has already been taken into account in the previous step.
- $P[\text{Plugged}] = 1 - \varepsilon$ where ε is the residual non-detection probability used to model human errors (EdF use a value of 10^{-4}).
- $P[\text{detection}/a]$ is the probability of detection (POD). The POD was assumed to follow the well known exponential law. The detection probability specific to the RPC method is as follows [66]:

$$POD = 1 - e^{-\left(\frac{a}{2.37}\right)^{3.25}} \qquad \textbf{Equation 22}$$

Equation 21 was applied at the "binned" level i.e. after a histogram was generated for the true defect size distribution. For a detailed description of this method see appendix E.

The resultant post inspection defect size distribution plots (for various plugging limits) are shown in the figure below.

Figure 24: Post Inspection Defect Size Distributions

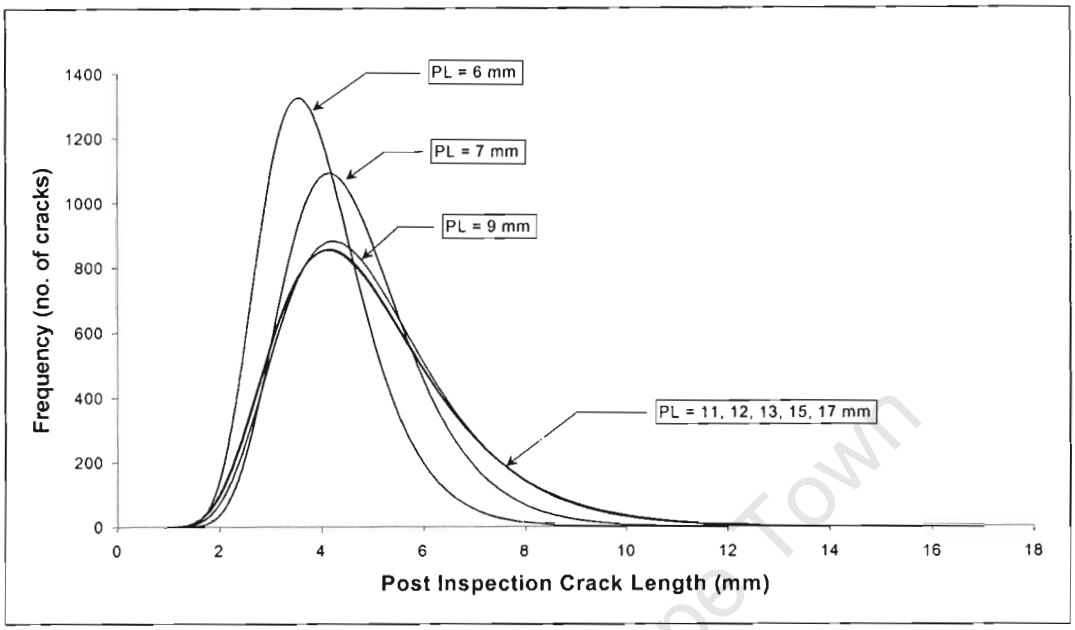

Since the above frequency distributions directly affect the tube rupture probabilities (particularly the weighting of the right tail), the following conclusions can be drawn:

- The frequency plots for PL of 11 to 17 mm are virtually indistinguishable. This implies that increasing the PL above 13 mm will not increase the tube rupture probability significantly.
- A significant decrease in tube rupture probability can only be achieved by applying a PL of 7 mm or lower. However, this would result in excessive plugging. The graph below (Figure 25) illustrates the required plugging frequency given a particular PL. Thus for a PL of 7 mm, an average of 180 tubes would have to be plugged. However, it will be shown, in subsequent chapters, that the tube rupture probability is well within limits even for the most penalising post inspection defect size distribution and thus there is no need to plug excessively.

Figure 25: Required Plugging Frequency vs PL (SG 95, Outage 113)*

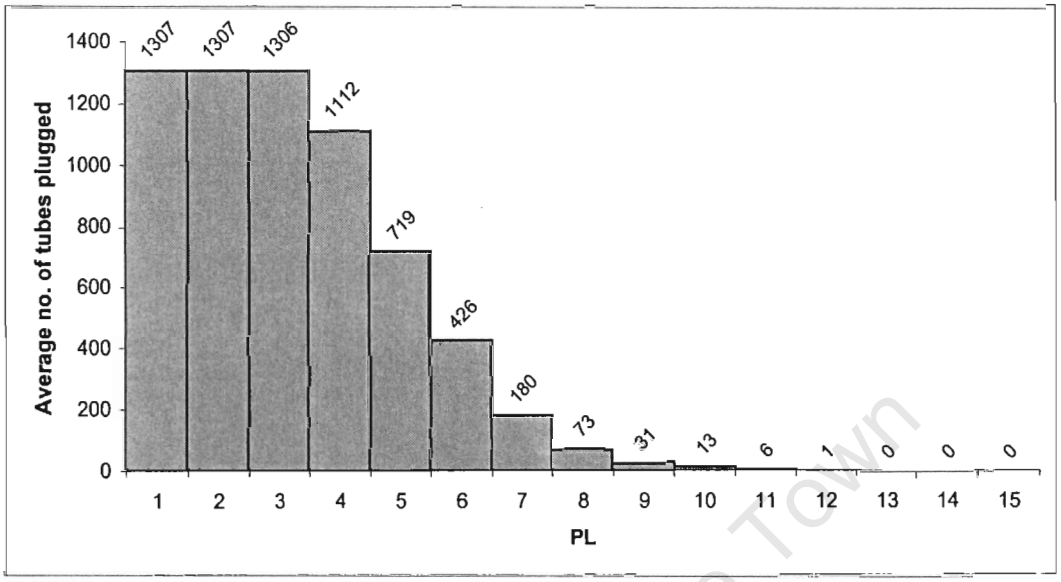

Barnier *et al.* [68] has developed a method, which appears to be more rigorous than the method described here. This method was used in the EdF approach and was adopted in 1995 by the JSI [74]. However, this method still requires a "subjective" judgement of the appropriate distribution type for the True Defect Size distribution e.g. the EdF analysis was based on a choice between a Log-normal ($\mu = 1.51, \sigma = 0.626$) and Weibull ($\alpha = 5.16, \beta = 1.53$) distribution for which the probability of having a crack length greater than 13 mm is 4.6E-02 and 1.6E-02 respectively. The difference is nearly 3 fold and may negate the need for such a rigorous approach.

* The vertical axis in this graph is representative of the average number of tubes requiring plugging. This is based on a factor of 2.53 cracks per tube (i.e. 3304 cracks / 1307 tubes affected).

7.3.4 Critical Crack Size Distribution

The critical crack length calculation is based on a correlation between burst pressure and plastic flow stress (σ_f). The equation defining critical crack size has been derived earlier (equation 16) and is repeated here for ease of reference.

$$a_c = \left(-0.128 + 1.020M^* - 6.976\, e^{-3.146M^*}\right)\sqrt{Rt}$$

where,

$$M^* = \frac{\sigma_f}{\sigma_\theta^*} = \frac{k\left(\sigma_Y + \sigma_{UTS}\right)}{P_f\left(\frac{R}{t} - 0.5\right)}$$

The defining parameters may be considered independent random variables (except for P_f) and may thus be subjected to a MCS. The probability distributions of these parameters are listed in the table below.

Table 12: Random Variables for MCS of Critical Crack Size distribution

Variable	Distribution			Unit	Truncation	Comment / Reference
	Type	Parameters				
t	Normal	$\mu = 1.27$	$\sigma = 0.04$	mm	$\pm 3\sigma$	[69]
ϕ	Normal	$\mu = 22.22$	$\sigma = 0.06$	mm	$-3\sigma / 2.2\sigma$	[69]
$\sigma_Y + \sigma_{UTS}$	Normal	$\mu = 914$	$\sigma = 30$	MPa	$\pm 3\sigma$	Koeberg Specific Data
k	Normal	$\mu = 0.58$	$\sigma = 0.01$	-	$\pm 3\sigma$	[69]

The pressure parameter P_f is considered to be deterministic since it is characteristic of a particular operating situation. The critical crack length is evaluated for two cases; Normal operating conditions ($P_f = 10$ MPa) and during the worst case accident scenario ($P_f = 17.2$ MPa). This latter scenario is attributed to a feed water line break accident [70].

A listing of the VBA code and the spreadsheet used to generate the Critical Crack size distributions is given in appendix D3.

The results are illustrated in Figure 26 below:

Figure 26: Critical Crack Size Distribution in RTZ (Generated by MCS)

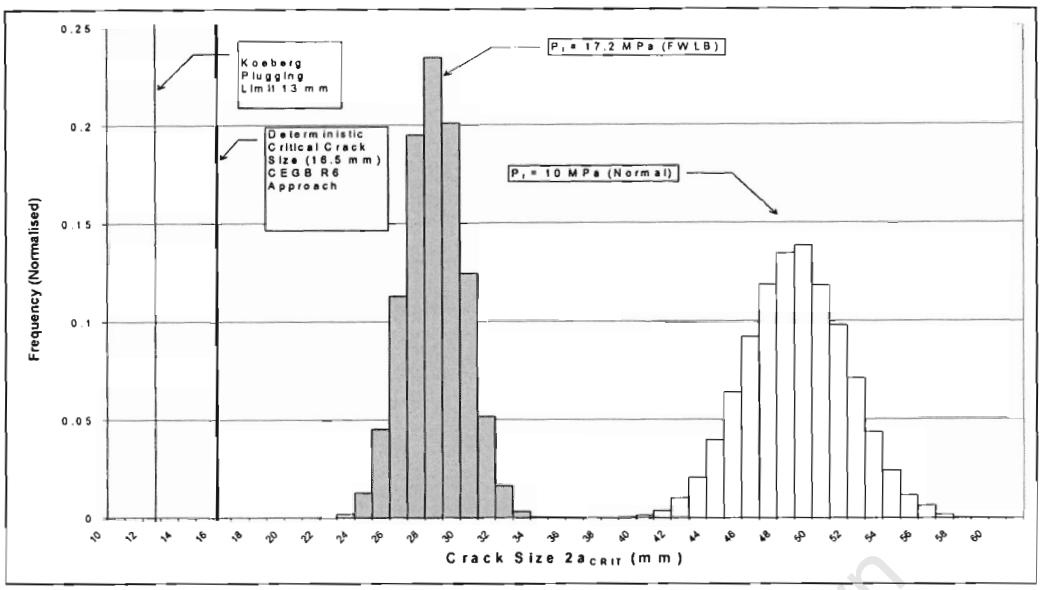

The critical crack size distributions, generated by MCS, has the following parameters:

Table 13: Critical Crack Size Distribution Parameters

Parameter	Value (mm)
Normal Operation	
μ (Mean)	48.13
σ (Std. Deviation)	2.87
FWLB	
μ (Mean)	27.58
σ (Std. Deviation)	1.66

It is clear from Figure 26 that the critical crack size is well above the plugging limit applied at Koeberg, even for the postulated accident condition (feed water line break - FWLB). The figure also indicates the advantage offered by the probabilistic approach in evaluating critical crack sizes. The conservatism associated with the deterministically calculated critical crack size of 16.5 mm, by the CEGB R6 approach, [25] is evident. The deterministic analysis also provides no information with regards to the uncertainty associated with the calculated value.

Whereas a deterministic approach gives a first impression of the influence of various parameters governing the critical crack size, a probabilistic calculation provides something "extra", since it provides the ability to quantify the influence of these parameters on the probability of a SG tube rupture.

A sensitivity analysis was performed to determine the effect of varying the parameters, which define the critical crack size. This was achieved by setting each parameter value to its mean and extreme values as listed in Table 13, and performing a MCS for each condition. The cumulative distribution for critical crack size (which is proportional to the failure probability) was then plotted for each simulation. The results are illustrated in the graphs below.

Figure 27: Sensitivity to Flow Stress Factor

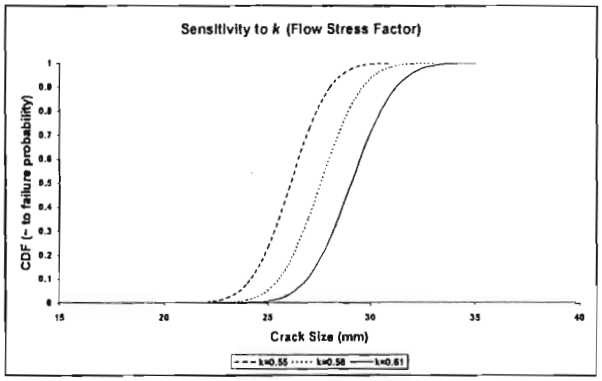

Figure 28: Sensitivity to Tube Outside Diameter

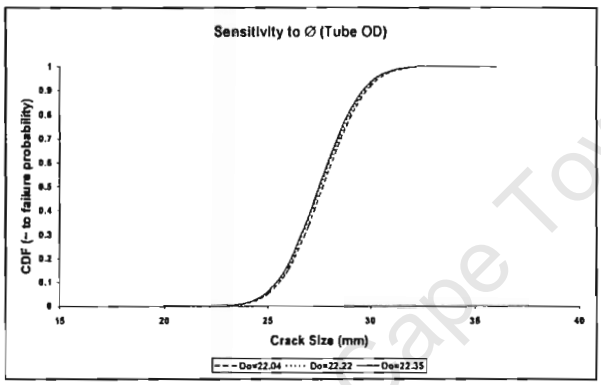

Figure 29: Sensitivity to Tube Wall Thickness

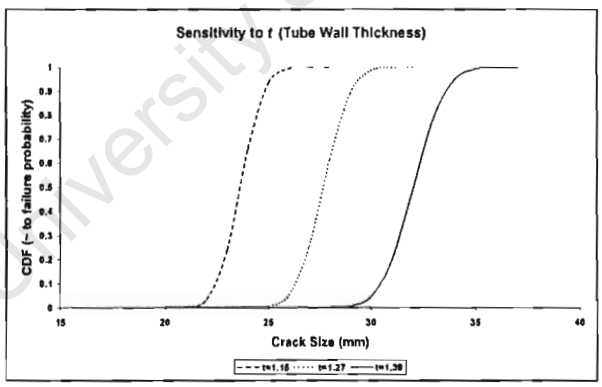

Figure 30: Sensitivity to $\sigma_Y + \sigma_{UTS}$

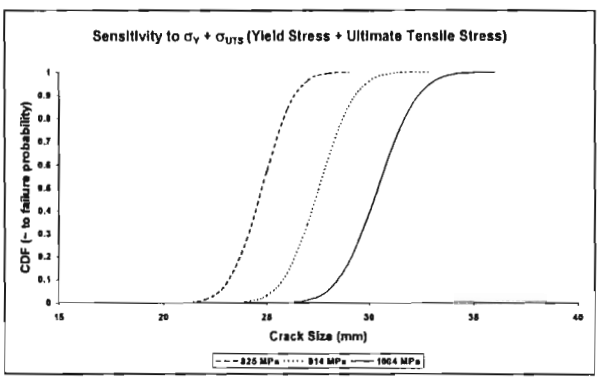

The cumulative distribution graphs are proportional to the tube rupture probability since curves to the left predict higher probabilities for smaller critical crack sizes. Thus, curves towards the left will yield higher tube rupture probabilities than curves to the right on the graphs above. These results demonstrate that it would be more important to know the distribution of tube thickness and mechanical properties rather than the distribution of tube diameters or flow stress parameters. These results may also be useful to future designers of SG tubes since it highlights the parameters, which would yield the most benefit if changed.

7.3.5 Crack Growth Law

The crack propagation model used by EdF (and adopted for this study) was derived from a model developed by Ford [84] for stainless steels and adapted to Inconel 600 on the bases of laboratory tests and operating experience. This model is based on a correlation* between the propagation rate da/dt and the stress intensity factor $K(a)$ having the following form [66]:

$$\frac{da}{dt} = C\left[K(a)\right]^m \quad (mm/hr) \qquad \textbf{Equation 23}$$

where da/dt has an upper bound of $1.5E-05\ mm/hr$ and

$$K(a) = -23.96\log a + 3.8a + 28.4 \qquad \textbf{Equation 24}$$

and $m \approx 1.07$

EdF has devoted considerable research to the development of the precise correlation between K and crack size [66]. This correlation is based on an evaluation of the local residual and operating stresses.

The total crack length, after a time interval Δt, may thus be defined as follows:

$$a_t = a + \Delta a \qquad \textbf{Equation 25}$$

where

$$\Delta a = \Delta t\, C\left[K(a)\right]^m \qquad \textbf{Equation 26}$$

One of the three parameters defining the crack propagation model, $C, K(a),$ or m, may be treated as a random variable. It should be noted that all three parameters cannot be treated as random variables simultaneously since they are not independent. As indicated in reference [66] only parameter C will be treated as a random variable in this study. This parameter is defined as follows:

Variable	Distribution			Unit	Truncation	Comment / Reference
	Type	Parameters				
C	Log-normal	$\alpha = -12.06$	$\beta = 0.84$	-	-	[66]

* This type of correlation is typically used to model Fatigue Crack growth, however, Stress Corrosion Cracking data may also be correlated by the Stress Intensity approach as indicated by Ewalds and Wanhill [5]

It should be noted that the correlation between da/dt and the stress intensity factor $K(a)$ developed by EdF compares well with that developed by Kawamura and Hirano [42], illustrated in Figure 12.

8 Results and Discussion

8.1 Tube Rupture Probability

A direct MCS was performed to calculate tube failure probabilities. The MCS source code and spreadsheet with which it interfaces is given in appendix D4. The MCS samples data from the Post Inspection crack length distribution, the crack growth factor (C), and the Critical Crack size distribution for postulated accident conditions. The spreadsheet then compares the crack length, at the time being considered, with the critical crack length for each realisation of these parameters. A failure occurrence is observed when the crack length (at time t) exceeds the critical crack length.

As indicated earlier, the tube failure probability is calculated from the number of numerical experiments, N, and the number of observed failure occurrences, N_f, as follows (equation 6):

$$\bar{p}_{TR} = \frac{N_f}{N}$$

where the number of iterations is determined by the convergence of the Coefficient of Variation as defined in chapter 6.2.1. A target value of 0.1 was used as suggested in reference [64].

Figure 31 below illustrates the Post Inspection crack length distribution and Critical Crack size distribution on the same horizontal scale. Since the tube rupture probability is proportional to the overlapping area, it is clear that very low tube rupture probabilities should be expected.

Figure 31: Post Inspection Crack Length (t = 0) and Critical Crack Size Distributions

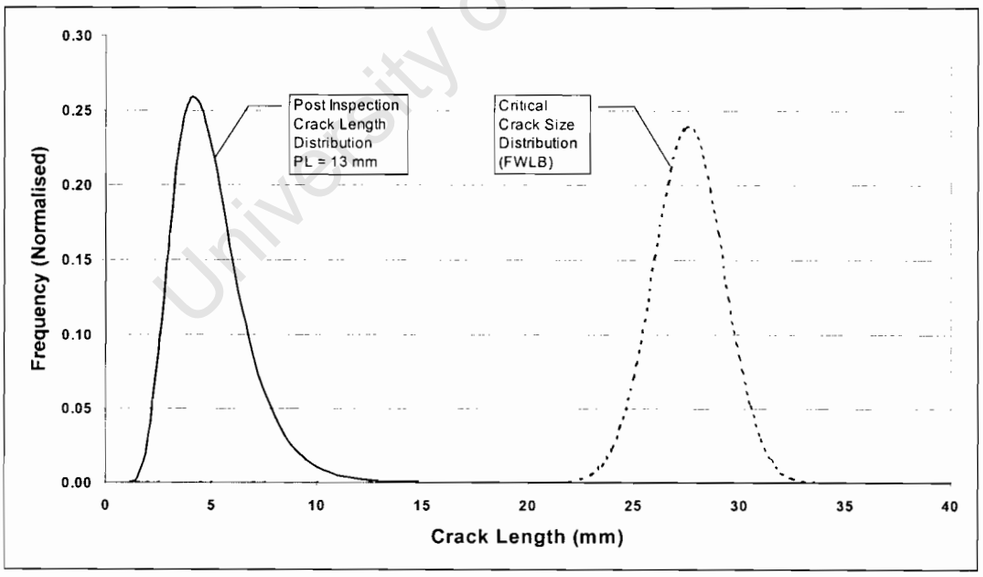

The expected low tube rupture probabilities have been verified by the MCS performed. After 5,000,000 iterations (given a Δt of 1 year) no failure occurrences were observed. Since the failure probability is simply the number of failure occurrences divided by the number of iterations, the tube rupture failure probability, given a plugging limit of 13 mm, may be considered less than 2E-07
(i.e. less than 1 / 5,000,000).

However, to verify the capability of the MCS method, developed in this study, particularly it's ability to converge to a particular solution, an artificial scenario was set up to increase the area of overlap and thus the failure probability. This was achieved by removing the restriction on the upper bound crack growth rate as defined in chapter 7.3.5. The results are listed in the table below:

Table 14: Tube Rupture Probabilities for Artificial Scenario

Δt	Δt = 0 yr	Δt = 0.25 yr	Δt = 0.5 yr	Δt = 0.75 yr	Δt = 1 yr
Tube Rupture Probability	8.03E-07	1.079E-05	1.831E-04	1.129E-03	2.738E-03

In all cases, the Direct MCS converged to the target value established earlier. A plot of tube rupture probability versus time is shown below.

Figure 32: Tube Rupture Probability vs Time (Artificial Scenario)

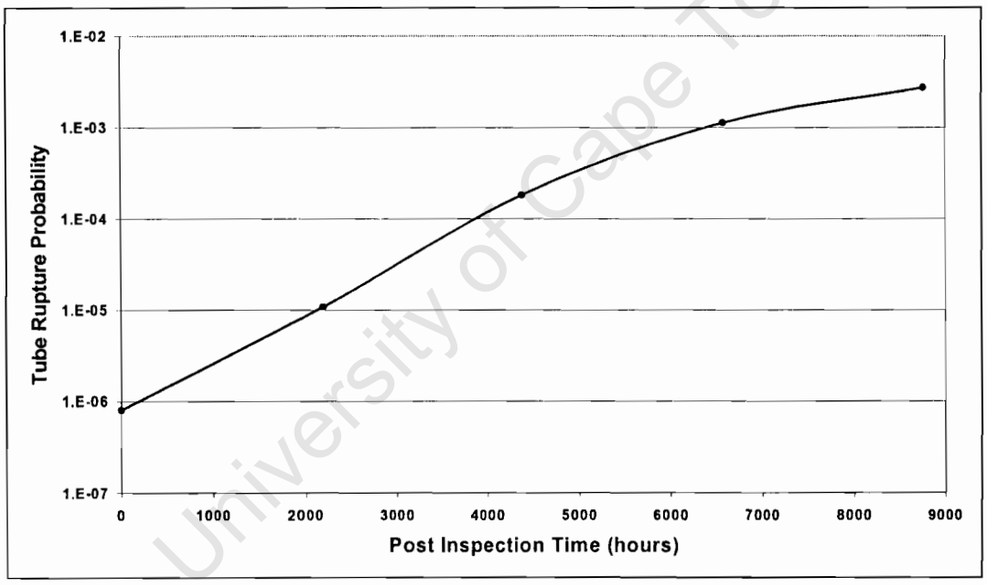

8.2 SGTR Probability

Assuming that a SG tube failure can be described by a Poisson's process*, the probability P_{SGTR} of having one or more tubes failed in a SG tube bundle containing M cracks is given by [75] (for large values of M):

$$P_{SGTR} = 1 - e^{(-M P_{TR})} \qquad \text{Equation 27}$$

The parameters and resultant solution of the equation 27 is given below for the Koeberg SGTR Probability:

Table 15: Koeberg SGTR Probability

Parameter	Value
SG	SG 95 (Unit 1)
Outage	113
PL	13 mm
Operating Condition	FWLB
P_{TR}	< 2.00E-07
M	1307
P_{SGTR}	< 2.61E-04

This is well within the upper limit established earlier of 1E-02. This implies that the maintenance regime (inspection frequency and plugging limit) serves its purpose well and may in fact be too restrictive.

Due to the low failure probabilities being considered it is difficult to establish the effect of plugging limit on the eventual SGTR probability. However, it is clear from Figure 24 that plugging limits of 11 to 17 mm are virtually indistinguishable and would result in essentially the same tube rupture probability. Reducing the plugging limit would result in SGTR probabilities lower than the value quoted above due to the reduction in weighting of the right tail of the distributions.

It should be noted that these observations are specific to the SG being considered and the crack population found during the outage being considered. SG 95 is considered the most degraded SG at Koeberg and as such establishes a bounding case for the SGTR probabilities of the other SG's.

* Poisson's processes are characterised by their time dependence, namely, the fact that certain events do or do not occur (depending largely on chance) at regular intervals of time or throughout continuous intervals of time. The mathematical model used to describe processes of this type is the Poisson's distribution [65].

Equation 27 leads to an interesting consideration. This equation indicates that the SGTR probability is a function of both the Tube Rupture probability and the number of cracked tubes in the tube bundle. Plugging criteria have always been focussed on minimising the individual tube rupture probabilities P_{TR}, however, a situation may arise where the population of cracked tubes may be the critical parameter. For example, a cracked tube population of 1307, in combination with tube rupture probabilities in excess of 7.67E-06, would result in an SGTR probability which exceeds the limit set earlier of 1E-2. Thus plugging would be required due to the number of cracked tubes and not due to conventional plugging criteria. This situation is illustrated in the figure below:

Figure 33: SGTR Probability vs Number of cracked tubes (Special Case)

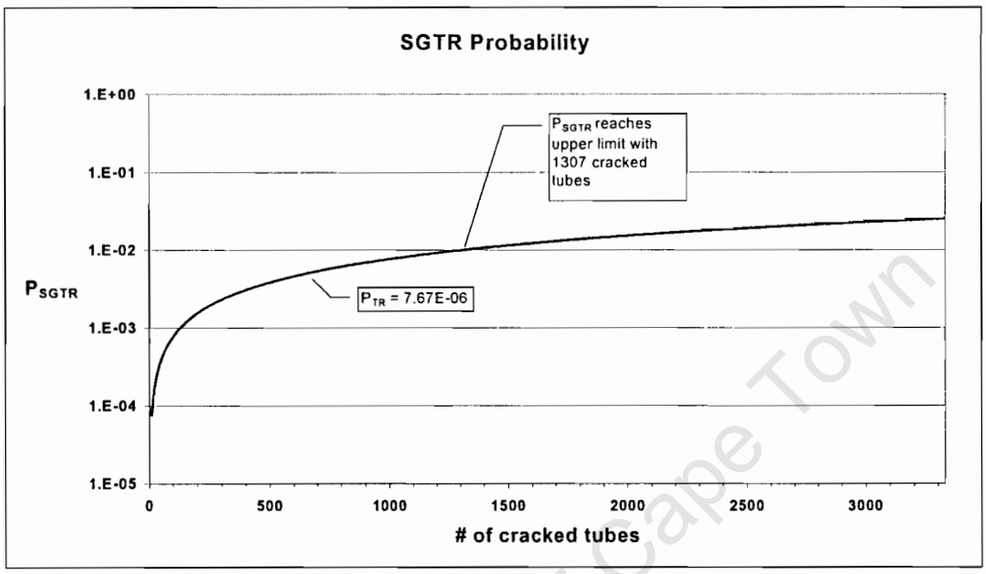

9 Concluding Remarks and Recommendations

9.1 Concluding Remarks

The initial literature review hinted at promising trends between certain metallurgical parameters and tube cracking susceptibility. However, a study of these parameters, using the Koeberg SG database, could not confirm any of these trends. It would however be useful to study these parameters again at a later date when more data has been collected, since a larger database might reveal trends not evident at this stage. These metallurgical trends might be used to develop "intelligent" inspection scopes focussing on the most susceptible tubes.

The probabilistic fracture mechanics model developed in this study has been based on various aspects of the EdF and JSI approaches. A direct Monte Carlo Simulation was used to determine the True Crack length distribution, the Critical Crack length distribution, and the resultant Tube Rupture probability. This particular study was based on the Outage 113 data for SG 95, considered the most degraded SG at Koeberg.

The Post Inspection crack length distribution generated for various plugging limits indicated that plugging limits of 11 to 17 mm would yield identical tube rupture probabilities. A significant decrease in tube rupture probability can only be obtained by reducing the plugging limit to 7 mm, however this would lead to excessive plugging and subsequent analysis showed that decreasing the plugging limit is not justified. The generation of the Post Inspection crack length distribution was based on a subjective choice of various distributions. In all cases, the distribution was chosen, which had the "heaviest" right hand tail and would thus lead to the most conservative tube rupture probabilities. The EdF and JSI approaches, although different to the method used in this study, also rely on this subjective choice of distributions.

The Critical Crack length distribution revealed the disadvantages of typical deterministic approaches and also indicated that the plugging limit of 13 mm, as used at Koeberg, is well within acceptable limits even for the postulated accident condition. The parameters defining the Critical Crack length was subjected to a sensitivity analysis. This analysis suggested that it would be more beneficial to know the exact distributions of tube thickness and the mechanical properties of the SG tubes as opposed to the flow stress factor and tube diameter. This allows future research to be more focussed on the parameters that really count. This sensitivity analysis highlights the usefulness of probabilistic methods as opposed to the traditional deterministic approach.

Even before the MCS was performed to determine the Tube Rupture probability, it was evident that the probabilities would be very low. This was based on an inspection of the area of overlap between the Post Inspection crack length distribution and the Critical Crack length distribution. The MCS performed indicated zero failure occurrences even after 5,000,000 iterations. This indicated that the Tube Rupture probability was less than 2E-07 (i.e. less than 1 / 5,000,000). This implies that the overall SGTR probability is less than 2.61E-04, which is well below the established upper limit. These results indicate that the current SG maintenance and operating regime (plugging limit, inspection scope, ORT, chemistry, etc.) have contributed to a very safe SG.

It should be noted that the current study only considers axial PWSCC in the RTZ. The other degradation mechanisms, such as U-bend cracking and secondary side intergranular attack have not been evaluated.

To verify the capability of the MCS method, particularly it's ability to converge to a particular solution, an artificial scenario was set up to increase the area of overlap and thus the failure probability. This was achieved by removing the restriction on the upper bound crack growth rate. The results indicated much higher Tube Rupture probabilities and converged successfully at each time increment.

The equation defining the SGTR probability includes the Tube Rupture probability and the number of cracked tubes. It was shown that the limit of 1E-02 would be exceeded for the current cracked tube population of 1307 if the individual Tube Rupture probabilities exceeded 7.67E-06. Therefore, this may be considered an additional factor to respect when evaluating SG tube bundles after future outages.

This study has thus quantified the benefits of the various measures in place at Koeberg to ensure the safe operation of the SG's. It has also highlighted the advantages of probabilistic methods, particularly the ability of Monte Carlo simulation methods to analyse complex situations.

The significant potential for risk based SG life-time optimisation is thus evident.

9.2 Recommendations

The MCS method developed in this study is considered adequate as an initial attempt. Various aspects of the model can be refined and extended. This can be achieved easily as the model has been set up in a modular form. The following recommendations should be considered in future developments:

- Variance Reduction Techniques such as Importance Sampling or Stratified Sampling should be included since these methods increase the efficiency and accuracy of the simulation. These methods require a relatively small number of simulation cycles, however, the level of computational difficulty for each simulation cycle increases.
- The current model does not take credit for the leak detection ability available to the operators. The model developed by EdF accounts for this ability in the form of leak detection probabilities. However, information regarding this model is not very clear but may be worth further investigation.
- The metallurgical trends discussed earlier warrants further investigation, as this would highlight susceptible tube batches. This information could be used to develop "intelligent" inspection scopes and may also be added as a sub-module in the current MCS model. The effect of this modified inspection scope could then be quantified.
- The sensitivity analysis performed on the parameters defining the Critical Crack size indicated that the tube thickness and mechanical properties were most significant. It may be beneficial to verify these parameters for use in future models.
- The method used by EdF to generate the Post Inspection defect size distribution appears to be more rigorous than the method used in this study, and should be considered for future revisions of this model.
- Other degradation mechanisms such as circumferential cracking, U-bend cracking, and secondary side intergranular attack should be included in future revisions of the model depending on the availability of the instability criteria and crack propagation laws defining these degradation mechanisms.

List of References

1. Kirk-Othmer
   Encyclopedia of chemical technology (4th Edition), Volume 17
   John Wiley and Sons Inc., 1996

2. Younes, C M, Morrissey, F H, Allen, G C
   Interface Analysis Centre, University of Bristol, UK
   McIntyre, P
   National Power plc Research and Engineering, UK.
   'Effect of heat treatment on grain boundary chemistry and resistance to intergranular corrosion of alloys 600 and 690'
   BRITISH CORROSION JOURNAL, Vol. 32, no. 3, 1997, pg. 185-192

3. Sung, J K
   Materials and Processes Research Centre, Research Institute of Industrial Science and Technology (RIST), Korea
   'Effect of Heat Treatment on Caustic Stress Corrosion Cracking behaviour of Alloy 600.'
   CORROSION – NACE, Vol. 55, no.12, December 1999, pg.1144-1154.

4. Anderson, T L
   FRACTURE MECHANICS
   Fundamentals and Applications (2nd Edition)
   CRC Press, Inc. 1995

5. Ewalds, H L and Wanhill, R J H
   FRACTURE MECHANICS
   Edward Arnold (Publishers) Ltd., 1984

6. Roberts, J T Adrian
   EPRI Palo Alto, California
   STRUCTURAL MATERIALS IN NUCLEAR POWER SYSTEMS
   Plenum Press, New York, 1981

7. Crombie, R
   AEA Technology
   'Koeberg Steam Generator Tube Degradation Safety Justification'
   Ref. No.: AEA/RESI/24072002/R/002 Final Issue
   Prepared for Koeberg NPS
   September 1997

8. Coriou, H, Grall, L, Le Grall, Y, and Vettier, A
   'Corrosion sous contraite de l'Inconel dans l'eau a'haute temperature'
   Third Metallurgy Conference on Corrosion, Saclay, North Holland Publishing Co., Amsterdam, p. 161 (1959)
   Cited by
   Domain *et al.* [19]

9. Stein, A A and Deleon, A
   Stone and Webster Engineering Corporation, Boston, USA
   A R McIlree
   Electric Power Research Institute (EPRI)
   'Predicting Stress Corrosion Cracking in Steam Generator tubing'
   POWER ENGINEERING, May 1985, pg. 53-56.

10. Newman R.C. and Proctor R.P.M.
Corrosion and protection centre, University of Manchester,
Institute of Science and Technology.
'Stress Corrosion Cracking: 1965 – 1990'
BRITISH CORROSION JOURNAL, 1990, vol. 25, no. 4, pg. 259-269.

11. Tsai, W T and Kuoh C C
Department of Materials Science and Engineering, National Cheng kung University, Taiwan, Republic of China.
'Corrosion Fatigue Crack Growth Rate in Sensitized Alloy 600 in Thiosulfate Solution at room temperature'
CORROSION – NACE, Vol. 55, no. 6, June 1999, pg. 554-560

12. Totsuka, N
Corrosion Laboratoy, Kawasaki Steel Corp., Japan
Szklarska – Smialowska, Z
The Ohio State University, Dept. of Metallurgical Engineering, Columbus.
'Effect of electrode potential on the Hydrogen – Induced IGSCC of Alloy 600 in an aqueous solution at 350 ^{0}C'
CORROSION - NACE, vol. 43, no. 12, December 1987.

13. Thomas, L E and Bruemmer, S M
Pacific Northwest National Laboratory, Richland, WA 99352
'High-Resolution Characterisation of Intergranular Attack and Stress Corrosion Cracking of Alloy 600 in High-Temperature Primary Water.'
CORROSION – NACE, Vol. 56, no.6, June 2000, pg. 572-587.

14. Bouecke, R, Odar, S and Stellwag, B
Siemans AG, Power Generation Group (KWU)
'Operating experience with Steam Generators'
Service Report, Power plants, Dec. 1989

15. Wicker, C A
Eskom, TRI
'Steam Generator Health Care – Nuclear Engineering Position Paper.'
Ref. No.: KBA 0022 N NEPO NEPP 016
August 1995

16. Norring, K, Studsvik Energiteknik AB, Nyköping, Sweden
Engström, J, Swedish State Power Board, Vällingby, Sweden
Norberg, P, AB Sandvik Steel, Sandviken, Sweden.
'IGSCC in steam generator tubing. Testing of alloy 690 and alloy 600 tubes.'
THE METALLURGICAL SOCIETY, 1988

17. Woodward, J, van Rooyen, D and McIlree, A R
Brookhaven National Laboratory, New York
'In-Situ stress relief of expanded alloy 600 steam generator tubing.'
Prepared for Electric Power Research Institute (EPRI)
May 1983.

18. Scott, P M
Framatome, France
'Stress Corrosion Cracking in Pressurized Water Reactors – Interpretation, Modelling, and Remedies'
Presented as the F N Speller Award Lecture at CORROSION 2000, March 2000, Orlando, FL
CORROSION – NACE, Vol. 56, no.8, August 2000, pg. 771-782.

19. Domain, H A, Emanuelson, R H, Sarver, L W, Theus, G J and Katz, L
Babcock and Wilcox
'Effect of microstructure on stress corrosion cracking of Alloy 600 in high purity water.'
CORROSION – NACE vol. 33, no. 1, January 1977, pg. 26-37.

20. Stein, A A
Stone and Webster Engineering Corporation, Boston, USA
'Predicting stress corrosion cracking of alloy 600 steam generator tubing in primary water.'
CORROSION PREVENTION AND CONTROL, Dec. 1986.

21. Economy, G, Jacko, R J
Westinghouse Research and Development Centre, Pittsburgh.
Pement, F W
Westinghouse Service Technology Division, Pittsburgh.
'IGSCC Behaviour of Alloy 600 Steam Generator Tubing in Water or Steam Tests above 360 ^{0}C'
CORROSION - NACE, vol. 43, no. 12, December 1987, pg. 727-738.

22. Nicholls, D.R
Eskom, Koeberg Nuclear Power Station, Nuclear Engineering Division
'Steam Generator Tubes Roll Transition Intergranular Stress Corrosion Cracking Safety Case'
Report RR3684 / Submission KSS 6.46
November 1987

23. Andresen, P L
'Effects of temperature on crack growth rate in sensitised type 304 SS and alloy 600'
CORROSION, Sept. 1993, pg. 714-725.

24. Ashby, M F and Jones, D R H
ENGINEERING MATERIALS 1
An introduction to their properties and Applications
Pergamon Press Ltd., 1980

25. Hutin, J.P, EdF SPT, France
Billon, F, Framatome, France
'Flaw Analysis in SG tubes.'
INT. J. PRES. VES. & PIPING **25** (1986) 267 – 278

26. Lemaire, P EdF
Approved by Senne, A EdF
Nuclear Power Plant Operation Division, Maintenance Department
'Maintenance Policy – EdF Steam Generator Tube bundles'
Doc. No.: D4002-42-57/97-058 NT, Issue 0
February 1997

27. Bruemmer, S M, Charlot, L A and Henager, C H, Jr.
Battelle, Pacific Northwest Laboratories, Washington
'Microstructure and Microdeformation effects on IGSCC of Alloy 600 Steam Generator tubing.'
CORROSION, November 1988, pg. 782-788.

28. Tsai, C H, Kai, J J, Yu, G P and Hsu, S S
National Tsing Hua University
Hsinchu, Taiwan, ROC
'On the critical chromium concentration of Inconel 600 in different test methods'
THE METALLURGICAL SOCIETY, 1988

29. Sedriks, A J, Floreen, S and McIlree, A R.
The International Nickel Company, Inc., New York.
'The effect of Nickel content on the Stress Corrosion cracking resistance of Fe-Cr-Ni Alloys in an elevated temperature caustic environment.'
CORROSION - NACE , October 1975

30. Owens, C M
Combustion Engineering, Inc., Windsor
'Stress corrosion cracking performance of mill – annealed, Inconel – 600 tubing in steam generators'
Presented during CORROSION/85,Paper No. 93, NACE, Houston, TX, 1985
MATERIALS PERFORMANCE, January 1986, pg. 49-54.

31. Stein, A A
Stone & Webster Engineering Engineering Corporation, Boston, Massachusetts
'Development of microstructural correlations and tubing specification for Alloy 600.'
Prepared for Electric Power Research Institute (EPRI)
March 1985.

32. Ashby, M F and Jones, D R H
ENGINEERING MATERIALS 2
An introduction to Microstructures, Processing and Design.
Pergamon Press Ltd., 1986

33. EPRI NP-3051
'Optimisation of Metallurgical Variables to Improve Corrosion Resistance of Inconel Alloy 600.'
Final Report, Research Project 1708-1, Electric Power Research Institute, July 1983.
Cited by
Green S J (EPRI) [37]

34. Bandy, R and van Rooyen, D
Department of Nuclear Energy Corrosion Science Group, Brookhaven National Laboratory, Upton, NY
'Stress Corrosion Cracking of Inconel Alloy 600 in High Temperature Water – An Update'
CORROSION - NACE, vol. 40, no. 8, August 1984.

35. ASM Handbook Committee
ASM Handbook, 8th Edition
Metals Handbook, Vol. 9
METALLOGRAPHIC TECHNIQUES AND MICROSTRUCTURES
ASM International, 1998

36. Le, N V
University of Quebec in Montreal, Mechanical Department, Montreal, Canada
'Nuclear Steam Generator tube failures: Analysis and Recommendations'
American Society of Mechanical Engineers (Paper) Published by ASME, New York, USA
ASME paper 84 - WA/DE – 20, 1984

37. ASM Handbook Committee
ASM Handbook, 6th Edition
Metals Handbook, Vol. 13
CORROSION
ASM International, 1998

38. Kishida, A and Takamatsu, H, The Kansai Electric Power Co., Inc.
Kitamura, H and Isobe, S, Kyushu Electric Power Co. , Inc.
Onimura, K, Ariska, K, Hattori, T, Arai, T and Sato, M
Mitsubishi Heavy Industries, Ltd
'The causes and remedial measures of steam generator tube intergranular attack in Japanese pressurised water reactors.'
THE METALLURGICAL SOCIETY, 1988

39. Partridge, M J, Dominion Engineering, Inc.
Paine, J P N, Electric Power Research Institute
Williams , C L, Electric Power Research Institute
'Crevice flushing as a remedy for IGA / IGSCC.'
THE METALLURGICAL SOCIETY, 1988

40. Navas, M, Gomez, D, Garcia-Mazario, M
Centro de Investigaciones Energeticas Medioambientales y Tecnologicas (CIEMAT), Madrid, Spain.
McIlree, A R
EPRI
Effect of Silicon compounds on Stress Corrosion Cracking of Alloy 600 in Caustic Solutions.
CORROSION – NACE, Vol. 55, no.7, July 1999, pg. 674-685.

41. Hwang, I S
Department of Nuclear Engineering, Seoul National University, Seoul, Korea.
Park, I G
Division of Materials Science and Engineering, Sun Moon University, Chungnam, Korea.
'Control of Alkaline Stress Corrosion Cracking in Pressurised-Water Reactor Steam Generator Tubing'
CORROSION – NACE, Vol. 55, no. 6, June 1999, pg. 616-625.

42. Kawamura, H and Hirano, H
Central Research Institute of the Electric Power Industry, Komae Research Laboratory, Japan
'Intergranular Attack and Stress Corrosion Cracking Propogation behaviour of Alloy 600 in high temperature caustic solution'
CORROSION – NACE, Vol. 55, no. 6, June 1999, pg. 566-575.

43. EPRI NP-3029
'Evaluation of Steam Generator tube R12C66 from Indian Point 3.'
Final Report, Research Project S138-6, Electric Power Research Institute, May 1983.
Cited by
Green S J (EPRI) [37]

44. Garnsey, R Central Electricity Generating Board, UK
'Corrosion of PWR Steam Generators'
Report RD/L.N/4/79, Job No. VF163 (March 1979)
Cited by
Roberts, J T A [6]

45. Van Rooyen, D and Weeks, J R Brookhaven National Laboratory, New York
'Denting of Inconel Steam Generator Tubes in Pressurized Water Reactors'
Final Report, BNL-NUREG-50778 (January 1978)
Cited by
Roberts, J T A [6]

46. Davies, M A
AEA Technology
'A review of the current status of the steam generators at Koeberg (Units 1 and 2)'
Ref. No.: AEA/RESI/24072002/R/001 Final Issue
Prepared for Koeberg NPS
December 1997

47. Horrocks, P J AEA Technology, March 1994
'International working group on life management of NPP. Specialist meeting on steam generator problems and replacement. 13-16 December 1993, Madrid, Spain.'
IAEA
Cited by
Davies, M A [46]

48. Haasbroek, A C
Eskom, Koeberg Nuclear Power Station, Design Engineering Division
'Koeberg Nuclear Power Station Steam Generator Tubing Integrity Safety Case'
Submission KSS 6.48

49. de Surgy, J, Hutin, J P and Serres, R
EdF, Service de la Production Thermique, Paris, France
'Tube performance at EdF 900Mwe units – an update'
NUCLEAR ENGINEERING INTERNATIONAL, January 1988, pg. 21-23.

50. ASM Handbook Committee
ASM Handbook, 9th Edition
Metals Handbook, Vol. 17
NONDESTRUCTIVE EVALUATION AND QUALITY CONTROL
ASM International, 1992

51. Gutzwiller, J E and Glass, S W, Babcock and Wilcox Company
'New options for improved steam generator U-bend integrity.'
INT. J. PRES. VES. & PIPING **34**, (1988) 95 – 108

52. Pement, F W and Economy, G, Westinghouse Electric Corp.
A R McIlree, Electric Power Research Institute (EPRI)
Gorman, J A, Dominion Engineering, Inc
'Treatment of alloy 600 simulated tube – tube sheet transitions for improved resistance to primary water SCC. Performance of treated specimens in accelerated environments.'
THE METALLURGICAL SOCIETY, 1988

53. Vaccaro, F P, Theus, G J, Miglin, B P, Monter, J V, Helmley, J M, Jenkins, A L and Lauer, J A.
Babcock and Wilcox Company
'Remedial measures for stress corrosion cracking of alloy 600 steam generator tubing.'
THE METALLURGICAL SOCIETY, 1988

54. Slama, G
Steam Generator Department, Framatome, France.
'Five years of Shot-Peening experience.'
FRAMATOME NEWSLETTER No. 39, 1990

55. Tait, R B
Associate Professor, Department of Mechanical Engineering, University of Cape Town
Personal Interview, 29 April 1999.

56. Stubbe, M J, Hernalsteen, P (BELGATOM-Laborelec)
Lablois C (BELGATOM-Tractebel)
Gelpi, M A, Michaut, B, Slama, G (FRAMATOME)
'Repair of Steam Generator Tubing by Nickel Plating'
FRAMATOME–Nuclear Products and Services, 1989

57. Bourdelet, M and Brocard, C
Framatome, France
'Chemical cleaning of steam generator secondary side'
FRAMATOME 3N91, PLANT OPERTION AND ITS ENVIRONMENT, October 1991

58. Kawamura, H and Hirano, H
Central research Institute of Electric Power Industry, Komae Research Laboratory, Tokyo, Japan
Shirai, S
Hokkaido Electric Power Co., Facilities Management Sec., Nuclear Power Dept., Higashi, Japan
Takamatsu, H, Matsunaga, T
The Kansai Electric Power Co., General Office of Nuclear and Fossil Power Production, Osaka, Japan
Yamaoka, K
The Shikoku Eectric Power Co., Ikata Nuclear Power Station, Kagawa, Japan
Oshinden, K
The Kyushu Electric Power Co., Genkai Nuclear Power Station, Fukuoka, Japan
Takiguchi, H
The Japan Atomic Power Co., Plant Engineering Dept., Tokyo, Japan
'Inhibitory effect of Zinc addition to High-Temperature Hydrogenated Water on Mill-Annealed and Prefilmed Alloy 600'
CORROSION – NACE, Vol. 56, no.6, June 2000, pg. 623-637.

59. Nicolson, H J H & Madlener, A F
Nuclear Engineering Department
ESKOM, Koeberg Nuclear Power Station
'Life Cycle Management of the Koeberg Steam Generators'
ICONE 5-2556
Proceedings of ICONE 5: 5th International Conference on Nuclear Engineering.
May 26-30, 1997, Nice, France

60. Lim, Y S and Kim, J S
Korea Atomic Energy Research Institute, Taejon, South Korea
Kwon, H S
Department of Materials Science and Engineering, Korea Advanced Institute of Science and Technology, Taejon, South Korea.
'Effects of sensitization treatment on the evolution of Cr carbides in rapidly solidified Ni-base Alloy 600 by a CO_2 laser beam.'
MATERIALS SCIENCE AND ENGINEERING A279 (2000) 192 – 200, February 2000.

61. Flesch, B
EdF, France
Cochet, B
Framatome, France
'Leak-Before-Break in Steam Generator Tubes.'
INT. J. PRES. VES & PIPING .**43** (1990), pg. 165-179.

62. Stein, A A
Stone and Webster Engineering Corporation, Boston, USA
'The use of activation energy for stress corrosion cracking to predict life of alloy 600 in primary water.'
Prepared for Electric Power Research Institute (EPRI)
March 1985

63. Elishakoff, I
PROBABILISTIC THEORY OF STRUCTURES
2ND Edition
Dover Publications, Inc. 1999

64. Sundararajan, C. (Editor)
PROBABILISTIC STRUCTURAL MECHANICS HANDBOOK
Theory and Industrial Applications
Chapman & Hall, 1995

65. Miller and Freund
PROBABILITY AND STATISTICS FOR ENGINEERS
5th Edition
Prentice-Hall International, Inc. 1994

66. Pitner, P, Riffard, T, Granger, B and Flesch, B, Electricité de France (EdF)
'Application of probabilistic fracture mechanics to optimise the maintenance of PWR steam generator tubes. '
NUCLEAR ENGINEERING AND DESIGN 142 (1993) 89-100

67. Mavko, B and Cizelj, L
Jozef Stefan Institute, Reactor Engineering Division
'Failure probability for axially cracked steam generator tubes: A probabilistic fracture mechanics model.'
NUCLEAR TECHNOLOGY, vol.98 May 1992, pg. 171-177.

68. Barnier, M, CEP Systèmes
Pitner, P and Riffard, T, (EdF)
'Estimation of crack size distribution from in-service inspection data for the calculation of failure probabilities'
European Safety and Reliability Conference, Copenhagen, 1992, pg. 527-538.

69. Pitner, P, Riffard, T and Flesch, B, Electricité de France (EdF)
'Failure analysis module for the probabilistic fracture mechanics code for pressurised water reactor steam generator tube maintenance'.'
SMiRT 11, Tokyo, 1991

70. Pitner, P, Riffard, T, Procaccia, H, Granger B, Faidy, C and Flesch, B, Electricité de France (EdF)
'Probabilistic fracture mechanics code for the pressurised water reactor steam generator tube maintenance.'
SMiRT 11, Tokyo, 1991

71. Cizelj, L and Mavko, B
Jozef Stefan Institute, Reactor Engineering Division, Slovenia
Riesch-Opperman, H
Institut für material forschung II, kernforschungszentrum, Germany
'Application of first and second order reliability methods in the safety assessment of cracked steam generator tubing'
NUCLEAR ENGINEERING AND DESIGN, vol. 147 (1994), no. 3, pg. 359 – 368

72. Cizelj, L and Mavko, B
Jozef Stefan Institute, Reactor Engineering Division, Slovenia
'On the Risk-Based Steam Generator Lifetime Optimisation'
Theoretical and Applied Fracture Mechanics 23 (1995) 129-137

73. Cizelj, L and Mavko, B
Jozef Stefan Institute, Reactor Engineering Division, Slovenia
Riesch-Opperman, H
Institut für material forschung II, kernforschungszentrum, Germany
'Propagation of Stress Corrosion Cracks in Steam Generator Tubes'
INT. J. PRES. VES. & PIPING **63** (1995) 35-43

74. Cizelj, L and Mavko, B, Vencelj, P
Jozef Stefan Institute, Reactor Engineering Division, Slovenia
'Reliability of Steam Generator Tubes with Axial Cracks'
Journal of Pressure Vessel Technology 118 (1996) 441-446.

75. Cizelj, L and Mavko, B
Jozef Stefan Institute, Reactor Engineering Division, Slovenia
'Application of probabilistic fracture mechanics to define steam generator tube plugging limit'
European Safety and Reliability Conference, Copenhagen, 1992, pg. 539-549.

76. Frederick, G, Mathonet, J, Hernalsteen, P, and Dobbeni, D
'Development and justification of new plugging criteria applicable to the cracking phenomena in the tubing of steam generators'
Belgatom, Brussels, Belgium (1989)
Cited by
Mavko, B and Cizelj, L [67]

77. Kastner, W, Röhrich, E, Schmitt, W, and Steinbuch, R
Kraftwerk Union AG, Erlangen, Federal Republic of Germany.
'Critical Crack Sizes in Ductile Piping'
INT. J. PRES. VES. & PIPING **9** (1981) 197 – 219

78. Hahn, G T *et al.*
'Criteria for crack extension in cylindrical pressure vessels.'
INTERNATIONAL JOURNAL OF FRACTURE MECHANICS
Vol 5, pg 187 – 210, 1969
Cited by
Kastner, W *et al.* [77]

79. Hernalsteen, P, Laborelec, Linkebeek, Belgium
'The influence of testing conditions on burst-pressure assessment for Inconel tubing'
INT. J. PRES. VES. & PIPING **52** (1992) 41 – 57,

80. Gentle, J E
RANDOM NUMBER GENERATION AND MONTE CARLO METHODS
Springer-Verlag New York, Inc., 1998

81. Hammersley, J M and Handscomb, D C
MONTE CARLO METHODS
John Wiley and Sons, Inc., 1965

82. Newman, T G and Odell, P L
THE GENERATION OF RANDOM VARIATES
Charles Griffin & Company Limited, 1971

83. Rubinstein, R Y
SIMULATION AND THE MONTE CARLO METHOD
John Wiley and Sons, Inc., 1981

84. Ford, F P
'Mechanistic interpretation of design and evaluation code for environmentally-assisted cracking'
CORROSION, Houston (1986)
Cited by*
Pitner et al. [66]

85. Hearne, D
Eskom, TRI
'Steam Generator Health Care – Nuclear Engineering Position Paper.'
Ref. No.: KBA 0022 N NEPO NEPP 016 Rev. 1
22 October 2002

* In some cases, specific journal articles could not be obtained due to proprietary or language constraints. However, the intent of these papers could often be determined by the context of the journal articles, which referenced them. These secondary articles are referenced as "Cited by:"

APPENDICES

A. Additional Tables

Table A1: Main Components of the Koeberg SG Tube Bundles [46]

Component	Description	Material
Tube sheet	A single piece forging with a diameter of 3454mm and thickness of 534mm. 2 x 3330 holes are drilled in the tube sheet to receive the heat exchanger tubes.	SA 508 class 3
Tube Bundle	3330 inverted U-shaped Vallourec tubes welded to the tube sheet. Tube dimensions: • OD: 22.2mm • Thickness: 1.27mm The bending radius varies from 55.6mm to 1519.9mm The straight sections have a maximum out of round tolerance of 1.4%. The curved sections have a maximum out of round tolerance of 6%*.	Mill Annealed Inconel 600 alloy [Nickel based alloy SB 163 (ASME)]†
Integral Tube Support Plates	The support plates are placed at appropriate height intervals to maintain proper tube spacing. The support plates transmit loads and displacements from the shell to the tube bundle. Seven 30mm thick, plates containing cruciform broached (quatrefoil design) tube penetration ports which support the tube in four places around the periphery of the tube with open areas to improve thermal hydraulic properties of the secondary water in the vicinity of the holes. The choice of material further reduces the risk of corrosion and constrictions in the penetrations.	Z10 C13(AFNOR) Martensitic Stainless Steel
Upper Tube Support Plate	Plate containing mainly cruciform broached (quatrefoil design) tube penetration ports. Towards the periphery of the plate some ports are drilled.	Z10 C13(AFNOR) Martensitic Stainless Steel
Tie Rods	Used to secure the support plates.	Stainless Steel 17-4-1
Blowdown System	The lower portion of the secondary system has two perforated tubes installed on top of the tube sheet.	
AVB	Anti-Vibration bars. Rods used to stabilise the upper tube bundle which is subject to vibration due to fluid – structure interaction.	Chrome plated, Inconel 600
Tube Wrapper	A cylinder surrounding the tube bundle.	SA 508 Class 3

* Out of round allowance is equal to the difference between the minimum and maximum diameters to the nominal diameters of the tube.

† Koeberg Unit 1, SG 3 was rejected by Eskom and replaced with a SG fitted with thermally treated Inconel 600 tubing.

Table A2: Tube Bundle Heat Certificate Data [46]

Property	Unit 1			Unit 2		
	SG 1 (96)	*SG 2 (95)*	*SG 3 (77)*	*SG 1 (98)*	*SG 2 (99)*	*SG 3.(100)*
C%	0.023	0.027		0.022	0.021	0.021
Si%	0.314	0.284		0.324	0.329	0.330
Mn%	0.718	0.710		0.718	0.720	0.714
Ni%	74.154	74.159		73.951	73.956	74.139
Cr%	15.985	16.047		15.980	16.022	16.021
Cu%	0.026	0.032		0.027	0.029	0.028
Co%	0.032	0.035		0.026	0.028	0.028
Ti%	0.273	0.208		0.316	0.301	0.294
Al%	0.175	0.176		0.208	0.206	0.209
Fe%	8.244	8.266		8.356	8.425	8.332
GS[*]	85.290	87.847		83.666	84.100	85.164
Yield Strength (MPa) (Room Temperature)	319.106	323.419		305.029	301.664	309.430
Yield Strength (MPa) (Op. Temperature)	253.635	256.135		248.050	245.846	250.909
UTS (MPa) (Room Temperature)	701.506	707.659		705.688	704.948	705.679
UTS (MPa) (Op. Temperature)	644.346	658.322		645.971	654.441	658.162

GS: Grain Size
UTS Ultimate Tensile Strength

[*] According to Afnor NF A04 102 (French Standard)

Table A3: Koeberg Unit 1 Inspection Summary [46]

Unit 1			
Inspection	SG 1 (96)	SG 2 (95)	SG 3 (77)
PSI	Bobbin Coil 100% DIA Test	Bobbin Coil 100% DIA Test	Bobbin Coil 100% DIA Test
RERUN	100% re-read of PSI BC tapes in hot leg	100% re-read of PSI BC tapes in hot leg	100% re-read of PSI BC tapes in hot leg
101	Bobbin Coil: • 1 in 8 • periphery (2 deep) • row 1 • Previous indications Visual Examination: • periphery	Bobbin Coil: • 1 in 8 • periphery (2 deep) • row 1 • Previous indications Visual Examination: • periphery	Bobbin Coil: • 1 in 8 • periphery (2 deep) • row 1 • Previous indications Visual Examination: • periphery
102	Bobbin Coil: • 1 in 8 • Previous indications Rotating Pancake Coil: • All BC crack indications Visual Examination: • Periphery Extension: • BC 1 in 4 in sludge zone	Visual Examination: • Periphery	Visual Examination: • Periphery
103	Visual Examination: • Periphery	Bobbin Coil: • 1 in 8 • periphery (2 deep) • Previous indications Rotating Pancake Coil: • 100% of sludge zone • High expansion anomalies • All BC crack indications • 2 leg extensions Visual Examination: • Periphery	Visual Examination: • Periphery
104	Bobbin Coil: • periphery (1 deep) • Previous indications Rotating Pancake Coil: • 1 in 8 • 100% of sludge zone • previous indications Visual Examination: • Periphery	Helium Leak Test Bobbin Coil: • periphery (1 deep) • Previous indications • He leaking Tubes Rotating Pancake Coil: • 1 in 8 • 100% of sludge zone • previous indications Visual Examination: • Periphery	Bobbin Coil: • 1 in 8 • periphery (2 deep) • row 1 • Previous indications Rotating Pancake Coil: • 100% of sludge zone • previous indications Visual Examination: • Periphery
105	Bobbin Coil: • 1 in 8 • periphery (1 deep) • rows 1 and 2 • Previous indications Rotating Pancake Coil: • 100% of SG tubes Visual Examination: • Periphery • Sludge zone	Bobbin Coil: • periphery (1 deep) • rows 1 and 2 • Previous indications Rotating Pancake Coil: • 100% of SG tubes Visual Examination: • Periphery • Sludge zone	Bobbin Coil: • periphery (1 deep) • rows 1 and 2 • Previous indications Rotating Pancake Coil: • 100% of Sludge zone • previous indications Visual Examination: • Periphery

Table continued on next page

Inspection	SG 1 (96)	SG 2 (95)	SG 3 (77)
106	Bobbin Coil: • 1 in 8 • periphery (1 deep) • reduced aseismic blocks • Previous indications Rotating Pancake Coil: • 100% of sludge zone • previous indications • All BC crack indications U-bend rotating pancake coil: • Row 1 (complete) • Row 2 (1 in 8) Visual Examination: • Periphery • Sludge zone	Bobbin Coil: • 1 in 8 • periphery (1 deep) • reduced aseismic blocks • Previous indications Rotating Pancake Coil: • 100% of sludge zone • previous indications • All BC crack indications U-bend rotating pancake coil: • Row 1 (complete) • Row 2 (1 in 8) Visual Examination: • Periphery • Sludge zone	Bobbin Coil: • 1 in 8 • periphery (1 deep) • reduced aseismic blocks • Previous indications Rotating Pancake Coil: • 100% of sludge zone • previous indications • All BC expansion anomalies U-bend rotating pancake coil: • Row 1 (complete) • Row 2 (1 in 8) Visual Examination: • Periphery
107	Hydrotest at 93 bar Bobbin Coil: • 1 in 8 • periphery (1 deep) • reduced aseismic blocks • Previous indications • Dents under TSP (AVB) • 1 in 4 under AVB's. Rotating Pancake Coil: • 100% of SG tubes U-bend rotating pancake coil: • Row 1 (complete) • Row 2 (1 in 8) Visual Examination: • Periphery • Sludge zone	Hydrotest at 93 bar Bobbin Coil: • 1 in 8 • periphery (1 deep) • reduced aseismic blocks • Previous indications • Dents under TSP (AVB) • 1 in 4 under AVB's. Rotating Pancake Coil: • 100% of SG tubes U-bend rotating pancake coil: • Row 1 (complete) • Row 2 (1 in 8) Visual Examination: • Periphery	Hydrotest at 93 bar Bobbin Coil: • 1 in 8 • periphery (1 deep) • reduced aseismic blocks • Previous indications • Dents under TSP (AVB) • 1 in 4 under AVB's. Rotating Pancake Coil: • 100% of sludge zone • previous indications U-bend rotating pancake coil: • None Visual Examination: • Periphery • Sludge zone
108	Bobbin Coil: • 1 in 8 • periphery (1 deep) • reduced aseismic blocks • Previous indications • Dents under TSP (AVB) • 1 in 4 under AVB's. Rotating Pancake Coil: • 100% of sludge zone • previous indications U-bend rotating pancake coil: • Row 1 (complete) • Row 2 (1 in 8) Visual Examination: • Periphery • Sludge zone	Bobbin Coil: • 1 in 8 • periphery (1 deep) • reduced aseismic blocks • Previous indications • Dents under TSP (AVB) • 1 in 4 under AVB's. Rotating Pancake Coil: • 100% of sludge zone • previous indications U-bend rotating pancake coil: • Row 1 (complete) • Row 2 (1 in 8) Visual Examination: • Periphery • Sludge zone	Bobbin Coil: • 1 in 8 • periphery (1 deep) • reduced aseismic blocks • Previous indications • Dents under TSP (AVB) • 1 in 4 under AVB's. Rotating Pancake Coil: • 100% of sludge zone • previous indications U-bend rotating pancake coil: • None Visual Examination: • Periphery • Sludge zone

Table continued on next page

Inspection	SG 1 (96)	SG 2 (95)	SG 3 (77)
109	Bobbin Coil: • Periphery (1 deep) • Reduced sludge zone • 1 in 8 • 1 in 4 under AVB's. • Previous indications • Expansion anomalies • Dents under AVB, wall loss & strike indications. Rotating Pancake Coil: • 100% of SG tubes Visual Examination: • Periphery	Bobbin Coil: • Periphery (1 deep) • Reduced sludge zone • 1 in 8 • 1 in 4 under AVB's. • Previous indications • Expansion anomalies • Dents under AVB, wall loss & strike indications. Rotating Pancake Coil: • 100% of SG tubes • Expansion anomalies (check for circumferential cracks) Visual Examination: • Periphery	Bobbin Coil: • Periphery (1 deep) • Reduced sludge zone • 1 in 8 • 1 in 4 under AVB's. • Previous indications • Expansion anomalies • Dents under AVB, wall loss & strike indications. Rotating Pancake Coil: • Reduced sludge zone • Previous indications • Expansion anomalies (Hot leg) Visual Examination: • Periphery
110	Bobbin Coil: • Periphery (1 deep) • Reduced sludge zone • 1 in 8 • 1 in 4 under AVB's. • Previous indications • Expansion anomalies (Relevant) • Wall loss & strike indications. Rotating Pancake Coil: • Reduced sludge zone • Previous indications with FL > 5mm • Expansion anomalies (Hot leg) U-bend rotating pancake coil: • Row 1 (1 in 2) • Row 2 (1 in 8) Visual Examination: • Periphery	Bobbin Coil: • Periphery (1 deep) • Reduced sludge zone • 1 in 8 • 1 in 4 under AVB's. • Previous indications • Expansion anomalies (Relevant) • Wall loss & strike indications. Rotating Pancake Coil: • Reduced sludge zone • Previous indications with FL > 5mm • Expansion anomalies (Hot leg) U-bend rotating pancake coil: • Row 1 (1 in 2) • Row 2 (1 in 8) Visual Examination: • Periphery	Bobbin Coil: • Periphery (1 deep) • Reduced sludge zone • 1 in 8 • 1 in 4 under AVB's. • Previous indications • Expansion anomalies (Relevant) • Wall loss & strike indications. Rotating Pancake Coil: • Reduced sludge zone • Previous indications • Expansion anomalies (Hot leg) U-bend rotating pancake coil: • Row 1 (1 in 2) • Row 2 (1 in 8) Visual Examination: • Periphery

Table A4: Koeberg Unit 2 Inspection Summary

	Unit 2		
Inspection	SG 1 (98)	SG 2 (99)	SG 3 (100)
PSI	Bobbin Coil 100% DIA Test	Bobbin Coil 100% DIA Test	Bobbin Coil 100% DIA Test
RERUN	100% re-read of PSI BC tapes in hot leg	100% re-read of PSI BC tapes in hot leg	100% re-read of PSI BC tapes in hot leg
201	Bobbin Coil: • 1 in 8 • periphery (2 deep) • row 1 • Previous indications Visual Examination: • periphery	Bobbin Coil: • 1 in 8 • periphery (2 deep) • row 1 • Previous indications Visual Examination: • periphery	Bobbin Coil: • 1 in 8 • periphery (2 deep) • row 1 • Previous indications Visual Examination: • periphery
202	Visual Examination: • Periphery	Bobbin Coil: • 1 in 8 • Previous indications Rotating Pancake Coil: • All BC crack indications Visual Examination: • Periphery	Visual Examination: • Periphery
203	Visual Examination: • Periphery	Visual Examination: • Periphery	Bobbin Coil: • 1 in 8 • periphery (2 deep) • row 1 • Previous indications Rotating Pancake Coil: • 100% of sludge zone • 2 leg extensions Visual Examination: • Periphery
204	Bobbin Coil: • 1 in 8 • periphery (1 deep) • row 1 • Previous indications Rotating Pancake Coil: • 100% of sludge zone • previous indications Visual Examination: • Periphery	Bobbin Coil: • 1 in 8 • periphery (1 deep) • row 1 • Previous indications Rotating Pancake Coil: • 100% of sludge zone • previous indications Visual Examination: • Periphery	Bobbin Coil: • 1 in 8 • periphery (1 deep) • row 1 • Previous indications Rotating Pancake Coil: • 100% of sludge zone • previous indications Visual Examination: • Periphery
205	Bobbin Coil: • 1 in 8 • periphery (1 deep) • reduced aseismic blocks • row 1 • HL expansion anomalies Rotating Pancake Coil: • 100% of sludge zone • all BC indications Visual Examination: • Periphery	Bobbin Coil: • 1 in 8 • periphery (1 deep) • reduced aseismic blocks • row 1 • previous indications Rotating Pancake Coil: • 100% of SG tubes Visual Examination: • Periphery	Bobbin Coil: • periphery (1 deep) • reduced aseismic blocks • row 1 • previous indications Rotating Pancake Coil: • 100% of sludge zone • previous indications • all BC indications Visual Examination: • Periphery

Table continued on next page

Inspection	SG 1 (98)	SG 2 (99)	SG 3 (100)
206	Bobbin Coil: • 1 in 8 • periphery (1 deep) • reduced aseismic blocks • Previous indications Rotating Pancake Coil: • 100% of SG tubes U-bend rotating pancake coil: • Row 1 (complete) • Row 2 (1 in 8) Visual Examination: • Periphery	Bobbin Coil: • 1 in 8 • periphery (1 deep) • reduced aseismic blocks • Previous indications Rotating Pancake Coil: • 100% of sludge zone • previous indications • all BC indications U-bend rotating pancake coil: • Row 1 (complete) • Row 2 (1 in 8) Visual Examination: • Periphery	Bobbin Coil: • 1 in 8 • periphery (1 deep) • reduced aseismic blocks • Previous indications Rotating Pancake Coil: • 100% of SG tubes U-bend rotating pancake coil: • Row 1 (complete) • Row 2 (1 in 8) Visual Examination: • Periphery
207	Hydrotest at 93 bar Bobbin Coil: • 1 in 8 • periphery (1 deep+wedges) • sludge zone • 1 in 4 AVB zone • Previous indications Rotating Pancake Coil: • 100% of sludge zone • previous indications • expansion anomalies U-bend rotating pancake coil: • Row 1 (complete) • Row 2 (1 in 8) Visual Examination: • Periphery • Sludge zone	Hydrotest at 93 bar Bobbin Coil: • 1 in 8 • periphery (1 deep+wedges) • sludge zone • 1 in 4 AVB zone • Previous indications Rotating Pancake Coil: • 100% of SG tubes U-bend rotating pancake coil: • Row 1 (complete) • Row 2 (1 in 8) Visual Examination: • Periphery	Hydrotest at 93 bar Bobbin Coil: • 1 in 8 • periphery (1 deep+wedges) • sludge zone • 1 in 4 AVB zone • Previous indications Rotating Pancake Coil: • 100% of sludge zone • previous indications • expansion anomalies U-bend rotating pancake coil: • Row 1 (complete) • Row 2 (1 in 8) Visual Examination: • Periphery • Sludge zone
208	Bobbin Coil: • Periphery (1 deep) • Reduced sludge zone • Expansion anomalies (cold leg) Cases 5a, 7, 8a, 12a, 12b, 12d, 12e • Wall loss, dents under TSP and AVB, Strike. Rotating Pancake Coil: • 100% of reduced sludge zone • previous indications • expansion anomalies (hot leg) U-bend rotating pancake coil: • Row 1 (complete) • Row 2 (1 in 8) Visual Examination: • Secondary side	Bobbin Coil: • Periphery (1 deep) • Reduced sludge zone • 1 in 8 • 1 in 4 AVB zone • Expansion anomalies Cases 7, 8a, 12e • Wall loss, dents under TSP and AVB, Strike. Rotating Pancake Coil: • 100% of reduced sludge zone • previous indications • expansion anomalies (hot leg) U-bend rotating pancake coil: • Row 1 (complete) • Row 2 (1 in 8) Visual Examination: • Secondary side	Bobbin Coil: • Periphery (1 deep) • Reduced sludge zone • Expansion anomalies Cases 3, 5a, 7, 8a, 12e • Wall loss, dents under TSP and AVB, Strike. Rotating Pancake Coil: • 100% of reduced sludge zone • previous indications • expansion anomalies (hot leg) U-bend rotating pancake coil: • Row 1 (complete) • Row 2 (1 in 8) Visual Examination: • Secondary side

Table continued on next page

Inspection	SG 1 (98)	SG 2 (99)	SG 3 (100)
209	Bobbin Coil: • Periphery (1 deep) • Reduced sludge zone (1 in 2) • 1 in 8 • 1 in 4 in AVB zone • Previous indications • Expansion anomalies (relevant) • Wall loss, Strike. Rotating Pancake Coil: • 100% of SG tubes Visual Examination: • Periphery	Bobbin Coil: • Periphery (1 deep) • Reduced sludge zone (1 in 2) • 1 in 8 • 1 in 4 in AVB zone • Previous indications • Expansion anomalies (relevant) • Wall loss, Strike. Rotating Pancake Coil: • 100% of SG tubes Visual Examination: • Periphery	Bobbin Coil: • Periphery (1 deep) • Reduced sludge zone (1 in 2) • 1 in 8 • 1 in 4 in AVB zone • Previous indications • Expansion anomalies (relevant) • Wall loss, Strike. Rotating Pancake Coil: • 100% of SG tubes Visual Examination: • Periphery
210	Bobbin Coil: • Periphery (1 deep) • Reduced sludge zone (1 in 2) • 1 in 8 • 1 in 4 in AVB zone • Previous indications • Expansion anomalies (relevant) • Wall loss Rotating Pancake Coil: • 100% of reduced sludge zone • Previous indications with FL > 5mm • Expansion anomalies (Hot leg) U-bend rotating pancake coil: • Row 1 (1 in 2) • Row 2 (1 in 8) Visual Examination: • Periphery	Bobbin Coil: • Periphery (1 deep) • Reduced sludge zone (1 in 2) • 1 in 8 • 1 in 4 in AVB zone • Previous indications • Expansion anomalies (relevant) • Wall loss Rotating Pancake Coil: • 100% of reduced sludge zone • Previous indications with FL > 5mm • Expansion anomalies (Hot leg) U-bend rotating pancake coil: • Row 1 (1 in 2) • Row 2 (1 in 8) Visual Examination: • Periphery	Bobbin Coil: • Periphery (1 deep) • Reduced sludge zone (1 in 2) • 1 in 8 • 1 in 4 in AVB zone • Previous indications • Expansion anomalies (relevant) • Wall loss Rotating Pancake Coil: • 100% of reduced sludge zone • Previous indications with FL > 5mm • Expansion anomalies (Hot leg) U-bend rotating pancake coil: • Row 1 (1 in 2) • Row 2 (1 in 8) Visual Examination: • Periphery

Table A5: Tube Inspection and Plugging History - Unit 1

UNIT 1								
Tube Inspection History [59]						**Tube Plugging [85]**		
						Tube #.		*Reason*
Outage	*Outage Start Dates*	*EFPD*	*SG no.*	*% Cracked Tubes*		*R*	*C*	
PSI	11/01/1982	0	**1**			02	01	Manufacture dent causing probe blockage
						03	01	Manufacture dent causing probe blockage
			2			10	93	Manufacture dent causing probe blockage
			3			19	85	ID wall loss (signal)
						24	83	ID wall loss (signal)
						25	78	OD wall loss
						43	42	ID wall loss (signal)
101	02/01/1986	300	**1**			27	84	OD wall loss (loose part)
			2			23	64	SCC initiation (abnormal expansion)
						23	66	SCC initiation (abnormal expansion)
						24	65	SCC initiation (abnormal expansion)
						24	67	SCC initiation (abnormal expansion)
102	15/08/1987	600	**1**			28	84	OD wall loss (loose part)
103	18/02/1989	912	**2**		(13)	-	-	-
104	17/08/1990	1263	**1**		(13)	26	83	Preventatively plugged due to tube
						26	84	R27 C84 damage
						26	85	"
						27	83	"
						28	83	"
						27	85	"
			2		(26)	05	94	Tube damage during He test
105	31/01/1992	1558	**1**	13	(19)	-	-	-
			2	18	(42)	-	-	-
106	20/08/1993	1901	**1**		(26)	21	60	SCC – Availability Plugging
			2		(48)	01	17	Preventatively plugged due to PWSCC at
						05	33	Tube expansion zone in order to reduce
						06	39	SG leak rate.
						06	44	"
						06	51	"
						11	32	"
107	12/02/1995	2222	**1**	23	(31)	28	78	OD wall loss (loose part)
						29	78	OD wall loss (loose part)
			2	31	(52)	-	-	-
108	14/06/1996	2538	**1**		(33)	01	92	ID wall loss in U-bend
			2		(54)	-	-	-
109	02/09/1997	2917	**1**	27	(36)	-	-	-
			2	35	(56)	-	-	-
110	15/01/1999	3334	**1**		*(41)*	-	-	-
			2		*(58)*			
111	14/04/2000	3722	**1**	30	(39)	02	52	U-bend SCC
						04	01	Dent causing Probe block
			2	37	(59)			
			3			35	32	OD wall loss – Mandatory Plugging
112	07/09/2001	4133	**1**	31	(40)			
			2	38	(59)	20	55	Axial SCC – 11 cracks in 270^0
113	17/01/2003	4539	**1**	31	(42)	01	02	Dent – Preventative plugging
						02	02	"
						02	03	"
						03	02	"
						03	03	"
						04	02	"
						04	03	"
						05	01	"
						05	02	"
						06	01	"
			2	39	(60)	25	43	Axial SCC – 11 cracks in 270^0
						Total Plugged:		**45**

Table A6: Tube Inspection and Plugging History - Unit 2

UNIT 2							
Tube Inspection History [59]					**Tube Plugging**		
					Tube #.		*Reason*
Outage	*OutageStart Dates*	*EFPD*	*SG #*	*% Cracked Tubes**	*R*	*C*	
PSI	22/11/1982	0	**1**		24	55	Manufacture; incorrect tube sheet drilling
					24	59	"
					24	63	"
			2		29	11	Tube sheet not drilled
							(no hole in TS on cold leg side)
			3		08	50	ID wall loss (signal)
					18	38	"
201	21/03/1987	308			-	-	-
202	20/08/1988	616	**2**		41	65	Loose Parts
					41	64	"
					42	64	"
203	22/12/1989	940			-	-	-
204	02/05/1991	1240	**1**	(4)	-	-	-
			2	(12)	-	-	-
			3	(4)	-	-	-
205	01/01/1993	1553	**1**	(8)	01	08	Preventatively plugged due to U-bend wall
							loss potentially affected by heat treatment
			2	**9 (20)**	-	-	-
			3	(9)	-	-	-
206	09/09/1994	1870	**1**	**4 (12)**	-	-	-
			2	(23)	-	-	-
			3	**8 (11)**	-	-	-
207	05/01/1996	2195	**1**	(13)	01	84	Indication in 8'th TSP – U-bend transition
			2	**13 (26)**	-	-	-
			3	(14)	-	-	-
208	20/02/1997	2503	**1**	*(15)*	01	27	U-bend RPC probe stuck in U-bend
			2	*(38)*			
			3	*(15)*			
209	22/04/1998	2861	**1**	**6 (15)**	-	-	-
			2	**15 (30)**			
			3	**11 (16)**			
210	18/09/1999	3282	**1**	*(16)*			
			2	*(42)*	01	18	Preventatively plugged due to U-bend
					01	71	indications
					01	75	"
			3	*(16)*			
211	12/01/2001	3683	**1**	**7 (16)**			
			2	**17 (32)**			
			3	**13 (19)**	15	89	Circumferential Crack (50 degrees)#
					19	87	Circumferential Crack (117 degrees)
212	05/04/2002	3974	**1**	**7 (16)**			
			2	**17 (33)**			
			3	**13 (19)**			
					Total Plugged:		**17**

* Values in brackets indicate percentage of cracked tubes in the sludge zone (300 tubes). Values in brackets and shaded in grey indicate percentage of cracked tubes in the reduced sludge zone (150 tubes). It was not possible to include some of the overall values since the inspection scopes covered 1 in 8 samples and previous indications. An indication refers to an eddy current signal ≥ 200 mV

Due to the greater risk involved with circumferential cracks, Koeberg is obliged (in accordance with the EdF maintenance policy) to perform full inspection scopes on all SG's, until it can be proven that the circumferential cracks detected in Outage 211 was an anomaly.

B. Known SG tube rupture incidents World-wide

1975: SGTR 1 (USA)
The U.S. nuclear industry experienced its first steam generator tube rupture at **Point Beach Unit 1** in Wisconsin. The steam generator tube rupture occurred in less than 5 years operation. Subsequent inspection revealed that 127 tubes had degraded wall thickness greater than 60%. The steam generators at Point beach were Westinghouse model 44's with mill-annealed Alloy 600 tubing and were replaced in 1984. These are the same steam generators that are still installed at Indian Point 2.

Cause: Wastage due to large sludge pile (ineffective cleaning)
Rupture Location: Above tubesheet, outer row on hot leg.
Leak Rate: 28,200 l/hr

1976: SGTR 2 (USA)
Surry Unit 2 reactor located near Williamsburg, Virginia, experiences the second steam generator tube rupture at a U.S. nuclear plant. The steam generator tube rupture occurred in less than 4 years operation. Subsequent inspection of nine U-bend sections of the steam generator tubes revealed a 4.5 inch crack, four of the other eight pulled tubes revealed cracking that was undetectable with inspection techniques available at the time.

Cause: PWSCC of top tube support plate – inward movement of tubes – high stresses and ovalisation of tubes at apex.
Rupture Location: Apex of U-bend (row 1, column 7).
Leak Rate: 75,000 l/hr

1975: SGTR 3 (Belgium)
Doel 2 (Belgium) experiences the first non-US steam generator tube rupture, 4 years after commissioning. The tube rupture occurred at the apex of U-bend (row 4, column 24), because of high residual stresses and ovalisation during fabrication.

Cause: PWSCC – high residual stresses and ovalisation during fabrication
Rupture Location: Apex of U-bend (row 1, column 24).
Leak Rate: 30,600 l/hr

1978: NRC Action
The NRC designates steam generator tube integrity as an Unresolved Safety Issue and plans were established to evaluate the safety significance of degradation in PWR steam generators.

1979: SGTR 4 (USA)
Prairie Island Unit 1 near Minneapolis, MN experienced a spontaneous tube rupture caused by a loose part in the steam generator. **NRC** issues **Information Notice 79-27** Steam Generator Tube Ruptures at Two PWR Facilities, documenting the accident at Prairie Island as well as a similar accident at the Doel 2 nuclear reactor in Belgium. Both reactors were Westinghouse 2-loop plants. The Prairie Island accident released approximately 30 curies of radiation into the environment.

Cause: Loose part – sludge lancing equipment left in SG.
Rupture Location: Periphary 76 mm above tubesheet on hot leg (row 4, column 1).
Leak Rate: 76,200 l/hr

1982: SGTR 5 (USA)
The **Ginna** reactor located near Rochester, NY experienced a spontaneous tube rupture caused again caused by a loose part in the steam generator. The steam generator tube rupture occurred in less than 5 years of operation. Inspections in April of 1981 revealed eddy-current indications that were not interpreted as needing plugging. The Ginna accident released 90 curies of radiation into the environment. Had there been any damage to the core of the reactor, the bypass of the containment would have provided highly radioactive fission materials a direct pathway into the environment.

Cause: Loose part – tube fretting on plugged tube(bundle base).
Rupture Location: Periphary 126 mm above tubesheet on hot leg (row 42, column 55).
Leak Rate: 174,000 l/hr

1982: Westinghouse Sued

Consolidated Edison sues Westinghouse over the Indian point 2 steam generators. Every utility, with the exception of the Tennessee Valley Authority, that has purchased a Westinghouse reactor has subsequently sued the corporation over problems with their steam generators.

1984: SGTR 6 (USA)

Fort Calhoun (military installation), near Omaha, NE, experienced a spontaneous tube rupture. The ruptured tube had been included in the last steam generator tube inspection and occurred after less than 10 years of operation. Re-evaluation of the data from that inspection revealed a 99% through wall defect where the tube eventually ruptured.

Cause: ODSCC – corrosion of carbon steel vertical support leading to tube ovalisation and excessive levels of stress.
Rupture Location: U-bend adjacent to vertical support bar (row 84, column 29).
Leak Rate: 25,500 l/hr

1987: SGTR 7 (USA)

North Anna Unit 1 near Fredricksburg, VA experienced a spontaneous tube rupture. The rupture was caused by a 360 degree through wall crack and occurred after less than 10 years of operation. The plants technical specifications did not require much inspection of the area that eventually ruptured because it was on the cold-leg side of the steam generator. Thus in the previous inspection only 13% of the tubes in this area were inspected. The tube that eventually ruptured was not among the 13%.

Cause: High cycle fatigue due to lack of AVB support and denting.
Rupture Location: Above upper support plate cold leg (row 9, column 51)
Leak Rate: 144,600 l/hr

1988: NRC Statement

NRC Commissioner Kenneth Rogers acknowledges that multiple tube ruptures can lead to a meltdown of the nuclear reactor:

> *The concern is with sudden multiple tube failures- common mode failures. For example, such failures could come about by having essentially uniform degradation of the tubes. Degradation would decrease the safety margins so that, in essence, we have a 'loaded gun,' an accident waiting to happen. Under those conditions, a pressure transient or a seismic event could rupture many tubes simultaneously. That could allow primary coolant to enter the secondary system and the resulting high pressure to lift the relief valves that are outside containment on the steam line, thus permitting primary water to by-pass containment and communicate with atmosphere directly, resulting in a LOCA (loss of coolant accident)*

1988: NRC Notice

NRC issues Information **Notice 88-31**: Steam Generator Tube Rupture Analysis

> *Deficiency acknowledging that if the break location becomes uncovered, a direct path might exist for fission products contained in the primary coolant to be released to the atmosphere. The licensee further concluded that the offsite dose consequences exceeded those calculated in the Updated Final Safety Analysis Report (UFSAR) because tube uncovery could produce a direct path for fission product release.*

1988: SGTR 8 (USA)

Indian Point 3, located 35 miles (~56 km) from New York City, experiences an incipient tube rupture after 13 years of operation. A 456litres/hour leak developed over a two and a half hour period. This amount of leakage was 7 times the technical specification limit. Subsequent inspection revealed a 250 degree circumferential crack.

Cause: High cycle fatigue.
Rupture Location: Above upper tube support plate (row 45, column 51)
Leak Rate: 456 l/hr

1989: SGTR 9 (USA)

McGuire Unit 1, located near Charlotte, NC, experienced a spontaneous steam generator tube rupture after less than 8 years of operation. The rupture was caused by stress corrosion cracking involving multiple sites along the tube. Prior to the rupture, primary to secondary leak rate had been low. The rupture released approximately 30 curies of radiation in to the environment.

Cause: ODSCC – possibly a manufacturing defect.
Rupture Location: 711 mm above tubesheet cold leg (row 18, column 25)
Leak Rate: 114,000 l/hr

1989: SGTR 10 (USA)

Beaver Valley Unit 2, located near Pittsburg, PA, experiences an incipient tube rupture due to wear caused by loose parts. The subsequent inspection revealed that the loose part had removed 97% of the tube wall. Three adjacent tubes were also damaged with wear 62 to 97% through the tube wall.

Cause: Loose parts
Rupture Location: Above tube sheet hot leg (row 31, column 16)
Leak Rate: 80 l/hr

1990: Westinghouse Sued

Duke Power Company sues Westinghouse over the steam generators in the four reactors at Oconee and Catawba stations. Duke alleged that Westinghouse had hidden problems with Inconel or Alloy 600 since 1964. Internal Westinghouse memoranda were cited by Duke in support of their allegations:

> An August 17, 1964 Westinghouse memo stated, *"Mr. Simpson was informed that he was not to inform anyone with the exception of his boss of the inconel corrosion problem, to prevent a hold on steam generator production."*
>
> A June 11, 1968 Westinghouse memo contained the following hand written note: *"What do we tell them at this stage? That the alloy is crumbling before our eyes or that service experience is so far good?*

1990: SGTR 11 (USA)

Maine Yankee, located near Bath, ME experiences an incipient tube rupture. The licensees staff re-analysed their steam generator data from 1988 and found the indication that may have been the precursor to the accident.

Cause: ODSCC
Rupture Location: Apex of U-bend (row 6, column 43)
Leak Rate: 318 l/hr

1991: SGTR 12 (Japan)

Mihama Unit 2, Fukui, - SGTR, leaking 55 tonnes of radioactive primary (reactor) coolant water into the secondary steam-generating circuit. Some radioactivity was released to the atmosphere and the plant's emergency corecooling system was required. It was reported later that the accident was caused by human error, some anti-vibration bars being wrongly installed by workers and sawn off short to make them fit.

Cause: Fatigue (vibration of a wrongly positioned anti-vibration bar)
Rupture Location: 360^{0} rupture
Leak Rate: 158,900 l/hr

1992: SGTR 13 & 14 (USA)

McGuire Unit 1 and **Arkansas Nuclear One, Unit 2** both experience incipient tube ruptures. In both instances, inspections in the previous year missed indications of tube wear that exceed the 40% through wall threshold.

McGuire Unit 1

Cause: ODSCC
Rupture Location: Above lower tube support plate, cold leg (row 46, column 46)
Leak Rate: 37 l/hr

Arkansas Nuclear One, Unit 2

Cause: ODSCC
Rupture Location: Expansion transition zone (explosive expansion) hot leg (row 67, col 109)
Leak Rate: 57 l/hr

1992: Westinghouse Sued

Precipitating Portland General Electric's (PGE) decision to close the Trojan reactor in Oregon, Mr. Hopenfeld filed a differing professional opinion (DPO) regarding an NRC decision to allow the nuclear reactor to operate with seriously degraded steam generator tubes. The issue was that "a main steam line break (MSLB) outside containment could trigger a multiple steam generator tube failure which could then result in a core melt because of depletion of coolant inventory." NRC documents leaked to the Union of Concerned Scientists revealed that the risk of a meltdown at the Trojan reactor was 300 times greater than the NRC's Safety Goal standard. Trojan was eventually shutdown and PGE sued Westinghouse rather than replace the steam generators.

1992: NRC Statement

In a memo, which had been withheld from public disclosure, the NRC's Director of Nuclear Reactor Regulation reported that *"steam generator tube rupture (SGTR) events appear to be unavoidable."* The memo also points out that NRC regulation is less stringent than other countries. *"Regarding steam generator tube inspection programs, it is clear that the U.S. lags behind the major European countries in terms of scope of inspection.... Further, the leak rates allowed were reported to be consistently much lower than that allowed by U.S. Technical Specifications."*

1993: SGTR 15 (USA)

Palo Verde Unit 2 located near Phoenix, AZ experienced a spontaneous tube rupture after less than seven years of operation. A month prior to the tube rupture the licensee had observed an increasing trend in radiation monitoring activity. NRC's Augmented Inspection Team later determined that the licensees monitoring method had been inaccurate and had caused the leak rate to be underestimated by a factor of ten.

Cause: ODSCC due to bridging deposits
Rupture Location: Free span between 8'th and 9'th TSP's, hot leg (row 117, col 144)
Leak Rate: 54,600 l/hr

1994: Unit Retired

Maine Yankee was shut down in July due to steam generator tube cracks that had been present since 1990 but had gone undetected. The Maine Yankee Atomic Power Company claimed that, even with the circumferential cracks, the steam generator tubes could have withstood a worst-case-accident. Whether Maine Yankee s assertions were true or in fact it violated the NRC's requirements for steam generator tube integrity has never been determined. After attempting unsuccessfully to find a buyer for Maine Yankee, the utility retired the reactor.

1995: NRC Generic Letter 95-03

NRC issues Generic Letter 95-03: **Circumferential Cracking Of Steam Generator Tubes** to notify addressees about the recent steam generator tube inspection findings at Maine Yankee Atomic Power Station and their safety significance. Later that year the NRC issued **Generic Letter 95-05**, Voltage-Based Repair Criteria for Westinghouse Steam Generator Tubes Affected by Outside Diameter Stress Corrosion Cracking. The alternate repair criterion allows a greater number of tubes with crack indications to remain in service.

1995: Public Petition
Ms. Connie Hogarth filed a 2.206 petition with the U.S. Nuclear Regulatory Commission requesting that the operating licenses for Indian Point Nuclear Generating Units 2 and 3 be suspended until the licensees have completed the actions requested by Generic Letter 95-03.

1996: NRC Statement
NRC denies Ms. Hogarth's 2.206 petition stating that due to *"the steam generator inspections required by their technical specifications, both Indian Point Nuclear Generating Units 2 and 3 are required to monitor primary-to-secondary leakage to ensure that, in the event that steam generator tubes begin to leak, operators will be able to bring the plant to a depressurised condition before a tube ruptures."*

The NRC acknowledged that stress corrosion cracking of the Indian Point Unit 2 steam generator tubes was first detected during the 1993 refueling outage. However, Unit 2 steam generator tubes that showed signs of circumferential cracking have been removed from service.

1996: Unit Retired
Commonwealth Edison retires the **Zion Unit 2** reactor rather than replace the steam generators. Zion Unit 1 is shut down five months later. The reactors operated for less than 24 years.

1997: NRC Information Notice 97-79
NRC issues Information Notice 97-79: *Potential Inconsistency In The Assessment Of The Radiological Consequences Of A Main Steam Line Break Associated With The Implementation Of Steam Generator Tube Voltage-Based Repair Criteria.* The notice states that Commonwealth Edison's Braidwood reactor miscalculated the accident consequences of a main steam line break when it applied for license amendments to implement the new repair criteria. The notice goes on to acknowledge that other licensee had made the same mistake in their license amendment requests.

1998: NRC Action
NRC kills plans for a steam generator rulemaking and a proposed generic letter, instead deferring to the Nuclear Energy Institutes 97-06. The staff was leaning toward rulemaking and the generic letter because reactor technical specifications were not adequate to ensure safety from new, more severe from of steam generator tube degradation.

1999: NRC Action
NRC staff grants **Indian Point 2** a license amendment that allows Consolidated Edison to forego steam generator tube inspections required by their technical specifications. This was supposed to allow a one time exemption from the 24 month inspection interval and removed the requirement that the NRC approve the Indian Point 2 steam generator inspection program.

2000: SGTR 16 (USA)
Indian Point Unit 2 is forced to shut down on February 15th due to a steam generator tube failure. NRC later acknowledged that both Con-Ed and the NRC staff had mishandled the 1997 steam generator tube inspection and that the 1999 license amendment was based upon faulty analysis.

Cause:	PWSCC of top tube support plate – inward movement of tubes – high stresses and ovalisation of tubes at apex.
Rupture Location:	Apex of U-bend (row 2, column 5)
Leak Rate:	18,000 l/hr (~150 gpm)

2002: SGTR 17 (South Korea)

Uljin Unit 4. A guillotine rupture approximately 7.5 cm above the tube sheet was identified as triggered by significant circumferential and longitudinal cracking in the tube. The final investigation report concluded that the main causes were several cracks above the tube sheet. The tube leakage enlarged to a rupture as the unit was being shut down for maintenance, which is an unusual time for such an incident, and the cause for the leakage is still being sought. The steam generator tubes were inspected for degradation that might have caused the leak before the unit was restarted and only minor corrosion problems were found.

Cause: Stress corrosion cracking.
Rupture Location: Guillotine rupture about 7.5 cm above the tube sheet
Leak Rate:

It should be noted that no EDF SG has suffered an SGTR. However, numerous instances of unplanned outages due to high primary to secondary leaks have occurred. At the end of 1993 two instances of unplanned outages due to high primary to secondary leaks was recorded for Framatome type 51B SG's (same type as at Koeberg).

Source: www.wise-paris.org
www.citizen.org

C. Univariate Distributions and Methods of Random Variate Generation

This appendix lists the definitions of the univariate distributions used in this study and the procedures used for generating random variates from these distributions. Usually, more than one procedure is available for generating random variates from a particular distribution. These algorithms differ in speed, accuracy, storage requirements, and in complexity of coding. The particular algorithms used in this study were selected, based on their popularity and relative simplicity, from the following references: [80, 81, 82, 83].

The following notation will be used:

- The random variable X (with a specific value of x) has a Probability Density Function (PDF) $f_X(x)$ and Cumulative Distribution Function (CDF) $F_X(x)$. Where the CDF is defined as

$$F_X(x) = \int_D f_X(x)\,dx$$

- The sequence of uniform random numbers between 0 and 1 will be denoted as $U(0,1)$

Exponential Distribution		
Defining Parameter:	Hazard Rate $\lambda\,(>0)$	λ
Defining Equations:	PDF:	$f_X(x) = \lambda e^{-\lambda x} \quad 0 \le x < \infty$ $= 0 \quad$ *otherwise*
	CDF:	$F_X(x) = 1 - e^{-\lambda x}$
	Mean:	$\frac{1}{\lambda}$
	Variance:	$\frac{1}{\lambda^2}$
Random Variate Generation:	To Generate X by the Inverse Transform Method : Let $U(0,1) = F_X(x) = 1 - e^{-\lambda x}$ $\therefore X = -\frac{1}{\lambda}\ln(1-U)$ Since $(1-U)$ is distributed in the same way as U $X = -\frac{1}{\lambda}\ln(U)$ $\therefore X$ has an exponential distribution	
Algorithm:	1··· Generate u from $U(0,1)$ 2··· $-\frac{1}{\lambda}\ln u \rightarrow X$ 3··· Deliver X	

Normal Distribution		
Defining Parameters:	Location Parameter μ Scale Parameter σ	μ = Sample Mean of random variable X σ = Sample Std Deviation of random variable X
Defining Equations:	PDF:	$f_X(x) = \frac{1}{\sigma\sqrt{2\pi}} e^{\left[\frac{-(x-\mu)^2}{2\sigma^2}\right]} \quad \infty < x < \infty$ $= 0 \qquad$ *otherwise*
	CDF:	$F_X(x) = \int_{-\infty}^{x} f(x)\,dx$
	Mean:	μ
	Variance:	σ^2
Random Variate Generation:	The PDF for the normal distribution may be denoted as $N(\mu, \sigma^2)$ Since $X = \mu + \sigma Z$ where Z is the Standard Normal Variable $N(0,1)$ we only need to consider generation from $N(0,1)$. We use the Box - Muller method to generate random variates from $N(0,1)$: If u_1 and u_2 are independent random numbers from $U(0,1)$ then variates $Z_1 = \sqrt{-2\ln u_1}\cos(2\pi u_2)$ $Z_2 = \sqrt{-2\ln u_1}\sin(2\pi u_2)$ are Independent Standard Normal variates.	
Algorithm:	$1 \cdots$ Generate 2 independen t random numbers, u_1 & u_2 from $U(0,1)$ $2 \cdots$ Compute Z_1 & Z_2 $3 \cdots \mu + \sigma Z_i \rightarrow X_i \quad i = 1, 2$ $4 \cdots$ Deliver X_i	

Log-normal Distribution		
Defining Parameters:	Scale Factor $\alpha \quad (>0)$ Shape Factor $\beta \quad (>0)$	α = Mean of $\ln y$ β = Standard deviation of $\ln y$
Defining Equations:	PDF:	$f_Y(y) = \frac{1}{y}\frac{1}{\beta\sqrt{2\pi}} e^{\left[-\frac{(\ln y-\alpha)^2}{2\beta^2}\right]} \quad 0 \le y < \infty$ $= 0 \qquad$ *otherwise*
	CDF:	$F_y(y) = \int_0^y f(y)\,dy$
	Mean:	$\mu = e^{\alpha+\frac{\beta^2}{2}}$
	Variance:	$\sigma^2 = e^{2\alpha+\beta^2}\left(e^{\beta^2}-1\right)$
Random Variate Generation:	Adaptation of Box-Muller method for the Normal distribution.	
Algorithm:	$1\cdots$ Generate Z from $N(0,1)$ $2\cdots \mu + \sigma Z \rightarrow X$ $3\cdots e^{X} \rightarrow Y$ $4\cdots$ Deliver Y	

Weibull Distribution		
Defining Parameters:	Shape Factor $\alpha \quad (>0)$ Scale Factor $\beta \quad (>0)$	Parameter estimation by the Maximum Likelihood Method
Defining Equations:	PDF:	$f_X(x) = \frac{\alpha}{\beta^\alpha} x^{\alpha-1} e^{-\left(\frac{x}{\beta}\right)^\alpha} \quad 0 \le x < \infty$ $= 0 \qquad$ *otherwise*
	CDF:	$F_X(x) = 1 - e^{-\left(\frac{x}{\beta}\right)^\alpha}$
	Mean:	$\beta\Gamma\left(1+\frac{1}{\alpha}\right)$
	Variance:	$\beta^2\Gamma\left(1+\frac{2}{\alpha}\right) - \left[\beta\Gamma\left(1+\frac{1}{\alpha}\right)\right]^2$
Random Variate Generation:	To generate X by the Inverse Transform Method : Let $U(0,1) = F_X(x) = 1 - e^{-\left(\frac{x}{\beta}\right)^\alpha}$ $\therefore X = \beta\left[-\ln(1-U)\right]^{\frac{1}{\alpha}}$ Since $(1-U)$ is distributed in the same way as U $X = \beta\left[-\ln U\right]^{\frac{1}{\alpha}}$	
Algorithm:	$1 \cdots$ Generate u from $U(0,1)$ $2 \cdots \beta\left[-\ln U\right]^{\frac{1}{\alpha}} \rightarrow X$ $3 \cdots$ Deliver X	
Where $\Gamma(x) = (x-1)!$		

D. Visual Basic Source Code

The Visual Basic Source Code (with comments) used in this study, is presented in this appendix.

D1 – Generic MCS Source Code

The following algorithm was set up to sample from Normal and Log-normal Distributions. As described in appendix C, two uniformly distributed random numbers are required at each iteration for these types of distributions. Other distributions (Exponential and Weibull) require only one uniformly distributed random number at each iteration. The following Source code represents a generic MCS analysis case subject to a two parameter situation. The actual VBA source codes used in this study are variations of this algorithm.

```
Sub GenericMCS()
'
' GenericMCS (With Truncation)
' Macro recorded by R Damon (August 2003)
'

'This module generates random numbers and uses these to sample from parameter distributions
'according to the distribution type and truncation limits.

'Declare Variables
Dim n As Long                    'Declare variables as Long Integers
Dim rowans As Long
Dim iterations As Long

Let n = 0
Let rowans = 15
Let iterations = Range("B2").Value * 0.5

'Clear previous data
Range("C15:M65536").Select
Selection.ClearContents
Range("B3").Select

Do Until n = iterations

  Let n = n + 1
  Let Range("B3").Value = 2 * n

  'Generate Random Variables for Parameter 1

  Let Range("C9").Value = Rnd
  Let Range("C10").Value = Rnd

   Do Until Range("C13").Value > Range("C7").Value And Range("C13").Value < Range("C8").Value
    Let Range("C9").Value = Rnd
    Let Range("C10").Value = Rnd
   Loop                                                  'Truncate at Upper and Lower Bounds

  Let Cells(rowans, 3).Value = Range("C13").Value        'Write Data to List

   Do Until Range("C14").Value > Range("C7").Value And Range("C14").Value < Range("C8").Value
    Let Range("C9").Value = Rnd
    Let Range("C10").Value = Rnd
   Loop                                                  'Truncate at Upper and Lower Bounds

  Let Cells(rowans + 1, 3).Value = Range("C14").Value    'Write Data to List
```

```
'Generate Random Variables for Parameter 2

Let Range("D9").Value = Rnd
Let Range("D10").Value = Rnd

 Do Until Range("D13").Value > Range("D7").Value And Range("D13").Value < Range("D8").Value
  Let Range("D9").Value = Rnd
  Let Range("D10").Value = Rnd
 Loop                                              'Truncate at Upper and Lower Bounds

Let Cells(rowans, 4).Value = Range("D13").Value    'Write Data to List

 Do Until Range("D14").Value > Range("D7").Value And Range("D14").Value < Range("D8").Value
  Let Range("D9").Value = Rnd
  Let Range("D10").Value = Rnd
 Loop                                              'Truncate at Upper and Lower Bounds

Let Cells(rowans + 1, 4).Value = Range("D14").Value    'Write Data to List

Let Cells(rowans, 5).Value = Range("E13").Value        'Write Relationship result to List
Let Cells(rowans + 1, 5).Value = Range("E14").Value    'Write Relationship result to List

 Let rowans = rowans + 2

Loop

End Sub
```

The code interfaces with the following spreadsheet.

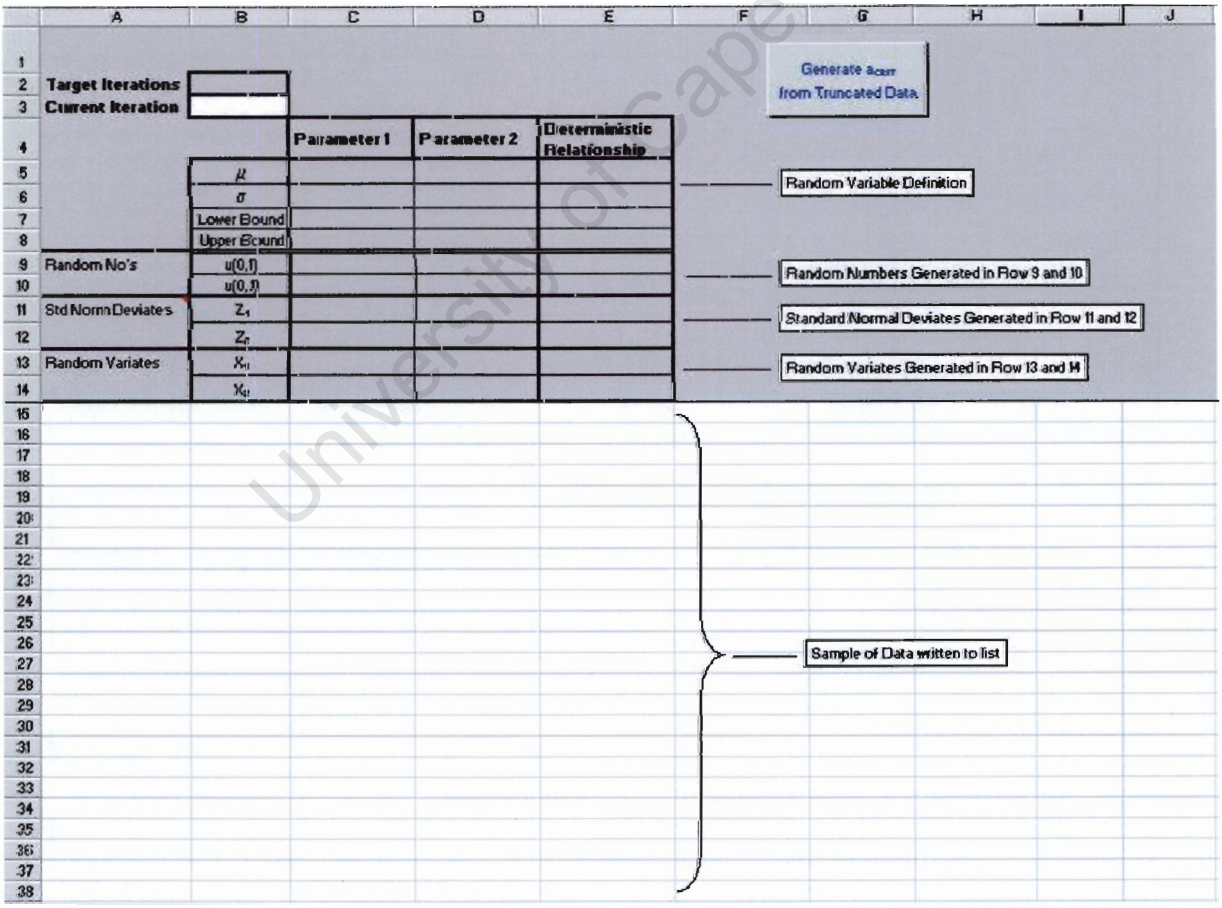

the Standard Normal Deviates and Random Variates are calculated as described in appendix C.

D2 – Source Code for the MCS of Initial Crack Length

```
Sub ainitial()
'
' ainitial Macro (With Truncation)
' Macro recorded by R Damon (August 2003)
'

'This module generates random numbers and uses these to sample from parameter distributions
'according to the distribution type and truncation limits.
'It then calculates the Initial crack length Distribution (with measurement errors)

'Declare Variables
Dim n As Long                    'Declare variables as Long Integers
Dim rowans As Long
Dim iterations As Long

Let n = 0
Let rowans = 15
Let iterations = Range("B2").Value * 0.5

'Clear previous data
Range("C15:M65536").Select
Selection.ClearContents
Range("B3").Select

Do Until n = iterations

  Let n = n + 1
  Let Range("B3").Value = 2 * n

  'Generate Random Variables for a MEASURED

  Let Range("C9").Value = Rnd
  Let Range("C10").Value = Rnd

  Let Cells(rowans, 3).Value = Range("C13").Value      'Write Data to List

  Let Cells(rowans + 1, 3).Value = Range("C14").Value  'Write Data to List

  'Generate Random Variables for MEASUREMENT ERROR

  Let Range("D9").Value = Rnd
  Let Range("D10").Value = Rnd

   Do Until Range("D13").Value > Range("D7").Value And Range("D13").Value < Range("D8").Value
    Let Range("D9").Value = Rnd
    Let Range("D10").Value = Rnd
   Loop                                                'Truncate at Upper and Lower Bounds

  Let Cells(rowans, 4).Value = Range("D13").Value      'Write Data to List

   Do Until Range("D14").Value > Range("D7").Value And Range("D14").Value < Range("D8").Value
    Let Range("D9").Value = Rnd
    Let Range("D10").Value = Rnd
   Loop                                                'Truncate at Upper and Lower Bounds

  Let Cells(rowans + 1, 4).Value = Range("D14").Value  'Write Data to List

  Let Cells(rowans, 5).Value = Range("E13").Value      'Write Measured + Error to List
  Let Cells(rowans + 1, 5).Value = Range("E14").Value  'Write Measured + Error to List


  Let rowans = rowans + 2

Loop

End Sub
```

The code interfaces with the following spreadsheet

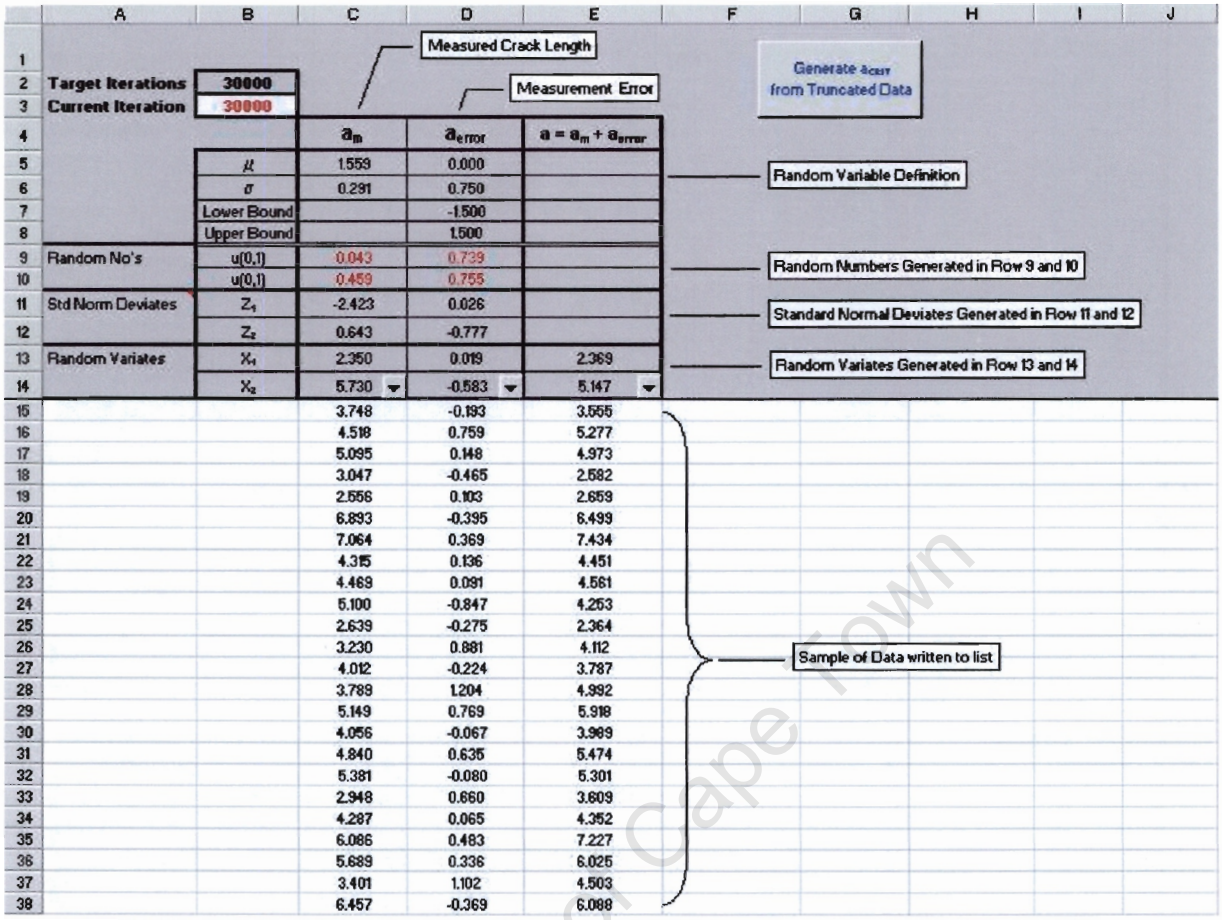

	A	B	C	D	E	F	G	H	I	J
1				Measured Crack Length						
2	**Target Iterations**	30000								
3	**Current Iteration**	30000		Measurement Error						
4			a_m	a_{error}	$a = a_m + a_{error}$					
5		μ	1.559	0.000						
6		σ	0.291	0.750						
7		Lower Bound		-1.500						
8		Upper Bound		1.500						
9	Random No's	u(0,1)	0.043	0.739						
10		u(0,1)	0.459	0.755						
11	Std Norm Deviates	Z_1	-2.423	0.026						
12		Z_2	0.643	-0.777						
13	Random Variates	X_1	2.350	0.019	2.369					
14		X_2	5.730	-0.583	5.147					
15			3.748	-0.193	3.555					
16			4.518	0.759	5.277					
17			5.095	0.148	4.973					
18			3.047	-0.465	2.582					
19			2.556	0.103	2.659					
20			6.893	-0.395	6.499					
21			7.064	0.369	7.434					
22			4.315	0.136	4.451					
23			4.469	0.091	4.561					
24			5.100	-0.847	4.253					
25			2.639	-0.275	2.364					
26			3.230	0.881	4.112					
27			4.012	-0.224	3.787					
28			3.789	1.204	4.992					
29			5.149	0.769	5.918					
30			4.056	-0.067	3.989					
31			4.840	0.635	5.474					
32			5.381	-0.080	5.301					
33			2.948	0.660	3.609					
34			4.287	0.065	4.352					
35			6.086	0.483	7.227					
36			5.689	0.336	6.025					
37			3.401	1.102	4.503					
38			6.457	-0.369	6.088					

Generate a_{CRIT} from Truncated Data

Random Variable Definition

Random Numbers Generated in Row 9 and 10

Standard Normal Deviates Generated in Row 11 and 12

Random Variates Generated in Row 13 and 14

Sample of Data written to list

D3 – Code for the MCS of Critical Crack Size

```
Sub acrittrunc()
'
' acrit Macro (With Truncation)
' Macro recorded by R Damon (August 2003)
'

'This module generates random numbers and uses these to sample from parameter distributions
'according to the distribution type and truncation limits.
'It then calculates critical crack length for each parameter selection

'Declare Variables
Dim n As Long                       'Declare variables as Long Integers
Dim rowans As Long
Dim iterations As Long

Let n = 0
Let rowans = 15
Let iterations = Range("B2").Value * 0.5

'Clear previous data
Range("C15:M65536").Select
Selection.ClearContents
Range("B3").Select

Do Until n = iterations

  Let n = n + 1
  Let Range("B3").Value = 2 * n

  'Generate Random Variables for TUBE THICKNESS

  Let Range("C9").Value = Rnd
  Let Range("C10").Value = Rnd

   Do Until Range("C13").Value > Range("C7").Value And Range("C13").Value < Range("C8").Value
    Let Range("C9").Value = Rnd
    Let Range("C10").Value = Rnd
   Loop                                             'Truncate at Upper and Lower Bounds

  Let Cells(rowans, 3).Value = Range("C13").Value         'Write Data to List

   Do Until Range("C14").Value > Range("C7").Value And Range("C12").Value < Range("C8").Value
    Let Range("C9").Value = Rnd
    Let Range("C10").Value = Rnd
   Loop                                             'Truncate at Upper and Lower Bounds

  Let Cells(rowans + 1, 3).Value = Range("C14").Value     'Write Data to List

  'Generate Random Variables for TUBE DIAMETER

  Let Range("D9").Value = Rnd
  Let Range("D10").Value = Rnd

   Do Until Range("D13").Value > Range("D7").Value And Range("D13").Value < Range("D8").Value
    Let Range("D9").Value = Rnd
    Let Range("D10").Value = Rnd
   Loop                                             'Truncate at Upper and Lower Bounds

  Let Cells(rowans, 4).Value = Range("D13").Value         'Write Data to List

   Do Until Range("D14").Value > Range("D7").Value And Range("D14").Value < Range("D8").Value
    Let Range("D9").Value = Rnd
    Let Range("D10").Value = Rnd
   Loop                                             'Truncate at Upper and Lower Bounds

  Let Cells(rowans + 1, 4).Value = Range("D14").Value     'Write Data to List
```

```
'Generate Random Variables for YIELD STRENGTH + UTS

Let Range("E9").Value = Rnd
Let Range("E10").Value = Rnd

 Do Until Range("E13").Value > Range("E7").Value And Range("E13").Value < Range("E8").Value
  Let Range("E9").Value = Rnd
  Let Range("E10").Value = Rnd
 Loop                                              'Truncate at Upper and Lower Bounds

Let Cells(rowans, 5).Value = Range("E13").Value     'Write Data to List

 Do Until Range("E14").Value > Range("E7").Value And Range("E14").Value < Range("E8").Value
  Let Range("E9").Value = Rnd
  Let Range("E10").Value = Rnd
 Loop                                              'Truncate at Upper and Lower Bounds

Let Cells(rowans + 1, 5).Value = Range("E14").Value 'Write Data to List

'Generate Random Variables for TUBE HEAT COEFFICIENT

Let Range("F9").Value = Rnd
Let Range("F10").Value = Rnd

 Do Until Range("F13").Value > Range("F7").Value And Range("F13").Value < Range("F8").Value
  Let Range("F9").Value = Rnd
  Let Range("F10").Value = Rnd
 Loop                                              'Truncate at Upper and Lower Bounds

Let Cells(rowans, 6).Value = Range("F13").Value     'Write Data to List

 Do Until Range("F14").Value > Range("F7").Value And Range("F14").Value < Range("F8").Value
  Let Range("F9").Value = Rnd
  Let Range("F10").Value = Rnd
 Loop                                              'Truncate at Upper and Lower Bounds

Let Cells(rowans + 1, 6).Value = Range("F14").Value 'Write Data to List

Let Cells(rowans, 8).Value = Range("H13").Value     'Write Flow Stress to List
Let Cells(rowans + 1, 8).Value = Range("H14").Value 'Write Flow Stress to List

Let Cells(rowans, 9).Value = Range("I13").Value     'Write Membrane Stress to List
Let Cells(rowans + 1, 9).Value = Range("I14").Value 'Write Membrane Stress to List

Let Cells(rowans, 10).Value = Range("J13").Value    'Write Bulging Factor to List
Let Cells(rowans + 1, 10).Value = Range("J14").Value 'Write Bulging Factor to List

Let Cells(rowans, 12).Value = Range("L13").Value    'Write a CRIT to List
Let Cells(rowans + 1, 12).Value = Range("L14").Value 'Write a CRIT to List

Let Cells(rowans, 13).Value = Range("M13").Value    'Write 2 x a CRIT to List
Let Cells(rowans + 1, 13).Value = Range("M14").Value 'Write 2 x a CRIT to List


Let rowans = rowans + 2

Loop

End Sub
```

The code interfaces with the following spreadsheet

	A	B	C	D	E	F	G	H	I	J	K	L	M	N	O
1			Clear DATA		Source for ($\sigma_Y + \sigma_U$)		Generate a_{CRIT} from Truncated Data		Generate a_{CRIT} No Truncation						
2	Target Iterations	30000			Koeberg - At Temperature										
3	Current Iteration	318													
4			t (mm)	ϕ (mm)	$\sigma_Y + \sigma_U$ (MPa)	k	Pressure (MPa)	σ_f (MPa)	σ_g* (MPa)	M*		a_{CRIT} (mm)	$2a_{CRIT}$ (mm)		
5		μ	1.270	22.220	914.456	0.580	FWLB - 17.2 MPa				a	-0.128			
6		σ	0.040	0.060	28.973	0.010					b	1.829			
7		Lower Bound	1.150	22.040	824.536	0.550					c	-6.976			
8		Upper Bound	1.390	22.352	1004.377	0.610					d	-3.146			
9	Random No's	u(0,1)	0.395	0.618	0.673	0.087									
10		u(0,1)	0.097	0.108	0.310	0.633									
11	Std Norm Deviates	Z_1	1.116	0.756	-0.326	-1.483							27.498	μ	
12		Z_2	0.784	0.614	0.828	-1.639							1.601	σ	
13	Random Variable	X_1	1.315	22.266	904.695	0.565		511.31	137.06	3.73		14.07	28.14		
14		X_2	1.301	22.257	939.264	0.564		529.31	138.48	3.82		14.35	28.71		
15			1.237	22.205	921.638	0.582		536.36	145.73	3.68		13.44	26.88		
16			1.263	22.291	868.630	0.551		478.49	143.11	3.34		12.31	24.63		
17			1.263	22.092	918.557	0.594		545.29	141.77	3.85		14.18	28.36		
18			1.245	22.297	898.685	0.577		518.25	145.39	3.56		13.07	26.14		
19			1.290	22.207	918.109	0.560		513.93	139.48	3.68		13.74	27.48		
20			1.277	22.235	880.620	0.567		499.06	141.11	3.54		13.11	26.23		
21			1.255	22.185	905.486	0.583		527.68	143.39	3.68		13.53	27.06		
22			1.317	22.173	962.560	0.575		553.04	136.19	4.06		15.34	30.68		
23			1.311	22.224	939.818	0.564		529.66	137.19	3.86		14.54	29.09		
24			1.266	22.246	911.253	0.576		525.29	142.47	3.69		13.64	27.27		
25			1.355	22.273	939.954	0.586		551.23	132.80	4.15		15.95	31.90		
26	Sample of Data written to list		1.270	22.225	932.994	0.560		522.18	141.94	3.68		13.62	27.23		
27			1.331	22.151	958.501	0.579		554.36	134.54	4.12		15.65	31.29		
28			1.288	22.283	939.707	0.581		522.88	140.19	3.73		13.93	27.86		
29			1.304	22.151	880.298	0.576		507.23	137.47	3.69		13.82	27.64		
30			1.324	22.129	935.310	0.587		549.31	135.13	4.07		15.38	30.77		
31			1.280	22.125	849.540	0.580		492.46	140.04	3.52		13.02	26.04		
32			1.307	22.165	932.009	0.584		544.70	137.26	3.97		14.92	29.84		
33			1.250	22.203	894.484	0.591		528.31	144.86	3.65		13.41	26.82		
34			1.289	22.174	893.809	0.588		525.13	139.32	3.77		14.05	28.11		
35			1.255	22.233	834.994	0.576		481.13	143.72	3.35		12.29	24.58		
36			1.230	22.198	892.255	0.582		519.09	146.66	3.54		12.87	25.73		
37			1.235	22.153	878.729	0.595		523.03	145.69	3.59		13.07	26.14		
38			1.269	22.236	938.791	0.586		549.70	142.04	3.87		14.35	28.70		
39			1.337	22.110	871.987	0.561		489.15	133.66	3.66		13.86	27.72		

D4 – Code for the MCS of Tube Failure Probability

```
Sub FProbData()
'
' FProbData Macro (Without Truncation)
' Macro recorded by R Damon (August 2003)
'

'This module generates random numbers and uses these to sample from parameter distributions
'according to the distribution type.
'It then compares Post Inspection Crack Length plus Crack Growth to Critical Crack Length
'FProbData also Lists all generated data to the spreadsheet for further analysis

'Declare Variables
Dim n As Long                    'Declare variables as Long Integers
Dim nfail As Long
Dim rowans As Long
Dim cov
Dim covtarget

Let n = 0
Let nfail = 0
Let covtarget = Range("K9").Value
Let cov = Range("K10").Value
Let rowans = 15


'Clear previous data
Range("J8").Select
Selection.ClearContents
Range("B2").Select

Do While Range("K10").Value >= Range("K9").Value

  Let n = n + 1
  Let Range("B2").Value = 2 * n

  'Generate Random Variables for aINSP
  Let Range("C9").Value = Rnd
  Let Range("C10").Value = Rnd

  Let Cells(rowans, 3).Value = Range("C13").Value        'Write aINSP Data to List
  Let Cells(rowans + 1, 3).Value = Range("C14").Value    'Write aINSP Data to List

  'Generate Random Variables for C
  Let Range("D9").Value = Rnd
  Let Range("D10").Value = Rnd

  Let Cells(rowans, 4).Value = Range("D13").Value        'Write C Data to List
  Let Cells(rowans + 1, 4).Value = Range("D14").Value    'Write C Data to List

  Let Cells(rowans, 5).Value = Range("E13").Value        'Write K(aINSP)Data to List
  Let Cells(rowans + 1, 5).Value = Range("E14").Value    'Write K(aINSP)Data to List

  Let Cells(rowans, 6).Value = Range("F13").Value        'Write da/dt Data to List
  Let Cells(rowans + 1, 6).Value = Range("F14").Value    'Write da/dt Data to List

  Let Cells(rowans, 7).Value = Range("G13").Value        'Write delta a Data to List
  Let Cells(rowans + 1, 7).Value = Range("G14").Value    'Write delta a Data to List

  Let Cells(rowans, 8).Value = Range("H13").Value        'Write aTOT Data to List
  Let Cells(rowans + 1, 8).Value = Range("H14").Value    'Write aTOT Data to List
```

```
  'Generate Random Variables for aCRIT

  Let Range("I9").Value = Rnd
  Let Range("I10").Value = Rnd

  Let Cells(rowans, 9).Value = Range("I13").Value        'Write aCRIT Data to List
  Let Cells(rowans + 1, 9).Value = Range("I14").Value    'Write aCRIT Data to List

  Let Cells(rowans, 10).Value = Range("J13").Value       'Write Status to List
  Let Cells(rowans + 1, 10).Value = Range("J14").Value   'Write Status to List


   If Range("H13").Value >= Range("I13").Value Then      'Count Failures
     Let nfail = nfail + 1
     Let Range("J8").Value = nfail
   End If

   If Range("H14").Value >= Range("I14").Value Then      'Count Failures
     Let nfail = nfail + 1
     Let Range("J8").Value = nfail
   End If


  Let rowans = rowans + 2

  ActiveWindow.SmallScroll Down:=1                      'Scroll down one row

Loop

ActiveWindow.ScrollRow = (2 * n)                        'Scroll to end

End Sub
```

The code interfaces with the following spreadsheet

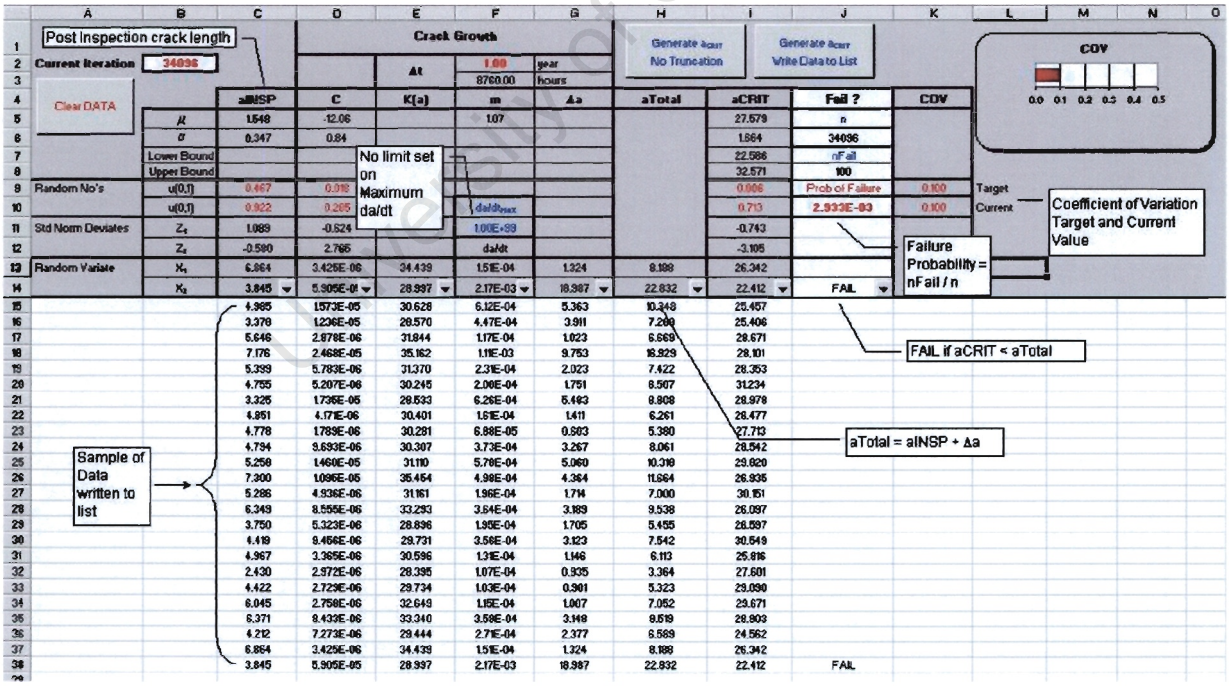

D5 – Histogram Source Code

The following code was developed to generate Histograms when required.

```
Sub Histogram()
'
' Histogram Macro
' Randolph Damon (August 2003).
'

'Histogram

Dim CountA, row, rowt, col, bin, rowans, colans, min, max, increment, binold, bino
' Declare Parameters

Worksheets("Histogram").Activate

Let min = Range("D3").Value
Let max = Range("D4").Value
Let increment = Range("D6").Value
Let rowt = Range("D7").Value

Let bin = min - increment
Let binold = bin
Let rowans = 2
Let colans = 7
Let bino = 0

Do Until bin >= max
    bin = bin + increment
    rowans = rowans + 1
    Range("F1").Value = bino
    bino = bino + 1

    CountA = 0
    row = 2
    col = 1
    Do Until row = rowt + 2
            row = row + 1

            ' Count each occurance between binold and bin i.e binold < x <= bin
            If Cells(row, col).Value > binold And Cells(row, col).Value <= bin Then
              CountA = CountA + 1
            End If

    Loop
    Cells(rowans, colans - 1).Value = bin
    Cells(rowans, colans).Value = CountA
    binold = bin

Loop

End Sub
```

The code interfaces with the following spreadsheet

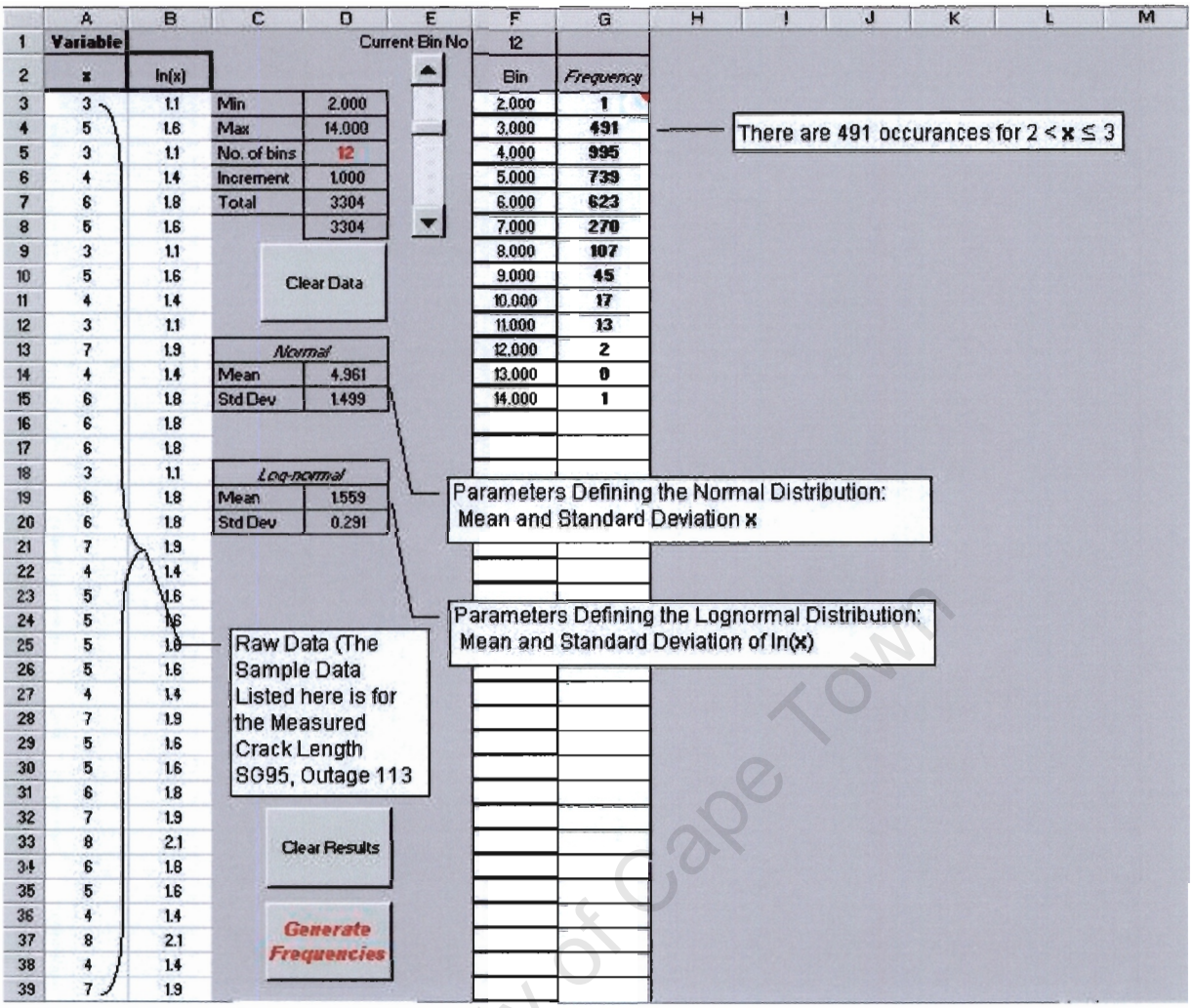

E. Determination of Post Inspection Defect Size Distribution

Given the True Defect Size Distribution generated by MCS, the Post Inspection Defect Size Distribution was determined by applying the equation defining the plugging probability at the "binned" level (i.e. the equation was calculated for each frequency class after a Histogram was generated for the True Defect Size Distribution). The process followed was as follows:

- Generate a Histogram for the True Defect Size Distribution.
- Calculate the Relative Frequency for each frequency class taking the plugging probability and POD into account.
- Fit various distributions to the new Histogram using the Excel Solver tool.
- Subjective choice of the most appropriate distribution.

An example of the Spreadsheet used for this purpose is illustrated below. This particular example is for a plugging limit of 13 mm.

POST INSPECTION DEFECT LENGTH DISTRIBUTION

p[insp/a]	1
p[PLG]	0.9999
PL	13
Sample	3304

No of iterations determine sample size

LogNormal Parameter		Weibull Parameters		Normal Parameters		Gamma Parameters	
Mean of ln x	1.534	Scale (β)	5.195	Mean	4.535	Shape (α)	8.662
Std Dev of ln x	0.353	Shape (α)	2.647	Std Dev	1.891	Scale (β)	0.551

Sum
30000

Sum
35037

Bin	Mid-Point	Frequency	Relative Frequency	POD	p[a≥PL/a]	P[PLG/a]	Freq [PLG]	Relative Freq [PLG]
1	0.5	15	5.00E-04	0.0063	0	0.000E+00	2364.563	6.75E-02
2	1.5	379	1.26E-02	0.2024	0	0.000E+00	1872.639	5.34E-02
3	2.5	2386	7.95E-02	0.6956	0	0.000E+00	3429.966	9.79E-02
4	3.5	6044	2.01E-01	0.9713	0	0.000E+00	6222.655	1.78E-01
5	4.5	7745	2.58E-01	0.9937	0	0.000E+00	7747.509	2.21E-01
6	5.5	6468	2.16E-01	1.0000	0	0.000E+00	6468.001	1.85E-01
7	6.5	3852	1.28E-01	1.0000	0	0.000E+00	3852.000	1.10E-01
8	7.5	1801	6.00E-02	1.0000	0	0.000E+00	1801.000	5.14E-02
9	8.5	821	2.74E-02	1.0000	0	0.000E+00	821.000	2.34E-02
10	9.5	291	9.70E-03	1.0000	0	0.000E+00	291.000	8.31E-03
11	10.5	119	3.97E-03	1.0000	0	0.000E+00	119.000	3.40E-03
12	11.5	48	1.60E-03	1.0000	0	0.000E+00	48.000	1.37E-03
13	12.5	18	6.00E-04	1.0000	1	9.999E-01	0.002	5.14E-08
14	13.5	6	2.00E-04	1.0000	1	9.999E-01	0.001	1.71E-08
15	14.5	3	1.00E-04	1.0000	1	9.999E-01	0.000	8.56E-09
16	15.5	4	1.33E-04	1.0000	1	9.999E-01	0.000	1.14E-08
17	16.5	0	0.00E+00	1.0000	1	9.999E-01	0.000	0.00E+00

The Error = the absolute value of the (Distribution value - the Relative Frequency).

Log-Normal	Error	Weibull	Error	Normal	Error	Gamma	Error
6.19E-09	6.75E-02	7.26E-03	6.02E-02	2.93E-02	4.58E-02	1.78E-05	6.75E-02
4.58E-03	4.89E-02	5.37E-02	2.30E-04	5.82E-02	4.73E-03	1.302E-02	4.04E-02
9.80E-02	1.09E-04	1.25E-01	2.74E-02	1.18E-01	2.03E-02	1.062E-01	8.32E-03
2.35E-01	5.75E-02	1.91E-01	1.33E-02	1.82E-01	3.99E-03	2.279E-01	5.03E-02
2.50E-01	2.90E-02	2.16E-01	4.85E-03	2.11E-01	1.02E-02	2.546E-01	3.35E-02
1.83E-01	1.95E-03	1.89E-01	3.17E-03	1.85E-01	6.25E-04	1.930E-01	8.40E-03
1.10E-01	3.22E-08	1.25E-01	1.50E-02	1.23E-01	1.30E-02	1.131E-01	3.13E-03
5.96E-02	8.17E-03	6.28E-02	1.14E-02	6.17E-02	1.03E-02	5.513E-02	3.73E-03
3.05E-02	7.04E-03	2.34E-02	2.07E-09	2.34E-02	8.13E-08	2.343E-02	1.49E-09
1.51E-02	6.81E-03	6.34E-03	1.97E-03	6.72E-03	1.58E-03	8.950E-03	6.44E-04
7.39E-03	3.99E-03	1.21E-03	2.18E-03	1.46E-03	1.94E-03	3.139E-03	2.58E-04
3.60E-03	2.23E-03	1.61E-04	1.21E-03	2.39E-04	1.13E-03	1.026E-03	3.43E-04
1.75E-03	1.75E-03	1.43E-05	1.43E-05	2.97E-05	2.96E-05	3.167E-04	3.17E-04
8.50E-04	8.50E-04	8.36E-07	8.19E-07	2.78E-06	2.77E-06	9.305E-05	9.30E-05
4.25E-04	4.25E-04	3.12E-08	2.27E-08	1.97E-07	1.89E-07	2.620E-05	2.62E-05
2.12E-04	2.12E-04	7.27E-10	1.07E-08	1.06E-08	8.41E-10	7.115E-06	7.10E-06
1.07E-04	1.07E-04	1.03E-11	1.03E-11	4.29E-10	4.29E-10	1.871E-06	1.87E-06
Average Error	1.39E-02	Average Error	8.29E-03	Average Error	6.69E-03	Average Error	1.28E-02

Bin: True Crack length frequency class

Relative Frequency = Frequency divided by sample size

POD Calculated at the midpoint of the Bin

Average Error minimised using the Excel SOLVER tool

The distribution parameters were determined by minimising the error between the proposed distributions (Log-normal, Weibull, Normal, and Gamma) and the calculated, Post Inspection, frequency distributions. This was achieved, using Excels Solver tool, which is illustrated below:

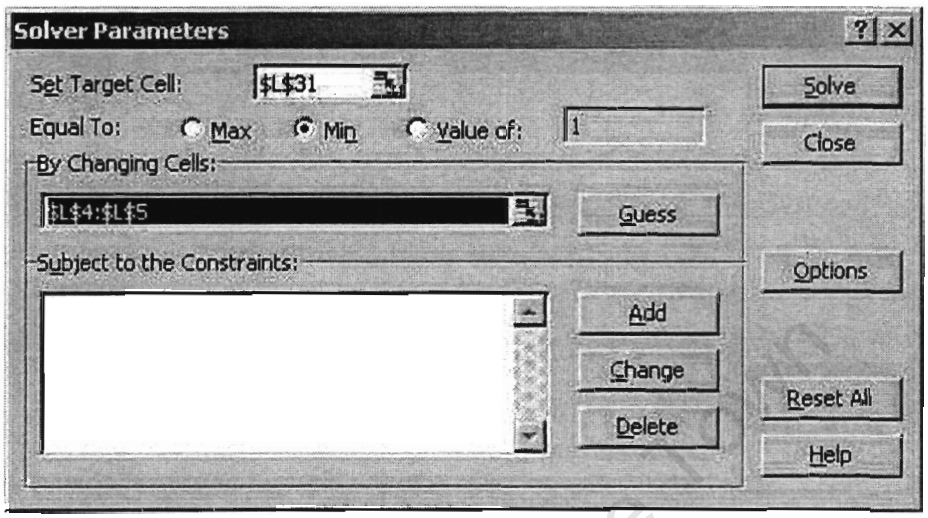

In this case, the target cell is the average error for the proposed distribution and the cells to be changed are the distribution parameters.

The choice of distribution was based mainly on the weight of the right hand tail section. The most conservative distribution (i.e. with the largest tail area) was chosen. This is illustrated below for the case of a 13 mm plugging limit.

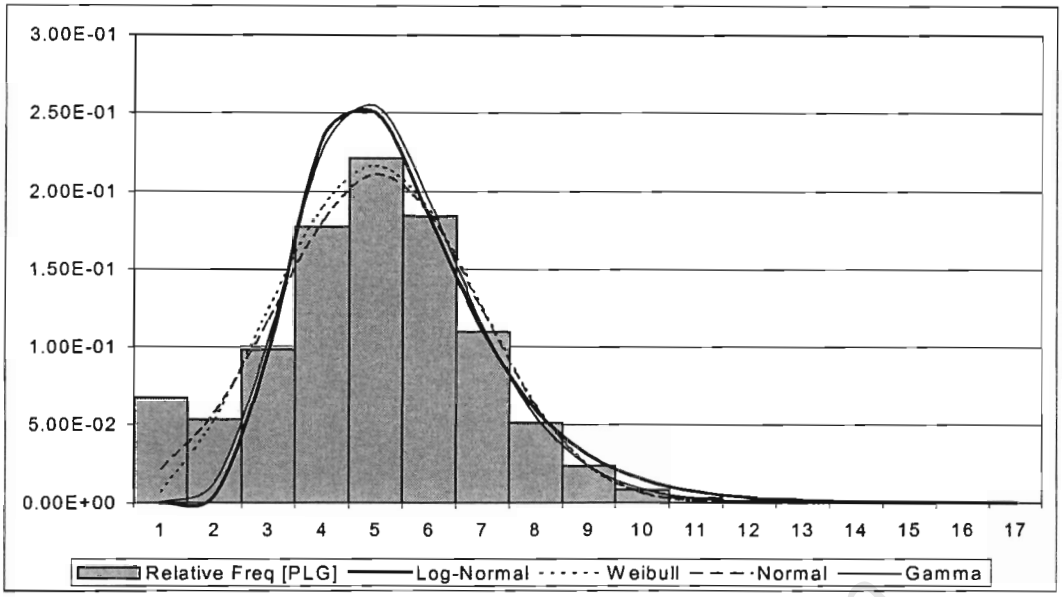

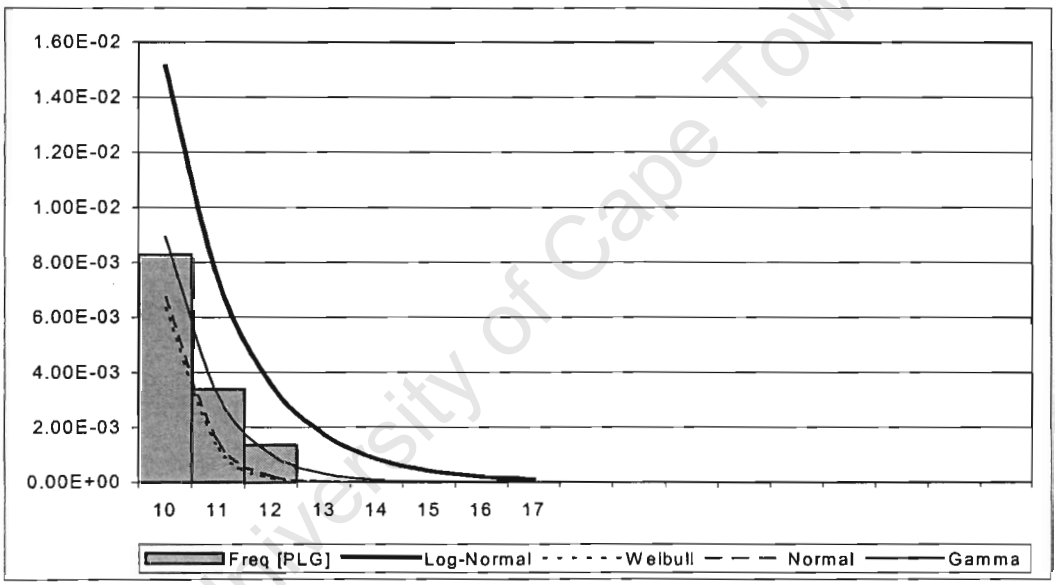

In all the cases investigated the Log-normal distribution displayed the "heaviest" tail and was thus chosen to model the Post Inspection Defect Size distribution.